UNIVERSIDADE ESTADUAL DE CAMPINAS
FACULDADE DE ENGENHARIA DE ALIMENTOS

FABIANA DE ASSIS PERRECHIL

PRODUÇÃO DE MICROGÉIS PARA ENCAPSULAÇÃO DE COMPOSTOS HIDROFÓBICOS

TESE DE DOUTORADO APRESENTADA À FACULDADE DE ENGENHARIA DE ALIMENTOS UNICAMP PARA OBTENÇÃO DO TÍTULO DE DOUTOR EM ENGENHARIA DE ALIMENTOS

PROFA. DRA. ROSIANE LOPES DA CUNHA
ORIENTADOR

Este exemplar corresponde à versão final da tese defendida por Fabiana de Assis Perrechil, aprovada pela comissão julgadora em 20/03/2012 e orientada pela Profa. Dra. Rosiane Lopes da Cunha

_____
Assinatura do Orientador

CAMPINAS, 2012

BANCA EXAMINADORA

_____

Profa. Dra. Rosiane Lopes da Cunha

Departamento de Engenharia de Alimentos / FEA / UNICAMP - Orientadora

_____

Profa. Dra. Ana Luiza Mattos Braga

Centro de Tecnologia e Desenvolvimento Regional / UFPB – Membro titular

_____

Prof. Dr. Carlos Raimundo Ferreira Grosso

Departamento de Alimentos e Nutrição / FEA / UNICAMP – Membro titular

_____

Dra. Fernanda Yumi Ushikubo

Departamento de Engenharia de Alimentos / FEA / UNICAMP – Membro titular

_____

Profa. Dra. Samantha Cristina de Pinho

Departamento de Engenharia de Alimentos / FZEA / USP – Membro titular

_____

Profa. Dra. Lucimara Gaziola de la Torre

Departamento de Processos Biotecnológicos / FEQ / UNICAMP – Membro suplente

_____

Dra. Renata Valeriano Tonon

EMBRAPA – Membro suplente

_____

Dra. Vanessa Martins da Silva

Departamento de Engenharia de Alimentos / FEA / UNICAMP – Membro suplente

Dedico este trabalho à minha família que esteve sempre ao meu lado em todos os momentos dessa caminhada e à Rosi que sempre me incentivou e acreditou em meu potencial

AGRADECIMENTOS

Primeiramente agradeço a Deus por iluminar meus caminhos, guiar meus passos e sempre me dar forças para seguir em frente;

À Faculdade de Engenharia de Alimentos e seus professores e funcionários pela oportunidade e estrutura oferecida, em especial ao Prof. Carlos Grosso pelos ensinamentos da disciplina TP357 que foram muito importantes para a realização deste trabalho;

À Capes, Fapesp e CNPq pela bolsa de doutorado e suporte financeiro;

À banca examinadora pelas correções que, com certeza, contribuíram muito para a melhoria do conteúdo apresentado neste trabalho;

À Profa. Dra. Rosiane Lopes da Cunha, gostaria de agradecer por todos os anos de convívio. Agradeço não só à orientação, mas também a sua amizade, seu incentivo, confiança, paciência, inúmeros conselhos e momentos de terapia. Obrigada por acreditar em mim em momentos em que nem eu mesma acreditava. Admiro muito seu profissionalismo, sua ética e seu amor à pesquisa;

Ao Gabriel, meu grande amor, muito obrigada por seu carinho, amizade, companheirismo, compreensão, apoio, paciência, e por tudo o que vivemos juntos nesses quase 7 anos. Seu amor me fortalece e me ajuda a vencer todos os obstáculos;

Aos meus pais, Julio e Suely, meus irmãos Marcus e Leca, minha avó Matilde e meu avô Valdy muito obrigada por sempre me apoiarem, por vibrarem comigo a cada conquista e, principalmente, por não me deixarem nunca desistir dos meus sonhos;

À Aninha... muito obrigada pela sua amizade, pela sua paciência pra aguentar todos os meus desabafos e minhas inúmeras crises, pelas inúmeras discussões sobre meus resultados, pelos conselhos, pelas risadas, pelos choros, pela companhia nas viagens para São Paulo... Obrigada por ser tão presente em minha vida. Com certeza esse trabalho é também um pouquinho seu!

ÍNDICE GERAL

Tese de doutorado

AUTORA: Fabiana de Assis Perrechil

TÍTULO: Produção de microgéis para encapsulação de compostos hidrofóbicos

ORIENTADORA: Profa. Dra. Rosiane Lopes da Cunha

Depto. Engenharia de Alimentos – FEA – UNICAMP

_____

RESUMO GERAL

A microencapsulação é uma técnica que vem sendo amplamente estudada para a proteção de compostos bioativos e controle de sua liberação. Neste contexto, o objetivo geral deste trabalho foi produzir micropartículas através da extrusão de emulsões estabilizadas por biopolímeros (caseinato de sódio e κ-carragena) em solução de cloreto de potássio para a encapsulação de compostos hidrofóbicos. Na primeira parte deste estudo, o processo de extrusão em um atomizador foi estudado através da produção de microgéis a partir de soluções aquosas de caseinato de sódio (Na-CN) e κ-carragena. Os efeitos da vazão de alimentação, vazão de ar comprimido no bico atomizador, viscosidade e tensão superficial das soluções foram avaliados experimentalmente e através da análise de parâmetros adimensionais. Os resultados mostraram que os menores microgéis foram obtidos com a menor vazão de alimentação, menor viscosidade da solução biopolimérica e maior vazão de ar comprimido. No entanto, a esfericidade dos microgéis foi principalmente influenciada pela tensão superficial das soluções. Na segunda etapa do trabalho, emulsões óleo-água (O/A) multicamadas estabilizadas por caseinato de sódio e κ-carragena foram estudadas com o intuito de determinar as condições de maior estabilidade em pH 7 e 3,5. Em pH 7, o fenômeno de floculação por depleção ocorreu em elevada concentração de κ-carragena, enquanto que em pH 3,5 foi observada a floculação por ponte (*bridging flocculation*) em menores concentrações de polissacarídeo. Emulsões estáveis foram produzidas na maior concentração de polissacarídeo (1% m/v) em ambos os valores de pH (7 e 3,5) devido ao aumento da viscosidade da fase contínua. Na terceira parte do estudo, microesferas com potencial para encapsulação de compostos hidrofóbicos foram produzidas a partir da gelificação iônica das emulsões multicamadas e avaliadas quanto à estabilidade em diferentes meios. As microesferas produzidas em pH 3,5 foram mais estáveis do que aquelas preparadas em pH 7, sendo que ambas foram altamente estáveis quando dispersas

em soluções de cloreto de potássio com concentrações superiores a 0,75% (m/v). Na última etapa do trabalho foi avaliado um exemplo de aplicação das microesferas para encapsulação de triptofano. Nesta etapa, as propriedades reológicas de suspensões de microgéis também foram estudadas com o intuito de verificar a sua influência na textura dos produtos. A eficiência de encapsulação do triptofano nas microesferas foi baixa (~30%), o que pode ser explicado pelo elevado tamanho dos poros do gel que não impediu a difusão desse composto de baixa massa molecular. No entanto, a liberação do bioativo foi bastante baixa quando as micropartículas foram diluídas em solução aquosa. Além disso, suspensões de microesferas com menores diâmetros e formatos mais esféricos apresentaram pouca influência na textura, mostrando sua potencial aplicação em produtos contendo elevada quantidade de água.

Palavras chave: Caseinato de sódio, κ-carragena, emulsão, extrusão, microestrutura, reologia

Ph. D. Thesis

AUTHOR: Fabiana de Assis Perrechil

TITLE: Encapsulation of hydrophobic compounds in microgels

SUPERVISOR: Profa. Dra. Rosiane Lopes da Cunha

Depto. Engenharia de Alimentos – FEA – UNICAMP

_____

ABSTRACT

Microencapsulation is a technique widely used for the protection of bioactive compounds and for controlling their release. In this context, the general purpose of this work was to produce microbeads through the extrusion of biopolymer-stabilized emulsions (sodium caseinate and κ-carrageenan) in a potassium chloride solution, aiming the encapsulation of hydrophobic compounds. In the first part of this work, the extrusion process was studied in an atomizer, producing microgels from aqueous solution of sodium caseinate (Na-CN) and κ-carrageenan. The effect of feed flow rate and compressed air flow rate in the atomizer nozzle, viscosity and surface tension of solutions were evaluated experimentally and through the analysis of dimensionless parameters. The results showed that smaller microgels were produced using lower feed flow rate, lower viscosity and higher compressed air flow rate. Nevertheless, the sphericity of microgels was mainly influenced by the surface tension of solutions. In the second step of this work, oil-in-water (O/W) multilayered emulsions stabilized by sodium caseinate and κ-carrageenan were studied in order to determine the conditions of higher stability at pH 7 and 3.5. At pH 7, depletion flocculation occurred at high κ-carrageenan concentrations, while at pH 3.5, bridging flocculation was observed at lower polysaccharide concentrations. Stable emulsions were produced in the highest polysaccharide concentration (1% w/v) in both pH values (7 and 3.5) due to the increase of viscosity of the continuous phase. In the third part of this study, microbeads potentially useful for encapsulation of hydrophobic compounds were produced by ionic gelation of multilayered emulsions and evaluated in relation to stability in different media. The microbeads produced at pH 3.5 were more stable than those prepared at pH 7 and both were highly stable when dispersed in solutions with more than 0.75% (w/v) potassium chloride. In the last step of this study, an example of microbead application for encapsulating tryptophan was evaluated. In this step, the rheological properties of

suspensions of microgels were also studied in order to verify their influence on the texture of products. The encapsulation efficiency of tryptophan in the microbeads was low (~30%), which was attributed to the large pore size of the gel matrix that could not hinder the diffusion of this low molecular weight compound. However, the release of bioactive was very low when the particles were diluted in aqueous solution. Moreover, suspensions of microbeads with smaller diameters and more spherical shape showed little influence on the texture, exhibiting their potential application in products with high water content.

Keywords: Sodium caseinate, κ-carrageenan, emulsion, extrusion, microstructure, rheology

CAPÍTULO 1.   Introdução Geral

1.1. INTRODUÇÃO

A encapsulação de compostos hidrofóbicos desperta o interesse em diversas indústrias, tais como a alimentícia, farmacêutica e médica. Dentre esses compostos hidrofóbicos encontram-se substâncias como lipídeos bioativos, *flavors*, antimicrobianos, vitaminas e antioxidantes (MCCLEMENTS et al., 2007). Emulsões simples (O/A ou A/O) apresentam elevado potencial para encapsulação de compostos ativos, principalmente por apresentarem regiões polares e apolares em sua composição, baixo custo de produção e relativa facilidade de produção (MCCLEMENTS et al., 2007). Como as emulsões são sistemas altamente instáveis, agentes emulsificantes e/ou estabilizantes devem ser adicionados (DICKINSON, 1992) para aumentar a estabilidade cinética. Dentre estes ingredientes, as proteínas e polissacarídeos são particularmente atrativos, principalmente por serem geralmente reconhecidos como seguros (*Generally recognized as safe* – GRAS) (KEPPELER et al., 2009). Alguns estudos demonstraram que a estabilidade das emulsões pode ser melhorada pela formação de complexos eletrostáticos proteína – polissacarídeo na interface das emulsões, produzindo as chamadas emulsões multicamadas. Neste caso, as emulsões são produzidas pela adição de um polissacarídeo carregado em uma emulsão estabilizada por uma proteína carregada com carga oposta (GU et al., 2004; GU et al., 2005; SURH et al., 2006; GUZEY & MCCLEMENTS, 2006; PALLANDRE et al., 2007).

A presença de biopolímeros nos sistemas ainda permite a formação de géis, tornando as emulsões mais estáveis e com maior resistência mecânica. Esses géis podem ser formados em escala micrométrica, sendo chamados de microgéis, de modo a apresentar a mesma estabilidade e resistência das matrizes de gel, porém podendo ser incorporados a diversos tipos de produtos com pouca alteração de suas características de textura. Além disso, os microgéis podem ser utilizados como modificadores de textura (ELLIS &

JACQUIER, 2009), podendo apresentar diferentes comportamentos dependendo de suas características, tais como composição, tamanho e formato. Assim, o conhecimento da reologia de suspensões é um modo de controlar as propriedades de tais materiais (ADAMS et al., 2004).

Diferentes métodos estão sendo estabelecidos para a produção de microgéis e a maioria deles combina a formação de gotas/partículas com o processo de gelificação, como o mecanismo de extrusão que envolve a formação de gotas pelo uso de uma seringa ou um bico atomizador, as quais são coletadas em uma solução contendo agente gelificante (HUNIK & TRAMPER, 1993; BLANDINO et al., 1999). O processo de gelificação geralmente utilizado para produzir microgéis de polissacarídeos a partir do método de extrusão é a gelificação ionotrópica (ZHANG et al., 2007; HERRERO et al., 2006; SMRDEL et al., 2008), a qual envolve a extrusão da solução de polissacarídeo em uma solução iônica, com difusão dos íons nas gotas de polissacarídeo. Ao escolher a utilização de tais métodos de produção, torna-se necessário levar em conta as propriedades das soluções de biopolímeros (viscosidade e tensão superficial) e condições de processo, como a vazão de solução no bico atomizador (RIZK & LEFEBVRE, 1980; BUREY et al., 2008; ALISEDA et al., 2008).

1.2. OBJETIVOS

O objetivo geral deste trabalho foi determinar os parâmetros de processo relevantes para produção de microgéis a partir da gelificação de emulsões contendo κ-carragena e caseinato de sódio para a encapsulação de compostos hidrofóbicos. Como exemplo de aplicação das micropartículas, a viabilidade de encapsular triptofano e/ou modificar a textura de produtos com elevado teor de água também foi avaliada.

Os objetivos específicos deste trabalho foram:

A) Estudar as variáveis de processo para a formação de microgéis a partir da gelificação de soluções de goma κ-carragena e / ou caseinato de sódio com o uso de cloreto de potássio. Os parâmetros adimensionais envolvidos no processo de extrusão (vazão de alimentação e de ar comprimido) foram avaliados, bem como a morfologia e estabilidade dos microgéis produzidos, além da reologia das suspensões de microgéis biopoliméricos;

B) Estudar a influência do pH e concentração de κ-carragena na estabilidade de emulsões O/A estabilizadas por caseinato de sódio em pH 7 e 3,5. Para isso, diâmetro médio de gotas, microestrutura, cobertura superficial das gotas, potencial zeta e propriedades reológicas foram avaliados;

C) Avaliar as variáveis de processo envolvidas na produção de microesferas por extrusão de emulsões multicamadas (diâmetro de saída de líquido do bico atomizador e distância entre o bico atomizador e a solução salina). A estabilidade das microesferas em diferentes meios foi avaliada de modo a obter potenciais matrizes para a encapsulação de compostos hidrofóbicos;

D) Estudar a viabilidade de encapsular triptofano nas microesferas produzidas a partir de emulsões multicamadas, avaliando a eficiência de encapsulação e a liberação dos compostos encapsulados, bem como a influência da incorporação dos mesmos na textura dos produtos.

1.3. ORGANIZAÇÃO DA TESE EM CAPÍTULOS

A apresentação deste trabalho foi organizada em 6 capítulos como descrito a seguir:

Capítulo 1: **Introdução geral**

Capítulo 2: **Revisão Bibliográfica**

Neste capítulo são abordados aspectos teóricos dos sistemas estudados, bem como uma revisão bibliográfica relatando a literatura recente e mais relevante sobre o tema deste trabalho.

Capítulo 3: **κ-Carrageenan – sodium caseinate microgel production by atomization: Critical analysis of the experimental procedure**

Nesta parte foi realizado um estudo da produção de microgéis a partir das soluções de caseinato de sódio e κ-carragena utilizando-se o processo de extrusão em solução de cloreto de potássio. A partir deste estudo foi possível entender os fatores que afetam o processo de extrusão, a interação entre as soluções biopoliméricas durante o processo de formação de gel, a estabilidade dos microgéis e o comportamento reológico dos microgéis em suspensões.

Capítulo 4: **Stabilization of multilayered emulsions by sodium caseinate and κ-carrageenan**

Neste capítulo foi avaliada a influência do pH e da concentração de polissacarídeo na formação de complexos eletrostáticos entre caseinato de sódio - κ-carragena na interface das emulsões O/A. Foram utilizadas técnicas de microscopia, difração a laser, potencial zeta e reologia para a avaliação da interação entre proteína e polissacarídeo, bem como a determinação das condições necessárias para a formação de emulsões estáveis.

Capítulo 5: **Development of Na-CN - κ-carrageenan microbeads for encapsulation of lipophilic compounds**

Neste capítulo foi feito o estudo da produção de microesferas a partir da gelificação das emulsões multicamadas estudadas no Capítulo 4. A partir deste trabalho foi possível avaliar alguns fatores que afetam o processo de extrusão, a interação entre a proteína e polissacarídeo na formação das microesferas, o efeito do pH e a estabilidade das microesferas em diferentes meios.

Capítulo 6: **Encapsulation of tryptophan using microbeads of sodium caseinate and κ-carrageenan produced by atomization**

Este capítulo apresenta um exemplo de aplicação das microesferas estudadas no Capítulo 5. Nesse estudo foi avaliada a viabilidade da encapsulação de triptofano através da eficiência de encapsulação, a cinética de liberação de triptofano em solução aquosa e propriedades reológicas de suspensões de microesferas em solução salina.

Capítulo 7: **Conclusões gerais**

Neste capítulo são relatadas as principais conclusões sobre os resultados obtidos.

1.4. REFERÊNCIAS

ADAMS, S.; FRITH, W. J.; STOKES, J. R. Influence of particle modulus on the rheological properties of agar microgel suspensions. **Journal of Rheology**, v. 48, n. 6, p. 1195-1213, 2004.

ALISEDA, A.; HOPFINGER, E. J.; LASHERAS, J. C.; KREMER, D. M.; BERCHIELLI, A.; CONNOLLY, E. K. Atomization of viscous and non-newtonian liquids by a coaxial, high-speed gas jet. Experiments and droplet size modeling. **International Journal of Multiphase Flow**, v. 34, n. 2, p. 161-175, 2008.

BLANDINO, A.; MACIAS, M.; CANTERO, D. Formation of calcium alginate gel capsules: Influence of sodium alginate and $CaCl_2$ concentration on gelation kinetics. **Journal of Bioscience and Bioengineering**, v. 88, n. 6, p. 686-689, 1999.

BUREY, P.; BHANDARI, B. R.; HOWES, T.; GIDLEY, M. J. Hydrocolloid gel particles: formation, characterization, and application. **Critical Reviews in Food Science and Nutrition**, v. 48, n. 5, p. 361-377, 2008.

DICKINSON, E. **An Introduction to Food Colloids**. Oxford University Press: Oxford, 1992.

ELLIS, A.; JACQUIER, J. C. Manufacture of food grade κ-carrageenan microspheres. **Journal of Food Engineering**, v. 94, n. 3-4, p. 316-320, 2009.

GU, Y. S.; DECKER, E. A.; MCCLEMENTS, D. J. Influence of pH and ι-carrageenan concentration on physicochemical properties and stability of β-lactoglobulin-stabilized oil-in-water emulsions. **Journal of Agricultural and Food Chemistry**, v. 52, n. 11, p. 3626-3632, 2004.

GU, Y. S.; DECKER, E. A.; MCCLEMENTS, D. J. Influence of pH and carrageenan type on properties of β-lactoglobulin stabilized oil-in-water emulsions. **Food Hydrocolloids**, v. 19, n. 1, p. 83-91, 2005.

GUZEY, D.; MCCLEMENTS, D. J. Formation, stability and properties of multilayer emulsions for application in the food industry. **Advances in Colloid and Interface Science**, v. 128-130, p. 227-248, 2006.

HERRERO, E. P.; MARTÍN DEL VALLE, E. M.; GALÁN, M. A. Development of a new technology for the production of microcapsules based in atomization processes. **Chemical Engineering Journal**, v. 117, n. 2, p. 137-142, 2006.

HUNIK, J. H.; TRAMPER, J. Large-scale production of κ-carrageenan droplets for gel-bead production: theoretical and practical limitations of size and production rate. **Biotechnology Progress**, v. 9, n. 2, p. 186-192, 1993.

KEPPELER, S.; ELLIS, A.; JACQUIER, J. C. Cross-linked carrageenan beads for controlled release delivery systems. **Carbohydrate Polymers**, v. 78, n. 4, p. 973-977, 2009.

MCCLEMENTS, D. J.; DECKER, E. A.; WEISS, J. Emulsion-based delivery systems for lipophilic bioactive components. **Journal of Food Science**, v. 72, n. 8, p. R109-R124, 2007.

PALLANDRE, S.; DECKER, E. A.; MCCLEMENTS, D. J. Improvement of stability of oil-in-water emulsions containing caseinate-coated droplet by addition of sodium alginate. **Journal of Food Science**, v. 72, n. 9, p. E518-E524, 2007.

RIZK, N. K.; LEFEBVRE, A. H. The influence of liquid film thickness on airblast atomization. **Journal of Engineering for Power**, v. 102, n. 7, p. 706-710, 1980.

SMRDEL, P.; BOGATAJ, M., ZEGA, A.; PLANINSEK, O.; MRHAR, A. Shape optimization and characterization of polysaccharide beads prepared by ionotropic gelation. **Journal of Microencapsulation**, v. 25, n. 2, p. 90-105, 2008.

SURH, J.; DECKER, E. A.; MCCLEMENTS, D. J. Influence of pH and pectin type on properties and stability of sodium-caseinate stabilized oil-in-water emulsions. **Food Hydrocolloids**, v. 20, n. 5, p. 607-618, 2006.

ZHANG, J.; LI, X; ZHANG, D.; XIU, Z. Theoretical and experimental investigations on the size of alginate microspheres prepared by dropping and spraying. **Journal of Microencapsulation**, v. 24, n. 4, p. 303-322, 2007.

CAPÍTULO 2.   Revisão Bibliográfica

2.1. EMULSÕES

Uma emulsão geralmente é composta por dois líquidos imiscíveis (usualmente óleo e água), com um dos líquidos disperso no outro na forma de gotas. A substância ou solução que compõe as gotas é chamada de fase dispersa, enquanto que aquela que compõe o meio é chamada de fase contínua. As emulsões podem ser classificadas de acordo com a distribuição relativa das diferentes fases. Um sistema que consiste de gotas de óleo dispersas em uma fase contínua aquosa é chamado emulsão óleo em água (O/A) como, por exemplo, leite, maionese, sopas e molhos. Já o sistema formado por gotas de água dispersas em uma fase oleosa é chamado emulsão água em óleo (A/O), tendo como exemplos a margarina e a manteiga (DICKINSON, 1992; MCCLEMENTS, 2005; MCCLEMENTS et al., 2007).

As emulsões são comumente classificadas de acordo com o diâmetro das gotas em nanoemulsões (ou microemulsões) (10-100 nm), miniemulsões (100-1000 nm) e macroemulsões (0,5-100 µm) (WINDHAB et al., 2005). Enquanto as microemulsões são translúcidas e termodinamicamente estáveis, as miniemulsões e macroemulsões são sistemas termodinamicamente instáveis e tendem a se romper com o tempo através de diversos mecanismos físico-químicos, como cremeação, floculação e coalescência das gotas (DICKINSON, 1992; MCCLEMENTS, 2005). Para a formação das emulsões devem ser empregados ingredientes conhecidos como emulsificantes, que são espécies químicas (ou misturas de espécies) que são adsorvidas na superfície das gotas produzidas durante o processo de homogeneização, formando camadas protetoras que impedem a agregação da fase dispersa e reduzem a tensão interfacial (MCCLEMENTS et al., 2007). Existem duas grandes classes de emulsificantes: surfactantes de baixo peso molecular (monoglicerídeos, polissorbatos, lecitina, dentre outros) e emulsificantes macromoleculares (usualmente

proteínas, principalmente do leite, da soja e do ovo) (DICKINSON, 2003). Além disso, a estabilidade das emulsões pode ser aumentada através de adição de espessantes, que são componentes que apresentam a propriedade de aumentar a viscosidade ou gelificar a fase contínua das emulsões, retardando ou impedindo o movimento das gotas (MCCLEMENTS et al., 2007). Dentre os principais espessantes utilizados estão os polissacarídeos, como as gomas carragena, xantana, gelana e jataí.

Além dos ingredientes utilizados na formulação das emulsões, a estabilidade deste tipo de sistema depende do método de dispersão utilizado em seu preparo, o que vai influenciar diretamente o tamanho das gotas formadas. As emulsões podem ser preparadas a partir de dois diferentes tipos de metodologias denominadas de baixa energia (emulsificação espontânea e temperatura de inversão de fase) e alta energia (moinhos coloidais, homogeneizadores de alta pressão, sistemas de membranas, dentre outros). Nas metodologias de baixa energia, as gotas são formadas através da alteração das propriedades físico-químicas intrínsecas dos surfactantes, diferentemente das metodologias de alta energia, as quais utilizam uma elevada energia mecânica para a formação das gotas. Os métodos que utilizam alta pressão são atualmente os mais utilizados e apresentam a vantagem de dependerem apenas de parâmetros diretamente controláveis, tais como quantidade de energia, concentração de tensoativo e natureza dos componentes (ANTON et al., 2008).

2.2. EMULSÕES MULTICAMADAS

A formação de multicamadas na interface das emulsões O/A pode melhorar a qualidade e estabilidade de muitos produtos, bem como a capacidade de desenvolver novos sistemas de encapsulação e liberação controlada. Para a produção de emulsões

multicamadas, um emulsificante iônico é primeiramente adsorvido na superfície das gotas de óleo durante a homogeneização, produzindo uma emulsão primária (Figura 2.1A). Em uma segunda etapa, um polieletrólito contendo carga oposta é adicionado ao sistema, sendo adsorvido na superfície das gotas e produzindo uma emulsão secundária formada por gotas de óleo cobertas por uma interface composta por duas camadas (Figura 2.1B). Esse procedimento pode ser repetido de modo a formar três ou mais camadas (GUZEY & MCCLEMENTS, 2006). A primeira camada é geralmente produzida pela adsorção de uma proteína na interface da emulsão devido a suas propriedades interfaciais, enquanto que as demais camadas podem ser compostas por outros biopolímeros (proteínas ou polissacarídeos) que se associam à primeira camada devido a interações eletrostáticas (DICKINSON, 2008).
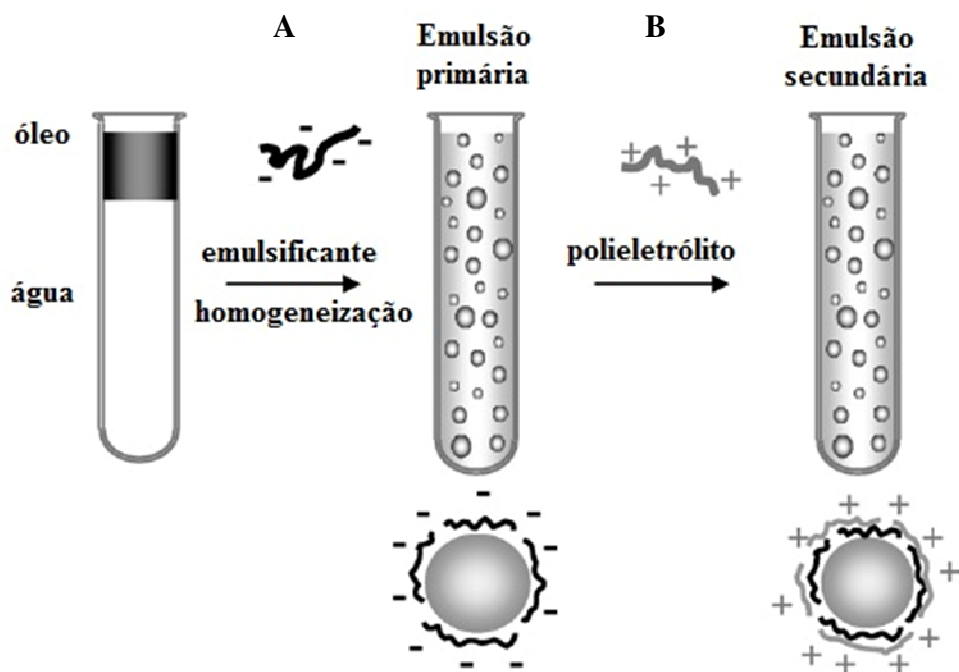
Figura 2.1. Representação esquemática do processo de formação de emulsões óleo em água A) primárias e B) secundárias (Fonte: GUZEY & MCCLEMENTS, 2006).

Antes da formação de uma nova camada, é necessário garantir que existe uma pequena quantidade (ou nenhuma) de polieletrólito livre presente na solução aquosa. Caso contrário, pode ocorrer a formação de complexos eletrostáticos fora da interface (GUZEY & MCCLEMENTS, 2006). Para isso, diferentes estratégias podem ser adotadas:

• Método de saturação – apenas a quantidade de polieletrólito necessária para cobrir completamente todas as gotas do sistema é adicionada, resultando em pequena quantidade de polieletrólito livre na fase aquosa. A concentração de saturação pode ser determinada experimentalmente através de medidas de potencial zeta ou pela determinação da concentração superficial de polieletrólito;

• Método de centrifugação – o excesso de moléculas de polieletrólito não-adsorvido é removido através de centrifugação da emulsão, seguido por suspensão em uma solução tampão apropriada;

• Método de filtração – o excesso de polieletrólitos não-adsorvido é removido através de filtração em membrana, de modo que as moléculas de polieletrólitos passem através da membrana e a emulsão filtrada é adicionada de solução tampão.

As emulsões multicamadas tendem a ser mais estáveis que as emulsões simples com relação a diferentes condições do meio (pH, sal, aquecimento, desidratação, etc.). No entanto, estas emulsões podem apresentar agregação das gotas dependendo da concentração de polieletrólitos (C) na multicamada (CHO & MCCLEMENTS, 2009).

• C = 0 → as emulsões são estáveis a agregação devido à forte repulsão eletrostática entre as gotas de óleo cobertas por emulsificante iônico.

• $0 < C < C_{sat}$ → floculação por ponte (*bridging flocculation*) ocorre quando a concentração de polieletrólito é insuficiente para saturar completamente a superfície das

gotas (C_{sat}). Neste caso, uma única molécula de polieletrólito se adsorve em duas gotas vizinhas, promovendo a floculação.

- $C_{sat} < C < C_{ads}$ → a floculação por ponte também ocorre quando a concentração de polieletrólito é suficiente para saturar a superfície das gotas, porém é muito baixa para garantir que as gotas sejam saturadas (C_{ads}) antes que ocorra colisão entre elas.

- $C_{ads} < C < C_{dep}$ → as emulsões são estáveis devido à completa e rápida saturação da superfície das gotas de óleo pelo polieletrólito, sendo a condição ideal para a produção de emulsões multicamadas estáveis.

- $C > C_{dep}$ → a concentração de polieletrólito livre em solução excede um valor crítico (C_{dep}), promovendo floculação por depleção (*depletion flocculation*), onde as forças de depleção são elevadas o suficiente para superar as forças repulsivas entre as gotas.

Assim, para a produção de emulsões multicamadas estáveis deve-se garantir que $C_{ads} < C < C_{dep}$, ou seja, a concentração de polieletrólito deve ser suficientemente alta para saturar a superfície das gotas, porém não tão elevada de forma a evitar que o excesso de polieletrólitos livre em solução promova floculação por depleção.

2.3. MICROGÉIS

A estabilidade das emulsões que utilizam biopolímeros como estabilizantes pode ainda ser aumentada pela gelificação da fase aquosa. Isso é possível devido à capacidade gelificante e de retenção de água das proteínas e de alguns polissacarídeos (WALSTRA, 2003). As matrizes biopoliméricas podem então ser utilizadas para incorporar e proteger compostos nutracêuticos (CHEN et al., 2006). No entanto, no caso de produtos semi-sólidos, é essencial que o tamanho da matriz do gel seja reduzido, formando microgéis, de

modo que estes possam ser incorporados nos produtos sem afetar sua textura (AUGUSTIN, 2003). Além disso, os microgéis podem ser utilizados para controle da textura ou reologia de alguns produtos (ELLIS & JACQUIER, 2009).

2.3.1. Encapsulação por microgéis

Os microgéis são utilizados para reter compostos ativos, visando reduzir a reatividade do material encapsulado (recheio) em relação ao meio (luz, oxigênio, umidade, temperatura, etc), evitar a evaporação de compostos voláteis, preservar ou mascarar sabores, controlar a taxa e local de liberação do mesmo, facilitando o manuseio do material encapsulado (SHAHIDI & HAN, 1993). Além disso, o uso de encapsulação por microgéis é particularmente atrativo, pois pode auxiliar na incorporação de materiais com baixa solubilidade e ainda permite a incorporação dos microgéis em produtos com elevada quantidade de água, o que não ocorre com partículas secas, como aquelas produzidas em "spray dryer" (BUREY et al., 2008). Deve-se atentar para a particularidade de que um microgel desenvolvido para proteger um determinado composto em um produto de baixa atividade de água não terá o mesmo desempenho quando aplicado em outro produto com maior umidade. Ou seja, no desenvolvimento de microcápsulas um dos pontos fundamentais a ser considerado é o tipo de produto a ser enriquecido.

Uma metodologia que vem mostrando grande eficácia no desenvolvimento de microcápsulas é a do "Retro-Design" (UBBINK & KRUEGER, 2006). A partir desta metodologia, o desenvolvimento de um ingrediente encapsulado é um resultado de uma pré-análise cuidadosa da aplicação desejada com relação a: 1) vida-de-prateleira do produto, 2) mercado consumidor alvo, 3) benefício esperado ao consumidor e 4) processo de produção e seus princípios físicos, incluindo a ciência dos materiais, físico-química e

biofísica. O conhecimento do mercado consumidor alvo permitirá a definição dos materiais a serem usados com relação à legislação local e, no caso de produtos alimentícios, com relação aos hábitos alimentares. O benefício esperado ao consumidor definirá onde e como o composto bioativo deverá ser liberado, por exemplo no produto ou no corpo humano, por difusão ou ruptura da microcápsula dentre outras possibilidades. No caso do benefício estar associado à nutrição, o composto ativo deve apresentar alta biodisponibilidade mesmo após encapsulado. O processo e o material a serem utilizados no preparo da microcápsula dependerão das características físico-químicas do produto a ser enriquecido e do composto bioativo, dos parâmetros do processo de produção, do local, do tempo e da forma como o composto será liberado. Após esta pré-análise, o pesquisador montará o "quebra-cabeça" entre possíveis processos e materiais a fim de identificar quais as tecnologias de encapsulação são as mais promissoras para obter sucesso na aplicação almejada. Além disto, na grande maioria dos casos, o pesquisador precisará desenvolver metodologias em sistemas modelo para avaliar as eficiências de encapsulação e de liberação do composto. Para este último, deve-se considerar todo o processo produtivo, condições de vida-de-prateleira e onde/como o composto será liberado (BRAGA & UBBINK, 2012).

É usual na indústria a encapsulação de ingredientes como aromas, vitaminas, minerais, enzimas, microrganismos, ácidos graxos e peptídeos. Alguns exemplos de aplicação em alimentos incluem a encapsulação de microrganismos probióticos em cápsulas produzidas a partir de gomas gelana e xantana (MCMASTER et al., 2005), partículas de κ-carragena e carboximetilcelulose para a encapsulação de beta-caroteno (MUHAMAD et al., 2011) e encapsulação de óleo essencial de eucalipto em cápsulas de alginato (CHANG & DOBASHI, 2003).

2.3.2. Controle de textura/reologia dos produtos

Os microgéis podem atender a diferentes aplicações dependendo de suas características, como composição dos polímeros, densidade da rede e tamanho de partícula. Alguns microgéis podem ser aplicados para formar a estrutura dos produtos, como é o caso do amido, ou ainda para fornecer uma textura sólida flexível, podendo substituir a gordura sem alteração da textura dos produtos (BUREY et al., 2008). O entendimento da reologia de suspensões de microgéis é a chave para o controle das propriedades de processamento e de utilização desses materiais (ADAMS et al., 2004).

2.4. MATERIAIS UTILIZADOS NO PREPARO DOS MICROGÉIS

Dentre os materiais utilizados para o preparo dos microgéis estão os biopolímeros, como polissacarídeos e proteínas, principalmente devido a sua biocompatibilidade e por serem produzidos a partir de fontes naturais (BUREY et al., 2008). Além disso, microgéis produzidos a partir de biopolímeros apresentam a capacidade de se degradar a partir da ação de estímulos biológicos, tais como alteração de pH ou interações com enzimas e proteínas (ZHANG et al., 2007). Existem diversos biopolímeros gelificantes de diferentes origens bastante importantes, principalmente na indústria de alimentos, sendo alguns deles apresentados na Tabela 2.1.

Tabela 2.1. Fontes de biopolímeros gelificantes industrialmente importantes (adaptado de Williams & Phillips, 2000)

Fonte	Biopolímero	Principal uso
Botânica	Amido, pectina, celulose, goma arábica	Agente espessante e/ou gelificante
Algas	Agar, carragena, alginato	Agente gelificante
Microbiana	Xantana, gelana, dextrana	Agente espessante e/ou gelificante
Animal	Gelatina, caseinatos, proteínas do soro, quitosana	Agente espessante e/ou gelificante

Dentre esses ingredientes, os materiais de particular interesse para esse trabalho (carragena e caseinato de sódio) serão descritos detalhadamente a seguir.

2.4.1. Carragena

A carragena é um polissacarídeo natural extraído a partir de algas vermelhas da classe das *Rhodophyceae*. Sua estrutura primária linear é formada por unidades alternadas de D-galactose e 3,6-anidro-D-galactose (3,6AG) com diferentes graus de sulfatação, unidas por ligações glicosídicas alternadas α-(1,3) e β-(1,4) (DE RUITER & RUDOLPH, 1997; IMESON, 2000). Os tipos mais comuns de carragena são chamados de kappa (κ), iota (ι) e lambda (λ), os quais podem ser observados na Figura 2.2. A estrutura destas três principais formas de carragena difere apenas no número de grupos sulfatados por unidade repetida de dissacarídeo: κ tem um, ι tem dois, e λ tem três (YUGUCHI et al., 2003).
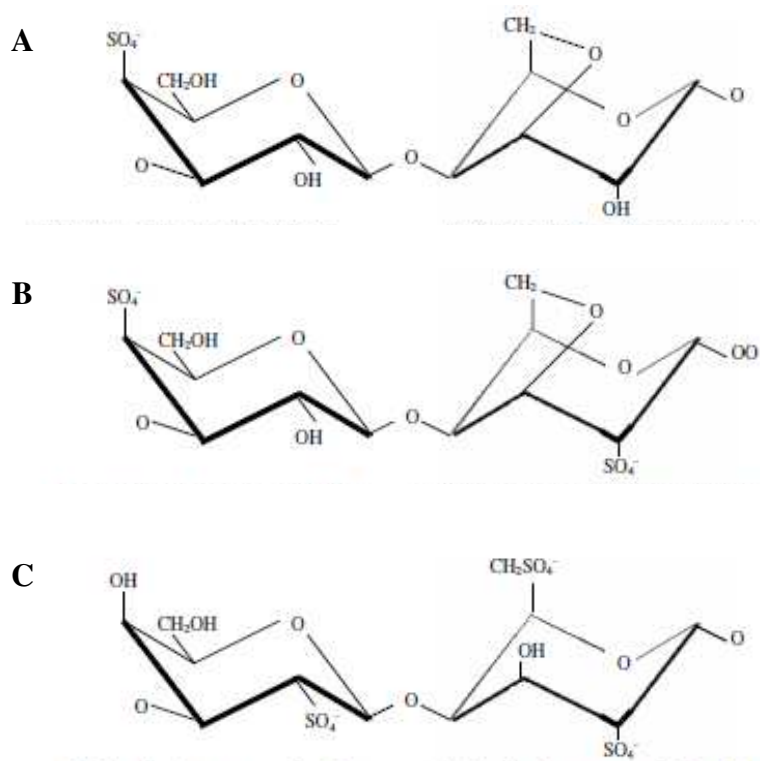
Figura 2.2. Tipos estruturais da carragena. A) κ-carragena, B) ι-carragena e C) λ-carragena (Fonte: BUREY et al., 2008).

Dentre as propriedades físicas deste polissacarídeo, destacam-se as capacidades gelificante e espessante, sendo que a propriedade gelificante é a mais importante para o desenvolvimento de microgéis. Diferentes propriedades podem ser observadas para cada tipo de carragena. Soluções quentes de κ e ι-carragena podem formar géis termicamente reversíveis quando resfriadas entre 40°C e 60°C, dependendo do cátion presente no sistema. A κ-carragena, por exemplo, seleciona íons potássio para estabilizar as zonas de junção formando géis caracteristicamente firmes, como apresentado na Figura 2.3A. Já a ι-carragena utiliza íons cálcio para formar ligações entre cadeias adjacentes (Figura 2.3B), formando géis tipicamente elásticos (IMESON, 2000).

A   B
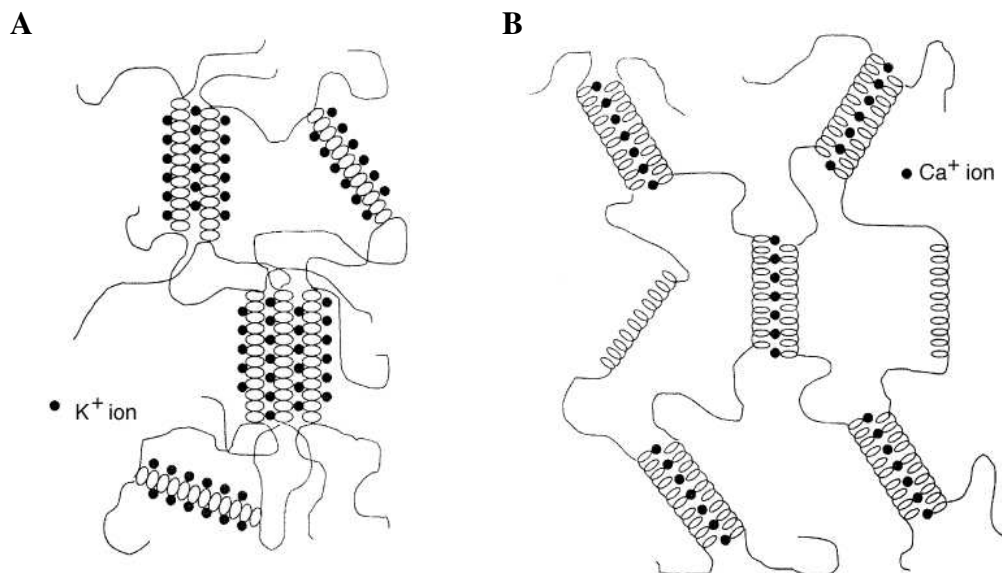
Figura 2.3. Gelificação da A) κ-carragena e B) ι-carragena com íons (Fonte: IMESON, 2000).

A carragena possui a capacidade de interagir com outros ingredientes, como a goma jataí e goma konjac. No entanto, a interação sinergística da carragena mais conhecida é aquela que envolve as proteínas do leite. Existem duas teorias que explicam as interações da κ-carragena com a caseína. A primeira teoria propõe que a κ-carragena carregada negativamente interage com uma região predominantemente positiva da κ-caseína, sendo então adsorvida na superfície da micela de caseína (DALGLEISH & MORRIS, 1988; SNOEREN et al., 1975). Já a segunda teoria propõe a formação de um gel fraco de κ-carragena, o qual mantém as micelas de caseína em suspensão (BOURRIOT et al., 1999), apesar das concentrações necessárias para a estabilidade serem inferiores à concentração crítica de gelificação.

2.4.2. Caseinato de sódio

O leite bovino é um sistema altamente complexo que contém aproximadamente 3,5% de proteína. As proteínas do leite são tradicionalmente divididas em duas principais frações: caseínas (~80%) e as proteínas do soro (~20%). A fração de caseína é composta por quatro principais proteínas chamadas α_{s1}-, α_{s2}-, β- e κ-caseínas, além da γ-caseína e diversas outras proteínas e peptídeos (ENNIS & MULVIHILL, 2000). Cerca de 95% da caseína existente no leite está na forma de micelas de caseína, que são associações coloidais com massa molecular de cerca de 10^8 Da e diâmetros médios na faixa de 100 nm. As micelas são compostas por sub-micelas esféricas contendo diferentes quantidades de caseínas e arranjadas de modo que a κ-caseína fique situada na superfície da micela (FOX & MULVIHILL, 1990). Fosfato de cálcio coloidal presente nas micelas de caseína promove interações hidrofóbicas entre proteínas e entre sub-micelas, contribuindo para a estabilidade da mesma. Além disso, os "cabelos" presentes na κ-caseína impedem a agregação das micelas de caseína através de repulsão eletrostática e estérica, mantendo o sistema estável.

O caseinato de sódio é um ingrediente preparado a partir da precipitação da caseína pela adição de ácido até o ponto isoelétrico (pH ~ 4,6), seguida por uma lavagem e dissolução em água utilizando-se hidróxido de sódio até atingir a neutralidade. A elevada proporção de cadeias laterais contendo aminoácidos hidrofóbicos na estrutura primária da caseína promove a formação de agregados (ou "sub-micelas") no caseinato de sódio quando este se encontra em solução aquosa (FARRELL et al., 1990). No entanto, as submicelas de caseína não conseguem se associar para a formação de micelas devido à ausência de cálcio. O caseinato de sódio é amplamente utilizado devido a suas propriedades funcionais que

incluem propriedades emulsificantes, espessantes, gelificantes e capacidade de retenção de água e de gordura (MULVIHILL, 1989).

2.5. METODOLOGIAS PARA PREPARO DOS MICROGÉIS

Existem dois principais mecanismos para a formação de microgéis: 1) formação da fase contínua ("*top-down*") e 2) formação da fase dispersa ("*bottom-up*"). Esses métodos diferem principalmente na ordem das etapas do processo. Na formação da fase contínua (*"top-down"*) existe primeiramente a produção de um macrogel a partir da solução de biopolímeros, seguida pela quebra do mesmo para a formação das micropartículas (BUREY et al., 2008). Já para a formação da fase dispersa (*"bottom-up"*), primeiramente ocorre a etapa de formação das gotas a partir de uma solução de biopolímero, sendo a segunda etapa caracterizada pela gelificação das gotas (ZHANG et al., 2007) (Figura 2.4). Como o mecanismo de formação da fase dispersa ("*bottom-up*") é de particular interesse para este trabalho, suas etapas de produção das gotas e gelificação serão detalhadas a seguir nos itens 2.5.1 e 2.5.2.
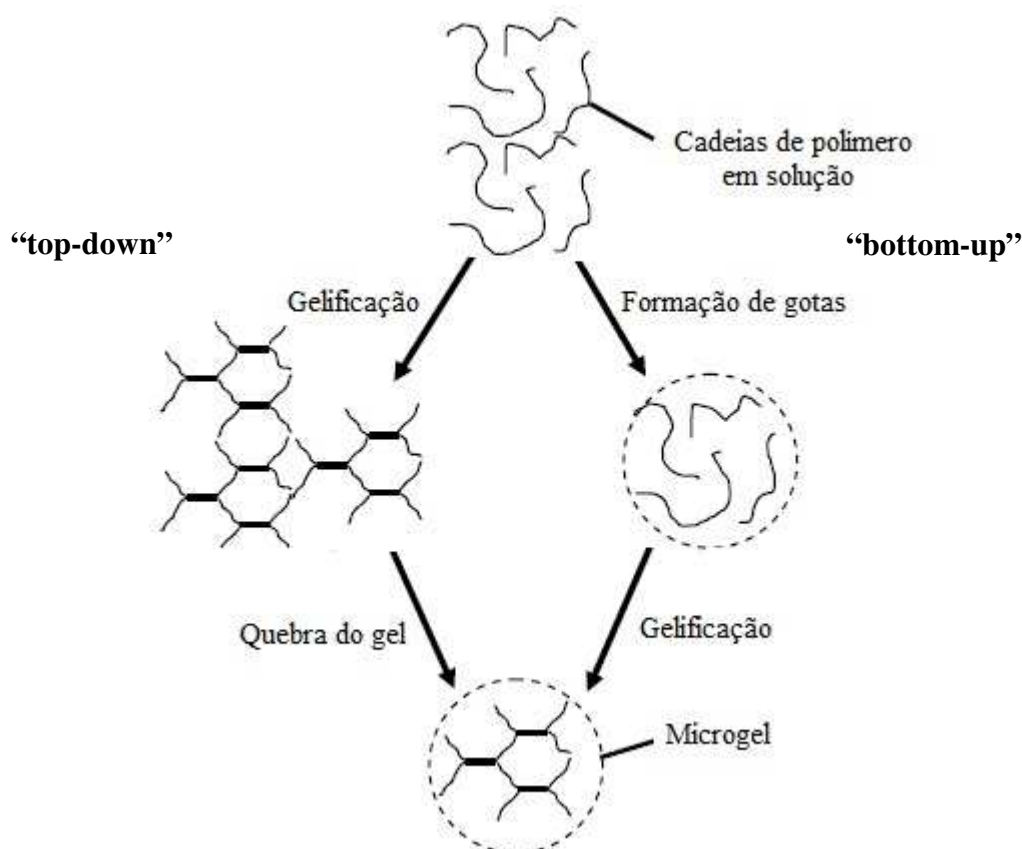
Figura 2.4. Esquema dos mecanismos de formação dos microgéis (Fonte: BUREY et al., 2008).

2.5.1. Produção das gotas

A etapa de produção das gotas é um dos estágios críticos para a formação dos microgéis pelo mecanismo "*bottom-up*", já que irá determinar o tamanho e a polidispersão das partículas produzidas. As gotas podem ser produzidas de forma simultânea através da agitação da solução de biopolímeros em uma fase dispersa oleosa, formando emulsões água em óleo (A/O), ou através de processos de gotejamento ou extrusão da solução biopolimérica (FREITAS et al., 2005; ZHANG et al., 2007).

A produção de partículas pela técnica de emulsificação consiste na suspensão de

uma solução biopolimérica em um meio não aquoso, geralmente óleo vegetal, formando uma emulsão A/O, seguida pela adição desta emulsão a uma solução promotora de gelificação (Figura 2.5). Neste caso, o tamanho das gotas formadas é dependente da viscosidade do óleo, razão óleo/solução biopolimérica, tipo de emulsificante e quantidade de energia utilizada para o preparo da emulsão (REIS et al., 2006).
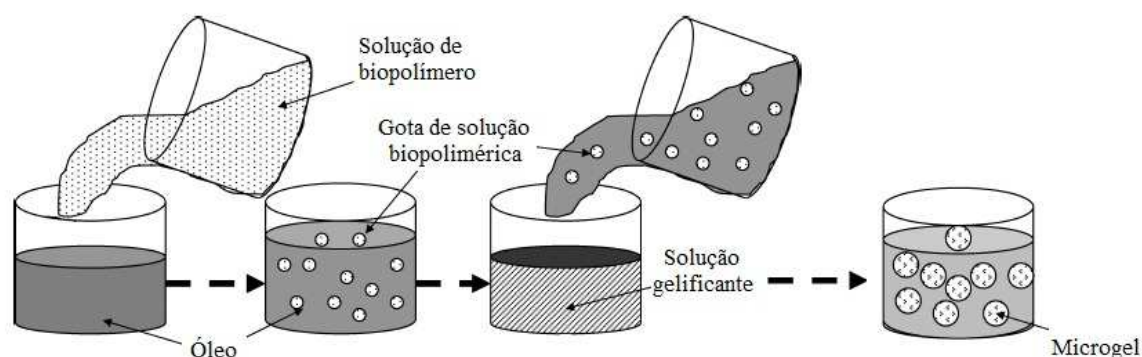
Figura 2.5. Produção de gotas pela técnica de emulsificação (Fonte: BUREY et al., 2008).

Já o processo de gotejamento / extrusão é bastante utilizado para a produção de partículas de gel. Nesse processo, uma solução de hidrocolóide é extrusada em uma solução promotora de gelificação (geralmente solução salina) através de uma seringa ou um bico atomizador (Figura 2.6) (BUREY et al., 2008). O mecanismo de formação de gotas através do uso de bicos atomizadores é bastante complexo, sendo influenciado por diversos parâmetros como a geometria do bico atomizador e as propriedades do fluido (ALISEDA et al., 2008). Dentre os diferentes bicos atomizadores que podem ser utilizados estão os atomizadores duplo fluido, cuja configuração apresenta um jato de líquido central que é atomizado por um fluxo de gás de alta velocidade anular co-corrente (VARGA et al., 2003). Um modelo físico para o processo de atomização foi sugerido através de estudos experimentais (VARGA et al., 2003), indicando que a quebra do jato de líquido é causada

por mecanismos de instabilidade que ocorrem na interface gás-líquido. Após a saída do bico atomizador, a superfície do jato de líquido é submetida à instabilidade Kelvin-Helmholtz, resultando na formação de ondas primárias (GOROKHOVSKI & HERRMANN, 2008). Essas ondas primárias são então expostas à corrente de gás em alta velocidade, o que leva à aceleração e desenvolvimento de instabilidades Rayleigh-Taylor (R-T) (VARGA et al., 2003; ALISEDA et al., 2008; GOROKHOVSKI & HERRMANN, 2008). Quando suficientemente amplificada, a instabilidade Rayleigh-Taylor leva à quebra do líquido em pequenas gotas (JOSEPH et al., 1999).
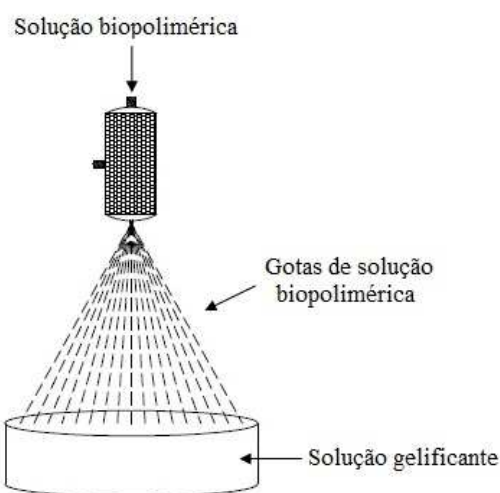
Figura 2.6. Produção de gotas pela técnica de extrusão.

2.5.2. Gelificação dos biopolímeros

A gelificação das gotas pode ocorrer através de processos químicos ou físicos do biopolímero. Ligações químicas são alcançadas através de reações de condensação ou polimerização do radical livre (ZHANG et al., 2007), enquanto que ligações físicas podem ser produzidas a partir de diversos mecanismos como a gelificação térmica ou a ionotrópica. A gelificação térmica requer a aplicação de calor à solução biopolimérica, o que leva à desnaturação / expansão das estruturas nativas e subsequente formação de uma

rede. Essa técnica é a menos utilizada para a formação de microgéis, sendo apenas utilizada quando aplicação de calor é requerida no processo produtivo. Já a gelificação ionotrópica ocorre através da ligação entre cadeias de biopolímeros pela adição de íons, geralmente cátions para a gelificação de polissacarídeos carregados negativamente. Existem duas principais técnicas cuja gelificação ionotrópica pode ocorrer: gelificação interna ou por difusão. A gelificação interna geralmente envolve a dispersão de sais insolúveis na solução biopolimérica, seguida pela solubilização dos íons através de alterações das propriedades da solução, como pH, por exemplo. Por outro lado, a difusão envolve a introdução da solução biopolimérica em uma solução iônica, com a gelificação ocorrendo pela difusão dos íons para a solução de biopolímeros (BUREY et al., 2008). Apesar da possibilidade de promover uma gelificação não homogênea das partículas de biopolímeros, a técnica de difusão é bastante simples e geralmente utilizada para o preparo de microgéis.

2.6. REFERÊNCIAS

ADAMS, S.; FRITH, W. J.; STOKES, J. R. Influence of particle modulus on the rheological properties of agar microgel suspensions. **Journal of Rheology**, v. 48, n. 6, p. 1195-1213, 2004.

ALISEDA, A.; HOPFINGER, E. J.; LASHERAS, J. C.; KREMER, D. M.; BERCHIELLI, A.; CONNOLLY, E. K. Atomization of viscous and non-newtonian liquids by a coaxial, high-speed gas jet. Experiments and droplet size modeling. **International Journal of Multiphase Flow**, v. 34, n. 2, p. 161-175, 2008.

ANTON, N.; BENOIT, J.-P.; SAULNIER, P. Design and production of nanoparticles formulated from nano-emulsion templates – A review. **Journal of Controlled Release**, v. 128, n. 3, p. 185-199, 2008.

AUGUSTIN, M. A. The role of microencapsulation in the development of functional dairy foods. **Australian Journal of Dairy Technology**, v. 58, n. 2, p. 156-160, 2003.

BOURRIOT, S.; GARNIER, C.; DOUBLIER, J. L. Micellar-casein - κ-carrageenan mixtures. I. Phase separation and ultrastructure. **Carbohydrate Polymers**, v. 40, n. 2, p. 145-157, 1999.

BRAGA, A. L. M.; UBBINK, J. An industrial approach to design / screen encapsulates for best performance in products: fish oil case. **Proceedings of the 1st South-American Symposium on Microencapsulation**. To be published in April 2012.

BUREY, P.; BHANDARI, B. R.; HOWES, T.; GIDLEY, M. J. Hydrocolloid gel particles: formation, characterization, and application. **Critical Reviews in Food Science and Nutrition**, v. 48, n. 5, p. 361-377, 2008.

CHANG, C. P.; DOBASHI, T. Preparation of alginate complex capsules containing eucalyptus essential oil and its controlled release. **Colloids and Surfaces B: Biointerfaces**, v. 32, n. 3, p. 257-262, 2003.

CHEN, L.; REMONDETTO, G. E.; SUBIRADE, M. Food protein-based materials as nutraceutical delivery systems. **Trends in Food Science and Technology**, v. 17, n. 5, p. 272-283, 2006.

CHO, Y.-H.; MCCLEMENTS, D. J. Theoretical stability maps for guiding preparation of emulsions stabilized by protein-polysaccharide interfacial complexes. **Langmuir**, v. 25, n. 12, p. 6649-6657, 2009.

DALGLEISH, D. G.; MORRIS, E. R. Interactions between carrageenans and casein micelles: electrophoretic and hydrodynamic properties of the particles. **Food Hydrocolloids**, v. 2, n. 4, p. 311-320, 1988.

DE RUITER, G. A.; RUDOLPH, B. Carrageenan biotechnology. **Trends in Food Science & Technology**, v. 8, n. 12, p. 389-395, 1997.

DICKINSON, E. **An Introduction to Food Colloids**. Oxford University Press: Oxford, 1992.

DICKINSON, E. Hydrocolloids at interfaces and the influence on the properties of dispersed systems. **Food Hydrocolloids**, v. 17, n. 1, p. 25-39, 2003.

DICKINSON, E. Interfacial structure and stability of food emulsions as affected by protein-polysaccharide interactions. **Soft Matter**, v. 4, n. 5, p. 932-942, 2008.

ELLIS, A.; JACQUIER, J. C. Manufacture of food grade κ-carrageenan microspheres. **Journal of Food Engineering**, v. 94, n. 3-4, p. 316-320, 2009.

ENNIS, M. P.; MULVIHILL, D. M. Milk proteins. In: **Handbook of Hydrocolloids**. Phillips, G. O.; Williams, P. A. (Eds.), CRC Press: Boca Raton, 2000.

FARRELL, H. M.; PESSEN, JR., H.; BROWN, E. M.; KUMOSLNSKL, T. F. Structural insights into the bovine casein micelle: small angle X-ray scattering studies and correlations with spectroscopy. **Journal of Dairy Science**, v. 73, n. 12, p. 3592-3601, 1990.

FOX, P. F.; MULVIHILL, D. M. Casein. In: **Food Gels**. Harris, P. (Ed.). Elsevier Applied Science Publishers: London, 1990.

FREITAS, S.; MERKLE, H. P.; GANDER, B. Microencapsulation by solvent extraction/evaporation: Reviewing the state of the art of microsphere preparation process technology. **Journal of Controlled Release**, v. 102, n. 2, p. 313-332, 2005.

GOROKHOVSKI, M.; HERRMANN, M. Modeling primary atomization. **Annual Review of Fluid Mechanics**, v. 40, p. 343-366, 2008.

GUZEY, D.; MCCLEMENTS, D. J. Formation, stability and properties of multilayered emulsions for application in the food industry. **Advances in Colloid and Interface Science**, v. 128-130, p. 227-248, 2006.

IMESON, A. P. Carrageenan. In: **Handbook of Hydrocolloids**. Phillips, G. O.; Williams, P. A. (Eds.), CRC Press: Boca Raton, 2000.

JOSEPH, D. D.; BELANGER, J.; BEAVERS, G. S. Breakup of a liquid drop suddenly exposed to a high-speed airstream. **International Journal of Multiphase Flow**, v. 25, n. 6-7, p. 1263-1303, 1999.

MCCLEMENTS, D. J. **Food emulsions: principles, practice and techniques**. CRC Press: New York, 2005.

MCCLEMENTS, D. J.; DECKER, E. A.; WEISS, J. Emulsion-based delivery systems for lipophilic bioactive components. **Journal of Food Science**, v. 72, n. 8, p. R109-R124, 2007.

MCMASTER, L. D.; KOKOTT, S. A.; SLATTER, P. Micro-encapsulation of *Bifidobacterium lactis* for incorporation in soft foods. **World Journal of Microbiology & Biotechnology**, v. 21, n. 5, p. 723-728, 2005.

MUHAMAD, I. I.; FEN, L. S.; HUI, N. H.; MUSTAPHA, N. A. Genipin-cross-linked kappa-carrageenan/carboxymethyl cellulose beads and effects on beta-carotene release. **Carbohydrate Polymers**, v. 83, n. 3, p. 1207-1212, 2011.

MULVIHILL, D. Casein and caseinates: Manufacture. In: **Developments in dairy chemistry — 4. Functional Milk Proteins**. Fox, P. F. (Ed.), Elsevier Applied Science: London, 1989.

REIS, C. P.; NEUFELD, R. J.; VILELA, S.; RIBEIRO, A. J.; VEIGA, F. Review and current status of emulsion/dispersion technology using an internal gelation process

for the design of alginate particles. **Journal of Microencapsulation**, v. 23, n. 3, p. 245–257, 2006.

SHAHIDI, F.; HAN, X. Q. Encapsulation of food ingredients. **Critical Reviews in Food Science and Nutrition**, v. 33, n. 6, p. 501-547, 1993.

SNOEREN, T. H. M.; PAYENS, T. A. J.; JEUNINK, J.; BOTH, P. Electrostatic interaction between κ-carrageenan and κ-casein. **Milchwissenschaft**, v. 30, p. 393-396, 1975.

UBBINK, J.; KRÜGER, J. Physical approaches for the delivery of active ingredients in foods. **Trends in Food Science & Technology**, v. 17, n. 5, p. 244-254, 2006.

VARGA, C. M.; LASHERAS, J. C.; HOPFINGER, E. J. Initial breakup of a small-diameter liquid jet by a high-speed gas stream. **Journal of Fluid Mechanics**, v. 497, p. 405-434, 2003.

WALSTRA, P. **Physical Chemistry of Foods**. New York: Marcel Decker, 2003.

WILLIAMS, P. A.; PHILLIPS, G. O. Introduction to Food Hydrocolloids. In: **Handbook of Hydrocolloids**. Phillips, G. O.; Williams, P. A. (Eds.), CRC Press: Boca Raton, 2000.

WINDHAB, E. J.; DRESSLER, M.; FEIGL, K.; FISCHER, P.; MEGIAS-ALGUACIL, D. Emulsion Processing—from single-drop deformation to design of complex processes and products. **Chemical Engineering Science**, v. 60, n. 8-9, p. 2101–2113, 2005.

YUGUCHI, Y.; URAKAWA, H.; KAJIWARA, K. Structural characteristics of carrageenan gels: various types of counter ions. **Food Hydrocolloids**, v. 17, n. 4, p. 481-485, 2003.

ZHANG, H.; TUMARKIN, E.; SULLAN, R. M. A.; WALKER, G. C.; KUMACHEVA, E. Exploring microfluidic routes to microgels of biological polymers. **Macromolecular Rapid Communications**, v. 28, n. 5, p. 527-538, 2007.

CAPÍTULO 3.   Produção de microgéis de κ-carragena e caseinato de sódio por atomização

κ-Carrageenan-sodium caseinate microgel production by atomization:

critical analysis of the experimental procedure

Perrechil, F. A.; Sato, A. C. K. and Cunha, R. L.∗

Department of Food Engineering, Faculty of Food Engineering, University of Campinas (UNICAMP), 13083-862 – Campinas, SP, Brazil.

∗ Corresponding author: Tel: +55-19-35214047; fax: +55-19-35214027;

e-mail: rosiane@fea.unicamp.br

ABSTRACT

The influence of atomization process to produce κ-carrageenan and κ-carrageenan/sodium caseinate microgels was studied experimentally (aspect ratio and particle size distribution) and theoretically (dimensionless parameters). Moreover, rheological behavior of microgel suspensions was evaluated to examine their potential application in food products. Experimental results demonstrated that the size of microgels was influenced by feed flow rate, compressed air flow rate and composition of solutions, while their shape depended on the viscosity and surface tension of biopolymer solutions. Regarding the dimensionless numbers, higher values of Reynolds number of liquid layer ($Re_{\lambda l}$) and Weber number (We_l) led to smaller particles, while the decrease of Ohnesorge number (Oh) was related to lower sphericity of microgels. Rheological behavior of suspensions depended not only on the morphology and size of microgels, but also on their

composition. Incompatibility between κ-carrageenan and sodium caseinate in mixed microgels led to suspensions with more complex rheological behavior at determined biopolymer concentrations.

Keywords: extrusion; ionic gelation; microscopy; rheology

3.1. INTRODUCTION

The development and preparation of microgels have attracted great interest in a number of areas, including the pharmaceutical, medical, cosmetics, agricultural and food industries. Specifically in the food industry, the microgels can be used for a variety of applications, for example as an encapsulation matrix to protect active compounds, or as a texture modifier (ELLIS & JACQUIER, 2009). Regarding the control of product texture/rheology, the microgels can be used for different applications depending on their characteristics, such as composition, size and shape. Thus the knowledge of the rheology of microgel suspensions is a way to control the properties of such materials (ADAMS et al., 2004).

Among the ingredients that can be used to produce microgels, the polysaccharides are particularly attractive, mainly due to their technological properties and because they are generally recognized as safe (GRAS) (KEPPELER et al., 2009). κ-Carrageenan is a polysaccharide with a structure composed of repeating D-galactose and 3,6-anhydrogalactose (3,6 AG) units, both sulfated and non-sulfated, joined by alternating α-(1,3) and β-(1,4) glycosidic links (DE RUITER & RUDOLPH, 1997; IMESON, 2000). Among the interesting technological properties of this polysaccharide, its gelling capacity is of special interest. The gelling process of κ-carrageenan involves a conformational

transition from the coil to the helix form (DE RUITER & RUDOLPH, 1997), which depends on the temperature, the ionic strength and the biopolymer concentration (MORRIS et al., 1980, MEUNIER et al., 2001). κ-Carrageenan can also interact with other ingredients, especially with milk proteins (IMESON, 2000). Even though it has long been known that κ-carrageenan can form complexes with casein micelles (DALGLEISH & MORRIS, 1988; LANGENDORFF et al., 1997; BOURRIOT et al., 1999; MARTIN et al., 2006; ARLTOFT et al., 2007), few studies have evaluated the interaction between κ-carrageenan and sodium caseinate (OAKENFULL et al., 1999; BELYAKOVA et al., 2003; RIBEIRO et al., 2004; SABADINI et al., 2010).

Different methods have been established to produce microgels and most of them combine droplet/particle formation with the gelation process. Emulsion formation and extrusion mechanisms are some techniques in which droplet formation occurs prior to gelation (BUREY et al., 2008). In the emulsion formation mechanism, the droplets are formed by dispersion of the biopolymeric solution into an oil phase, followed by the addition of a gelling agent to promote gelation (PONCELET et al., 1992; REIS et al., 2006; ELLIS & JACQUIER, 2009). In a different way, extrusion involves the formation of droplets by the use of a syringe or atomizer nozzle, and the droplets are then collected in a hardening solution containing the gelling agent, forming the microgels (HUNIK & TRAMPER, 1993, BLANDINO et al., 1999). The gelation process commonly used to produce polysaccharide microgels via extrusion method is that of ionotropic gelation by diffusion setting (ZHANG et al., 2007; HERRERO et al., 2006; SMRDEL et al., 2008), which involves the atomization of the polysaccharide solution into an ionic solution, with diffusion of the ions into the polysaccharide droplet. Both techniques can produce

microgels in a large range of sizes, depending on the conditions employed in the process, but the methodology of emulsion formation requires an additional process step to remove the oil phase from the microgels (BUREY et al., 2008).

Thus, the purpose of this work was to study the production of microgels composed of κ-carrageenan, with or without sodium caseinate, by extrusion into a salt solution, examining the influence of the process parameters on the morphology, the stability of microgels and rheological behavior of the microgel suspensions.

3.2. MATERIAL AND METHODS

3.2.1. Material

The ingredients used to prepare the systems were κ-carrageenan, gently supplied by CPKelco (Atlanta, USA), casein (Sigma-Aldrich Co., St. Louis, USA) and analytical-grade potassium chloride (Labsynth, Diadema, Brazil). The κ-carrageenan powder was characterized by atomic absorption (AA) spectroscopy, and the following composition of ions was obtained: Na = 1.32%, Ca = 2.54% and K = 1.83% (w/w).

3.2.2. Preparation of the stock solutions

The polysaccharide stock solution (3% w/v) was prepared by dissolving κ-carrageenan in deionized water, followed by heat treatment at 90°C for 60 minutes with magnetic stirring and subsequent cooling to 50°C. The pH was adjusted to 7.0 using HCl. Sodium caseinate (Na-CN) stock solution (6% w/v) was prepared by dispersing casein in deionized water using a magnetic stirrer, and maintaining the pH constantly adjusted to 7.0 with a 10 mol/L NaOH solution. After this, the protein solution was heated to 50°C and the

two stock solutions were diluted and mixed to prepare the microgels. The temperature of the solutions was maintained at 50°C using a thermostatic bath filled with distilled water. Pure microgels were obtained from the κ-carrageenan solution, whilst the mixed microgels were produced from the mixture of the κ-carrageenan and sodium caseinate solutions.

3.2.3. Visual phase diagrams

Visual κ-carrageenan/KCl and κ-carrageenan/Na-CN/KCl phase diagrams were constructed in order to establish the appropriate concentrations of salt and biopolymers for gel formation. In order to construct the visual phase diagrams, the biopolymer stock solutions were diluted to the desired concentration at 50°C, and 4 mL of each solution was mixed with 4 mL of each KCl solution at room temperature. For the κ-carrageenan/KCl phase diagram, the polysaccharide concentration varied between 0.5 and 3% (w/v) and the KCl concentration from 0.1 to 3% (w/v). For the κ-carrageenan/Na-CN/KCl diagram, the same salt concentration was used and the κ-carrageenan/Na-CN ratio varied between 0.2 and 5.0, with a total biopolymer concentration (protein + polysaccharide) of 3% (w/v). These mixtures were stirred at room temperature and placed into a temperature – controlled chamber (model TE-391, Tecnal, Brazil) at 10°C. After 24 hours of storage, the gel formation was visually evaluated. From these data it was possible to construct the sol-gel transition diagrams and to set up some of the conditions for microgel preparation.

3.2.4. Microgel production

The microgels were produced by the extrusion method using pure aqueous κ-carrageenan solutions and mixtures of κ-carrageenan and sodium caseinate solutions (Table

3.1). The surface tension of these solutions was measured using Du Nouy ring method by Sigma 70 tensiometer (KSV Instruments, Finland) at 50°C and the values are shown in Table 3.1. The viscosity of the biopolymer solutions was determined according to section 3.2.6.3.

In order to produce the microgels, hot biopolymer solutions (50°C) at pH 7.0 were extruded from an atomizer nozzle (1.2 mm diameter) into a 0.5% (w/v) KCl solution (concentration determined from the visual phase diagrams) at room temperature. The height from the atomizer nozzle to the KCl solution (Figure 3.1A) was fixed at H = 200 mm, which is greater than the distance for the completion of atomization (~50 mm) (ALISEDA et al., 2008). The feed flow rate varied between 0.3 and 1.0 L/h, while the compressed air flow rate at the nozzle varied from 0.3 to 1.2 m^3/h. The gelled particles were maintained in the salt solution for 30 minutes (CHAN et al., 2009) and then filtered through a sieve with opening of 0.053 mm. The microgels were stored at 10°C and the microstructure and rheology of their suspensions were evaluated.
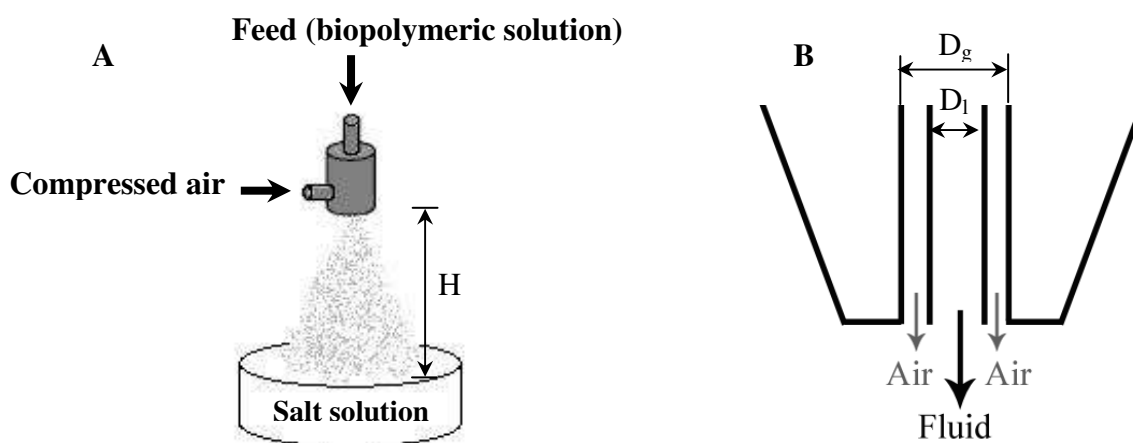
Figure 3.1. A) Extrusion formation of microgels and B) atomizer nozzle. H = height from the atomizer nozzle to the salt solution, D_l = diameter of the fluid nozzle exit and D_g = diameter of gas nozzle exit.

Table 3.1. Biopolymer concentration and surface tension at 50°C of the fluids used to prepare the microgels

PURE κ-CARRAGEENAN SOLUTIONS			
	κ-Carrageenan (%)	Na-CN (%)	Surface tension (mN/m)
	0.5	–	58.79 ± 0.63
	1.0	–	56.98 ± 0.81
	2.0	–	58.16 ± 1.26
	3.0	–	63.02 ± 1.32
MIXED κ-CARRAGEENAN – Na-CN SOLUTIONS			
κ-Carrageenan / Na-CN ratio	κ-Carrageenan (%)	Na-CN (%)	Surface tension (mN/m)
0.2	0.5	2.5	43.32 ± 0.59
0.5	1.0	2.0	44.73 ± 0.42
1.0	1.5	1.5	47.48 ± 0.19
2.0	2.0	1.0	46.99 ± 0.22
5.0	2.5	0.5	47.50 ± 0.20

3.2.5. Dimensionless numbers of the atomization process

The configuration of the atomizer nozzle used in this work is schematically shown in Figure 3.1B. It consists of a round liquid jet surrounded by a co-flowing annular gas stream. The diameter of the liquid jet was $D_l = 1.2$ mm and the gas nozzle exit diameter was $D_g = 3.0$ mm. The liquid and gas velocities (v_l and v_g) at the exit of the nozzle were calculated from the ratio between their respective volume flow rates ($\dot{\gamma}_l$ and $\dot{\gamma}_g$) and exit section areas (A_l and A_g).

The Reynolds numbers of the gas (Re_g) and liquid layers ($Re_{\lambda l}$) can be calculated from Equations 3.1 and 3.2, respectively.

$$\text{Re}_g = \frac{v_g b_g}{\nu_g} \tag{3.1}$$

$$\text{Re}_{\lambda l} = \frac{(v_c - v_l)\lambda_l}{\nu_l} \tag{3.2}$$

where ν_l and ν_g are kinematic viscosities (ratio between the liquid dynamic viscosity and its density) of the liquid and gas (m²/s), respectively, v_c is the velocity of the waves produced in the exit of nozzle ($v_c = \frac{\sqrt{\rho_l}\, v_l + \sqrt{\rho_g}\, v_g}{\sqrt{\rho_l} + \sqrt{\rho_g}}$) and λ_l is the wavelength ($\lambda_l \approx \frac{2Cb_g}{\sqrt{\text{Re}_g}} \frac{\sqrt{\rho_l}}{\sqrt{\rho_g}}$), where C is the coefficient of proportionality that depends on the nozzle design, which was considered as 1.2 (VARGA et al., 2003), ρ_l is the liquid density (kg/m³), ρ_g is the gas density (kg/m³) and b_g is the thickness of the gas layer ($b_g = \frac{D_g - D_l}{2}$).

Biopolymeric solutions can present non-Newtonian behavior depending on their concentration, which means that the viscosity values vary with the shear rate. The shear rate is a consequence of the hydrodynamics and in the atomization process it can be estimated using Equation 3.3 (ALISEDA et al., 2008).

$$\dot{\gamma} = \frac{v_c}{\lambda_l} \tag{3.3}$$

The Ohnesorge number (Oh), which relates the liquid viscosity to the surface tension, and the Weber number (We_l) that defines the ratio between the destabilizing dynamic pressure forces exerted by the gas on the liquid and the confining forces associated with the surface tension (VARGA et al., 2003), can be determined by Equations 3.4 and 3.5, respectively.

$$Oh = \frac{\eta_l}{\sqrt{\rho_l \sigma D_1}}$$ (3.4)

$$We_1 = \frac{\rho_g (v_g - v_1)^2 D_1}{\sigma}$$ (3.5)

where η_l is the liquid viscosity (Pa.s) at the process shear rate and σ is the surface tension (N/m).

3.2.6. Microgel evaluation

3.2.6.1. Optical microscopy and analysis of the microgel morphology

The morphology of the microgels was evaluated by optical microscopy using a Scope.A1 microscope (Carl Zeiss, Germany) with a 10× objective lens. For this, the microgels were stained with methylene blue, poured onto microscope slides and carefully covered with glass cover slips. At least 10 images were obtained for each sample.

The particle size distribution (PSD) and shape of the microgels were determined from image analysis using the public domain software Image J v1.36b (http://rsb.info.nih.gov/ij/). Measurements of the maximum (F_{max}) and minimum (F_{min}) Feret diameters were carried out for each particle, with a total of 400 particles per sample. The aspect ratio (AR) was obtained from the relation between F_{max} and F_{min} (Equation 3.6). The mean particle size ($\bar{d}$) was determined from the equivalent sphere area (Equation 3.7), considering that the particles had an ellipsoidal shape (PABST et al., 2006), and the volume-surface mean diameter (d_{32}) was calculated (Equation 3.8) in order to compare the size between different microgels.

$$AR = \frac{F_{max}}{F_{min}}$$ (3.6)

$$\overline{d} = \sqrt{F_{max} \cdot F_{min}} \tag{3.7}$$

$$d_{32} = \frac{\sum n_i d_i^3}{\sum n_i d_i^2} \tag{3.8}$$

The particle size distribution of the microgels was determined from the mean equivalent diameter ($\overline{d}$) and a log-normal frequency distribution function (Equation 3.9) (MCCLEMENTS, 2005).

$$f(\ln \overline{d}) = \frac{1}{\ln SD \sqrt{2\pi}} \exp\left[\frac{-(\ln \overline{d} - \ln \overline{d}_g)^2}{2 \ln^2 SD}\right] \tag{3.9}$$

where $\overline{d}_g$ and SD are the geometric mean and the standard deviation of the geometric mean, as given by Equations 3.10 and 3.11, respectively.

$$\overline{d}_g = \frac{\sum n_i \overline{d}_i}{N} \tag{3.10}$$

$$SD = \sqrt{\frac{\sum n_i (\overline{d}_i - \overline{d}_g)^2}{N}} \tag{3.11}$$

where n_i is the number of particles with diameter $\overline{d}_i$ and N is the total number of particles.

3.2.6.2. Evaluation of microgel stability in water and salt solutions

Microgels composed only of 3% (w/v) κ-carrageenan were used to evaluate their stability in aqueous solutions. Suspensions were prepared by dispersing 10% (v/v) microgels in deionized water or in the different potassium chloride solutions at concentrations of 0.05%, 0.1%, 0.5%, 1%, 5% and 10% (w/v). The microgel suspensions were stored at room temperature and aliquots were collected after pre-determined time periods (5, 10, 20 and 60 minutes) and observed using an optical microscope. The stability

was determined by the modification of size and shape of microgels within the evaluated period.

3.2.6.3. Rheological measurements of the suspensions

The rheological properties of the microgel suspensions (20%, 40% and 60% particles (w/w) dispersed in 10% w/v KCl solutions were evaluated. A modular compact rheometer Physica MCR301 (Anton Paar, Austria) with a rough parallel plate geometry (50 mm) and 2 mm gap was used for the measurements. Flow curves were obtained by an up-down-up steps program with the shear rate varying between 0 and 300 s^{-1}. All measurements were performed in triplicate at 25°C. Flow curves of biopolymeric solutions were obtained under the same conditions as the suspensions.

3.2.7. Statistical analysis

Significant differences were determined by the Tukey test. Statistical analyses were performed using the software STATISTICA 5.5 (Statsoft Inc., Tulsa, USA) and the level of confidence was 95%.

3.3. RESULTS AND DISCUSSION

3.3.1. Visual phase diagrams

Figures 3.2A and 3.2B show the visual phase diagrams obtained for κ-carrageenan and κ-carrageenan/Na-CN, respectively, in the presence of KCl. The phase diagrams were divided into two regions (sol and gel) and an approximate boundary line was traced between them. It is evident from Figure 3.2 that κ-carrageenan gel formation occurred at a

critical value of KCl concentration of approximately 0.5% (w/v) or above, whilst below this value, a coil-helix transition could take place but without helix aggregation or gelation (NÚÑEZ-SANTIAGO & TECANTE, 2007). An exception was the 3% (w/v) κ-carrageenan sample, which formed a gel without the need for salt addition. At 0.5% and 1% (w/v) KCl, the systems composed of pure κ-carrageenan (Figure 3.2A) gelled at all the biopolymer concentrations (between 0.5% and 3% w/v polysaccharide). However, the systems containing 0.5% (w/v) polysaccharide at higher salt concentrations (2 and 3% w/v) did not form gels. This result is consistent with the findings of Lai et al. (2000), who verified maximum elasticity during gelation (indicated by G' and tan δ) at salt concentrations around 1% (w/w) KCl (0.1 to 0.2 M).
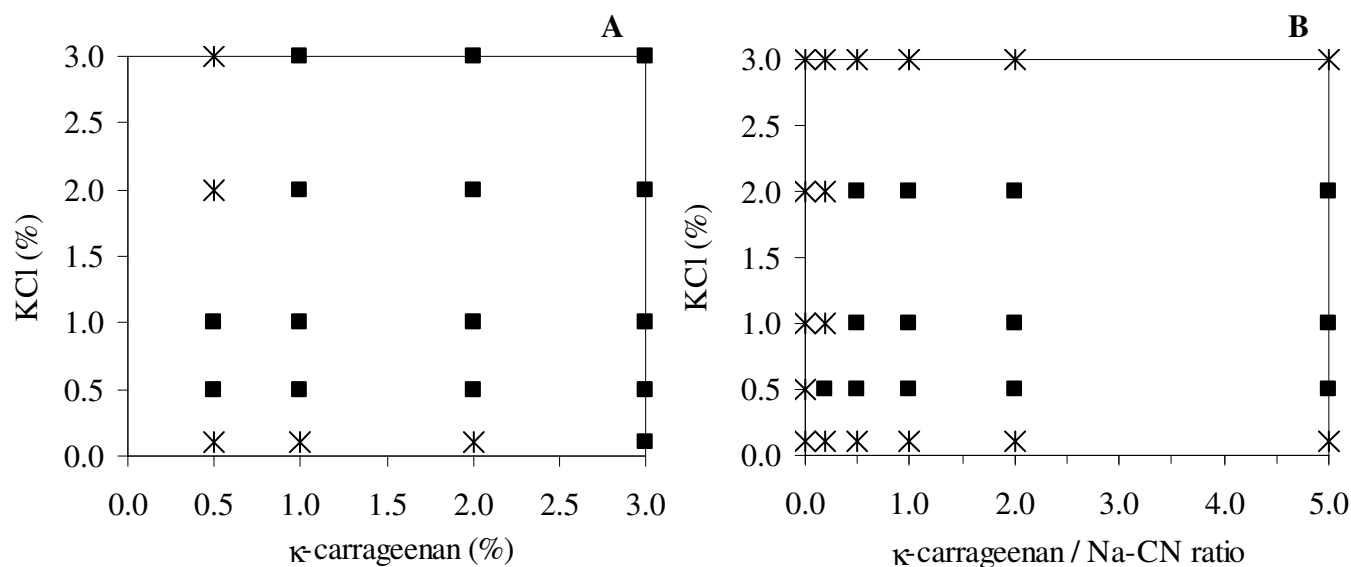
Figure 3.2. Visual phase diagram of A) κ-carrageenan/KCl systems and B) κ-carrageenan/Na-CN/KCl systems (total biopolymers concentration of 3% w/v). (■) Gel points and (✳) sol points.

κ-Carrageenan/Na-CN/KCl (Figure 3.2B) mixed systems showed gel formation for salt concentrations between 0.5% and 2% (w/v) and κ-carrageenan/Na-CN ratios above 0.5, showing the relevance of the presence of κ-carrageenan in gel formation. In particular, for 0.5% (w/v) KCl, all the mixed κ-carrageenan – sodium caseinate solutions showed gel formation. In contrast, the 3% (w/v) KCl solution did not promote gel formation for any of the systems studied. We can speculate that the elevated salt concentration could lead to a disordered aggregation of protein and polysaccharide molecules, with expulsion of water (syneresis) and without formation of a three-dimensional network. Comparing Figures 3.2A and 3.2B, it could be seen that both the pure and mixed systems formed gels when the κ-carrageenan concentration was above 0.5% (w/v), which means that this was the minimum biopolymer concentration to be used. Similar result was reported by Şen and Erboz (2010), who observed formation of gel structure of κ-carrageenan at concentrations above 0.7% (w/v). Since most of the systems showed gel formation when mixed in the 0.5% (w/v) KCl solution, this salt concentration was chosen to prepare the microgels.

3.3.2. Microgels

The main factors determining the final diameter of the microgels are: 1) biopolymer flow rate, 2) compressed air flow rate at the atomizer nozzle and 3) microgel composition (HERRERO et al., 2006). The influence of each factor was studied and the results are detailed below.

3.3.2.1. Effect of the feed flow rate

In order to evaluate the influence of feed flow rate on the final morphology of the microgels, the systems were produced at a fixed κ-carrageenan concentration of 2% (w/v), compressed air flow rate of 1.2 m^3/h (maximum value), and with a feed flow rate ranging from 0.3 to 1 L/h. Figure 3.3 illustrates the particle size distribution and morphology of the microgels produced under these conditions.

d_{32} = 117.9 μm	d_{32} = 167.9 μm	d_{32} = 161.0 μm
AR = 1.36	AR = 1.30	AR = 1.39
SD = 1.56	SD = 1.79	SD = 1.69
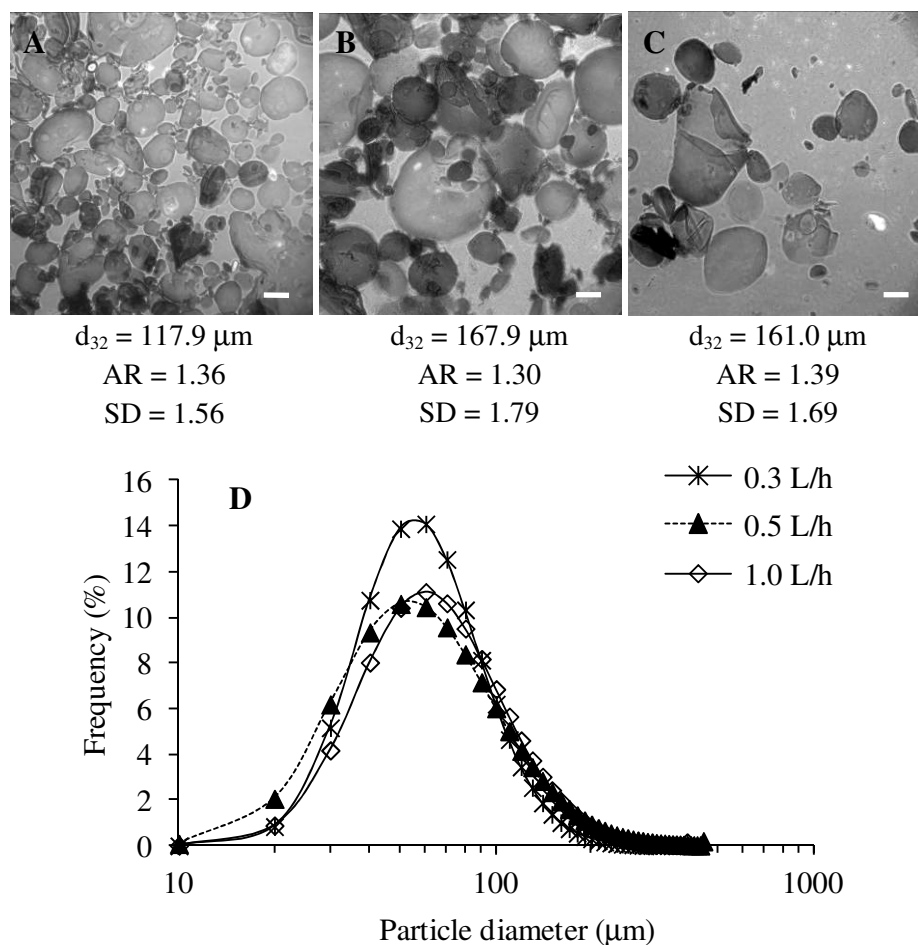
Figure 3.3. Microscopic images of 2% (w/v) κ-carrageenan microgels produced at a fixed compressed air flow rate and different feed flow rates: A) 0.3 L/h, B) 0.5 L/h and C) 1.0 L/h. Scale bar = 100 μm. E) Particle size distribution of these microgels.

47

Figure 3.3 shows that the mean diameter of the microgels increased with increase in the feed flow rate between 0.3 and 0.5 L/h, becoming almost constant between 0.5 and 1.0 L/h. The principle of atomization consists in the formation of a liquid film exiting the nozzle, which is exposed to an air flow moving at high velocity. The contact between liquid and air produces waves (primary instability) that disintegrate into fragments when the wave amplitude reaches a critical value. The fragments rapidly contract into unstable ligaments under the action of surface tension, which break up into droplets (HERRERO et al., 2006, RIZK & LEFEBVRE, 1980). An increase in feed flow rate leads to the formation of thicker films of liquid at the nozzle, which break down into bigger droplets (HERRERO et al., 2006, RIZK & LEFEBVRE, 1980). There are many dimensionless parameters that influence the breakup process when using coaxial atomizer nozzles (VARGA et al., 2003). The evaluation of the dimensionless parameters ($Re_{\lambda l}$ and We) involved in the atomization process showed little differences between the distinct conditions (results not shown), confirming the limited influence of this range of feed flow rate on the production of the microgels. The polidispersity of the microgels (SD) followed the same tendency as the mean diameter, and the aspect ratio of the microgels showed no significant differences with the change in feed flow rate. Thus, a feed flow rate of 0.3 L/h was chosen in order to produce microgels with smaller diameters and polidispersity.

3.3.2.2. Effect of compressed air flow rate

The effect of the air flow rate (0.3, 0.6, 0.9 and 1.2 m^3/h) on the atomizer nozzle was evaluated using fixed values for the κ-carrageenan concentration (2% w/v) and feed flow rate (0.3 L/h). As shown in Figure 3.4A, the microgel produced at the lowest

compressed air flow rate (0.3 m^3/h) showed a spherical shape and mean diameter (d$_{32}$) of around 1.5 mm, which is larger than the atomizer nozzle diameter (1.2 mm). In this case, the force exerted by the compressed air was probably not sufficient to overcome the surface tension force, and thus the droplets were formed when the gravity force on the liquid exceeded the surface tension force (LEFEBVRE, 1989), hindering the breakup of the droplets into smaller ones. The increase in the compressed air flow rate from 0.3 to 1.2 m^3/h led to a gradual reduction in the mean diameter of the microgels (Figure 3.4E) and an increase in the aspect ratio (Figures 3.4B, 3.4C and 3.4D). The influence of the compressed air flow rate on the particle size can once more be explained by the mechanism of film disruption and droplet formation. With the increase in compressed air flow rate, the liquid film disintegrated earlier and the ligaments were formed nearer the nozzle. These ligaments tended to be thinner and shorter, disintegrating into smaller droplets (RIZK & LEFEBVRE, 1980).

d$_{32}$ = 1536.3 µm AR = 1.18 SD = 1.12

d$_{32}$ = 353.4 µm AR = 1.19 SD = 1.66

d$_{32}$ = 138.7 µm AR = 1.28 SD = 1.59

d$_{32}$ = 117.9 µm AR = 1.36 SD = 1.56
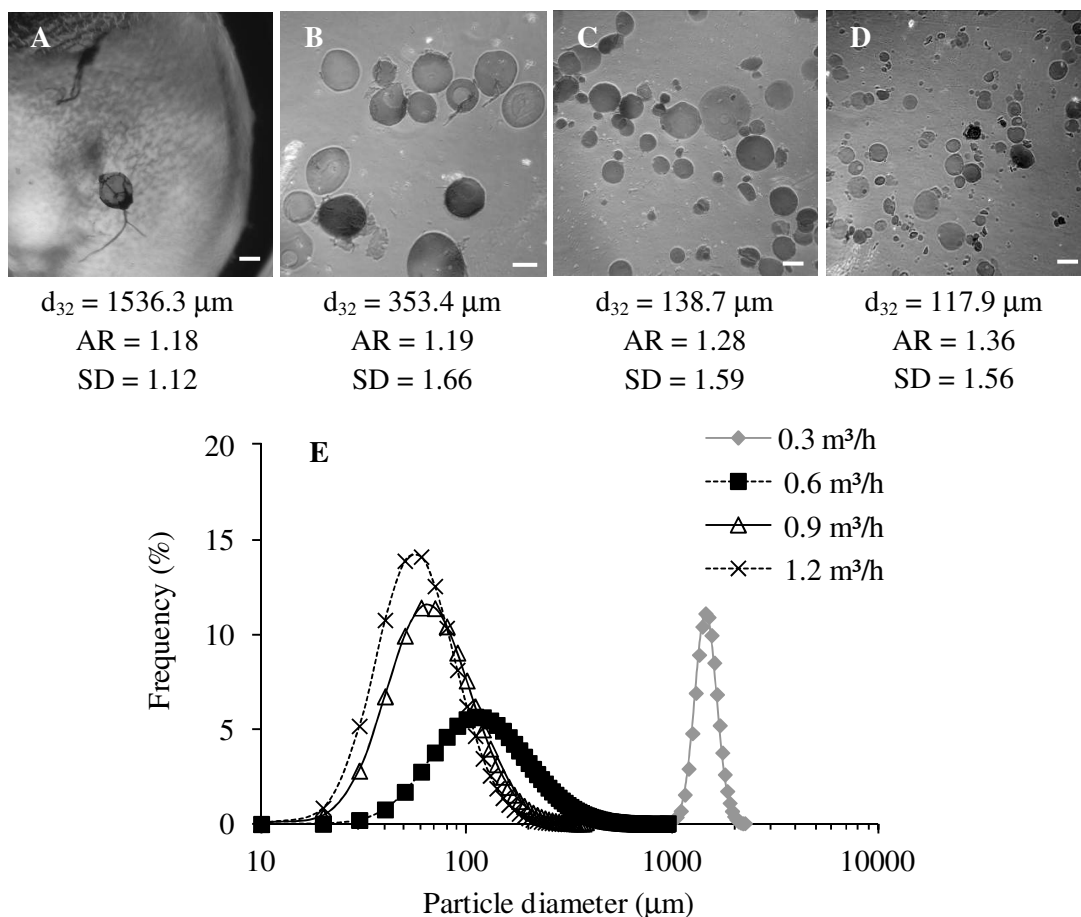
Figure 3.4. Micrographs of 2% (w/v) κ-carrageenan microgels produced at a fixed feed flow rate (0.3 L/h) and different compressed air flow rates: A) 0.3 m^3/h, B) 0.6 m^3/h, C) 0.9 m^3/h and D) 1.2 m^3/h. Scale bar = 100 µm. E) Particle size distribution of these microgels.

Table 3.2 shows the shear rate at the atomizer nozzle, the apparent viscosity of the 2% (w/v) κ-carrageenan solution and the dimensionless parameters calculated for the different conditions of compressed air flow rate. All the parameters were highly influenced by the change in compressed air flow rate. The shear rate at the outlet from the nozzle was estimated to be higher than the range tested experimentally (300 s^{-1}). Thus the viscosity of the biopolymer solution at the shear rate of atomization was estimated from the fitted

equation (power law or Herschel Bulkley), and this value was used to calculate the dimensionless parameters. The Reynolds number of the gas was highly influenced by the air flow rate, showing an increase in the turbulence at higher values of flow rate. The Reynolds number of the liquid layer also increased with the air flow rate and was higher than ~10 in all situations, which is the condition necessary to develop the primary instability (ALISEDA et al., 2008) and consequently droplet breakup. However, the value of $Re_{\lambda l}$ close to 10 in the lowest air flow rate reinforced the assumption that the compressed air was not efficient in the breakup of the droplets under this condition. The Ohnesorge number was only slightly influenced by the air flow rate, because the viscosity at the different shear rates was very similar. This dimensionless number can be related to the microgel sphericity (CHAN et al., 2009), which explains the tendency of aspect ratio to increase with the increment of compressed air flow rate (lower Oh). The Weber number increased at higher values of air flow rate (in the same way as the Reynolds number), indicating that the waves produced at the primary instability grew more quickly (ALISEDA et al., 2008), favoring the production of smaller droplets.

Table 3.2. Shear rate, solution viscosity and dimensionless parameters of the experiments at different compressed air flow rates

Air flow rate (m^3/h)	$\dot{\gamma}$(s^{-1})	η_l^* (mPa.s)	Re_g	$Re_{\lambda l}$	Oh	We_l
0.3	1311	36.0 ± 0.5	2637	15.2	0.14	15
0.6	3563	32.8 ± 0.4	5275	23.6	0.12	62
0.9	6456	31.0 ± 0.3	7912	30.6	0.12	139
1.2	9872	29.8 ± 0.3	10549	36.8	0.11	247

* Viscosity calculated at the shear rate of the extrusion process

From these results, a compressed air flow rate of 1.2 m^3/h was chosen to produce the microgels in the following steps of this study.

3.3.2.3. Evaluation of the microgel composition

For the evaluation of the composition on the microgel morphology, extrusion was carried out at a constant feed flow rate (0.3 L/h) and compressed air flow rate (1.2 m^3/h) as previously determined. Figure 3.5 shows the microstructure of the pure (0.5, 1, 2 and 3% κ-carrageenan) and mixed (κ-carrageenan/Na-CN ratios of 0.2, 0.5, 1.0, 2.0 and 5.0, with total biopolymer concentration of 3% w/v) microgels, from which a considerable dependence of the particle morphology on the biopolymer composition can be verified.
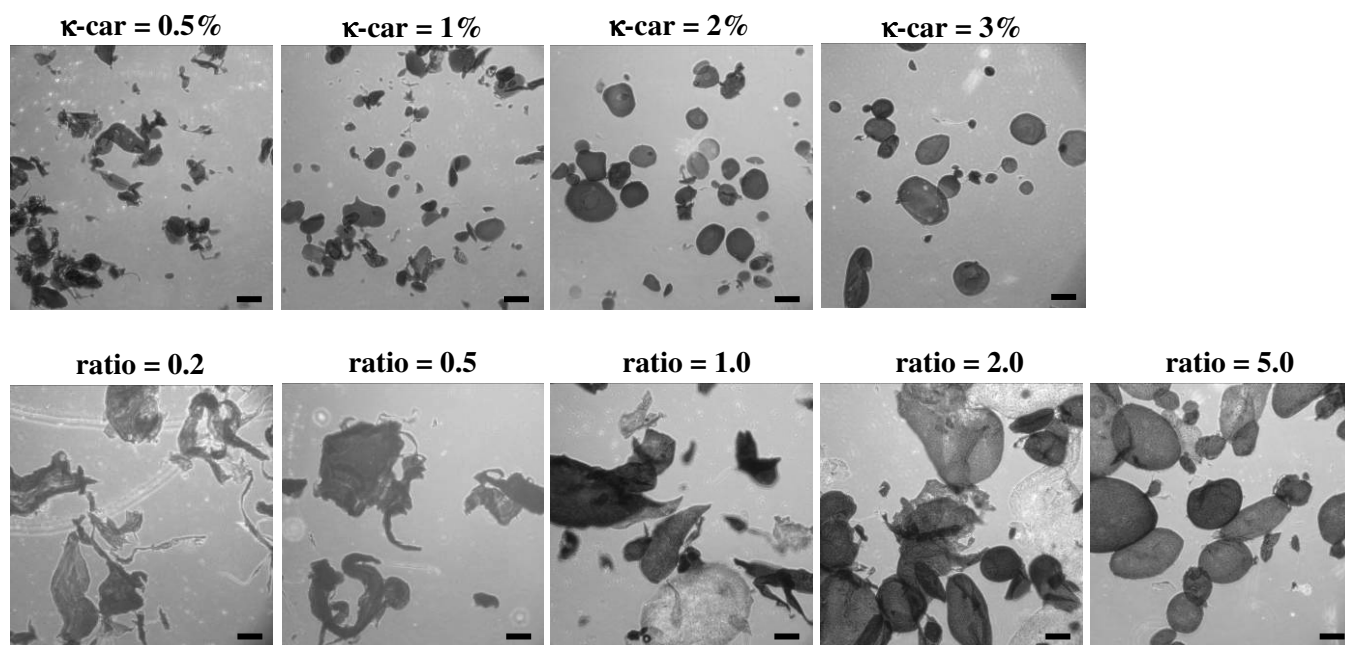
Figure 3.5. Microstructure of the microgels composed of κ-carrageenan (κ-car) and the mixture between κ-carrageenan and Na-CN (different ratios). Scale bar = 100 μm.

The results obtained for droplet diameter and aspect ratio (Table 3.3) indicated that an increase in the κ-carrageenan concentration and the κ-carrageenan/Na-CN ratio led to the formation of larger and more spherical particles. The increased size of the droplets could be related to the greater density of the biopolymers, which resulted in thicker films at the nozzle and consequently in an increase in droplet diameter (RIZK & LEFEBVRE, 1980). On the other hand, the more spherical shape could be associated with the higher surface tension and viscosity of the biopolymeric solutions (Tables 3.1 and 3.3) (CHAN et al., 2009).

The comparison between the pure and mixed microgels showed that the systems containing sodium caseinate presented higher values for the diameter and aspect ratio than the pure systems made with biopolymer solutions of similar viscosity i.e., the addition of protein led to the formation of larger and less spherical particles. This probably occurred because the addition of protein led to the formation of a more porous biopolymeric matrix due to the weak or even repulsive interactions between the protein and polysaccharide, especially for κ-carrageenan/Na-CN ratios of 2.0 and 5.0 (excess of polysaccharide), leading to an increase in particle diameter. Nono et al. (2011) also studied the interaction between κ-carrageenan and sodium caseinate and verified a process of phase separation above a critical concentration of either κ-carrageenan or Na-CN. The difference in morphology of the microgels probably occurred due to the slower gelation of mixed solutions. Thus, the droplets started to dilute into the salt bath before the complete gelation, resulting in particles with more irregular shapes.

Table 3.3 shows the evaluation of the dimensionless parameters involved in the atomization process, as well as the estimated viscosity of the biopolymer solutions used to

calculate these parameters. The values for viscosity were estimated from the flow curves of the solutions, using a shear rate of 9872 s^{-1} as determined from Equation 3.3. These data showed that the Reynolds number of the liquid layer decreased by increasing the apparent viscosity, but in all cases the $Re_{\lambda l}$ was higher than 10 (condition necessary for droplet breakup). On the other hand, the Ohnesorge number increased, demonstrating the greater influence of liquid viscosity in relation to surface tension (ALISEDA et al., 2008) and leading to the formation of more spherical particles (CHAN et al., 2009). As the process parameters (v_g, v_l and D_l) were maintained constant during the experiments, the Weber number was mainly related to the surface tension of the biopolymer solutions (Table 3.1), being lower for the pure polysaccharide solutions (higher σ values) and higher for the mixed solutions (lower σ values). The higher values for the We number should lead to the formation of smaller droplets (ALISEDA et al., 2008) as can be observed for the pure carrageenan beads. Nevertheless, the mixed solutions showed bigger particles than the pure ones. The incompatibility or repulsive interactions between the κ-carrageenan and the sodium caseinate associated to the slower gelation of systems containing protein, probably led to the production of larger microgels.

Table 3.3. Mean droplet diameter and aspect ratio of the microgels prepared from different biopolymer solutions and the dimensionless atomization process parameters

κ-Carrageenan (%)	d_{32} (μm)	AR	η_l^* (mPa.s)	Re_g	$Re_{\lambda l}$	Oh	We_l
0.5	83.7 ± 14.0	1.68 ±0.13	5.3 ± 0.1	10549	206	0.02	244
1.0	89.9 ± 14.1	1.47 ± 0.04	10.9 ± 0.0	10549	100	0.04	252
2.0	136.3 ± 25.0	1.36 ± 0.05	29.8 ± 0.3	10549	37	0.11	247
3.0	159.6 ± 17.6	1.33 ± 0.05	61.8 ± 2.1	10549	18	0.23	228
κ-Carrageenan / Na-CN ratio	d_{32} (μm)	AR	η_l^* (mPa.s)	Re_g	$Re_{\lambda l}$	Oh	We
0.2	142.8 ± 29.04	1.90 ± 0.12	6.0 ± 0.1	10549	183	0.03	331
0.5	161.7 ± 31.8	1.84 ± 0.10	14.2 ± 0.2	10549	77	0.06	321
1.0	165.9 ± 40.4	1.86 ± 0.07	23.5 ± 0.2	10549	47	0.10	302
2.0	224.1 ± 33.8	1.75 ± 0.16	32.0 ± 0.1	10549	34	0.14	305
5.0	235.1 ± 46.0	1.64 ± 0.13	47.2 ± 0.3	10549	23	0.20	302

* Viscosity calculated at the shear rate of the extrusion process

3.3.3. Evaluation of microgel stability

The systems composed of 3% (w/v) κ-carrageenan and κ-carrageenan/Na-CN ratio of 5.0 were used in the evaluation of particle stability in water and salt solutions, because of their more spherical shape as compared to the other pure and mixed microgels, respectively. The micrographs of the 3% (w/v) κ-carrageenan microgels dispersed in deionized water (Figure 3.6) showed that the particles were loosing their shape and seemed to swell during incubation. It was concluded that this type of microgel was not stable in deionized water because the leakage of the K^+ ions causing the disintegration of the gel.

| t = 0 | t = 5 min | t = 10 min | t = 20 min | t = 60 min |
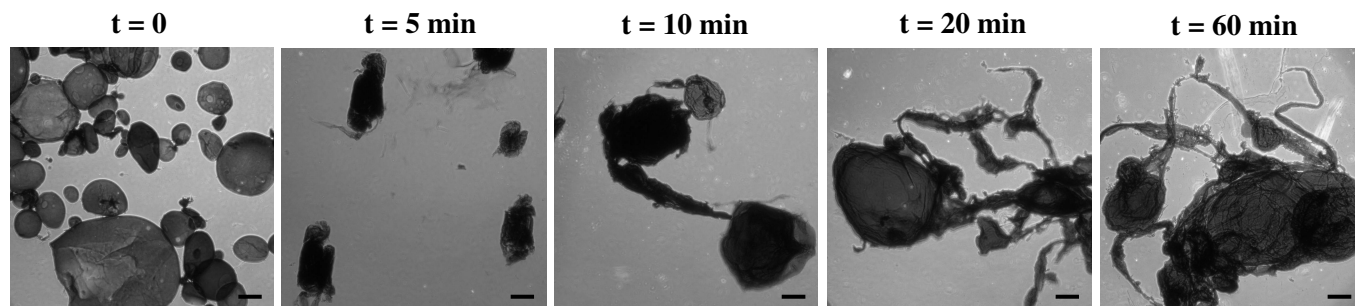
Figure 3.6. Evaluation of the stability of 3% (w/v) κ-carrageenan microgels dispersed in deionized water, where t is the time of incubation. Scale bar = 100 μm.

The evaluation of microgel stability in salt solutions was carried out using different concentrations of KCl (0.05%, 0.1%, 0.5%, 1%, 5% and 10%). Figure 3.7 shows the photos of pure (3% κ-carrageenan) and mixed (κ-carrageenan/Na-CN ratio of 5.0) microgels dispersed in the salt solutions after 1 hour of incubation, with the mean particle diameter (d_{32}). At salt concentrations up to 0.5% KCl, the microgels lost their shape and merged into each other. An increase in salt concentration (> 1% KCl) avoided the fusion of the particles, but they were still quite swollen and with an irregular shape. Only from KCl concentrations above 5%, the microgels became more spherical and at 10% KCl they were similar to the microgels with no dilution. A comparison of the values obtained for mean diameter indicated that an increase in KCl concentration led to a significant reduction in diameter of the microgels. Covalently cross-linked microgels of κ-carrageenan (ELLIS et al., 2009), alginate (MOE et al., 1993) and gellan gum (ANNAKA et al., 2000) showed the same tendency to increase the particle size with reduction in salt concentration, but the covalent bonds of the cross-linked microgels favored maintenance of the spherical shape. Thus, the

microgels probably lost their shape due to the higher affinity of KCl for the water, i.e., the salt that composed the microgel tended to migrate to the water, destabilizing the particles.

The difference in diameter of the microgels with salt concentration can be explained by the Donnan equilibrium, in which the difference in ionic concentration between the inside and outside of the microgel should be reduced when salt concentration in the surrounding medium is increased (ELLIS et al., 2009). At lower salt contents, the ion concentration inside the particles is higher than in the surrounding solution, so in order to minimize this disequilibrium, water penetrates into the microgels, making them swell. On the other hand, by increasing the salt concentration of the surrounding solution, the opposite effect occurs, leading to shrinkage of the particles (KEPPELER et al., 2009; ELLIS et al., 2009). Comparing the results obtained for the morphology and diameter of the microgels dispersed in different salt solutions, the 10% KCl solution was chosen as the dispersing medium for the study of suspension rheology (section 3.3.4).

| | 0.05% KCl | 0.1% KCl | 0.5% KCl | 1% KCl | 5% KCl | 10% KCl |

κ-carrageenan (3%)

κ-carrageenan / Na-CN (ratio 5.0)
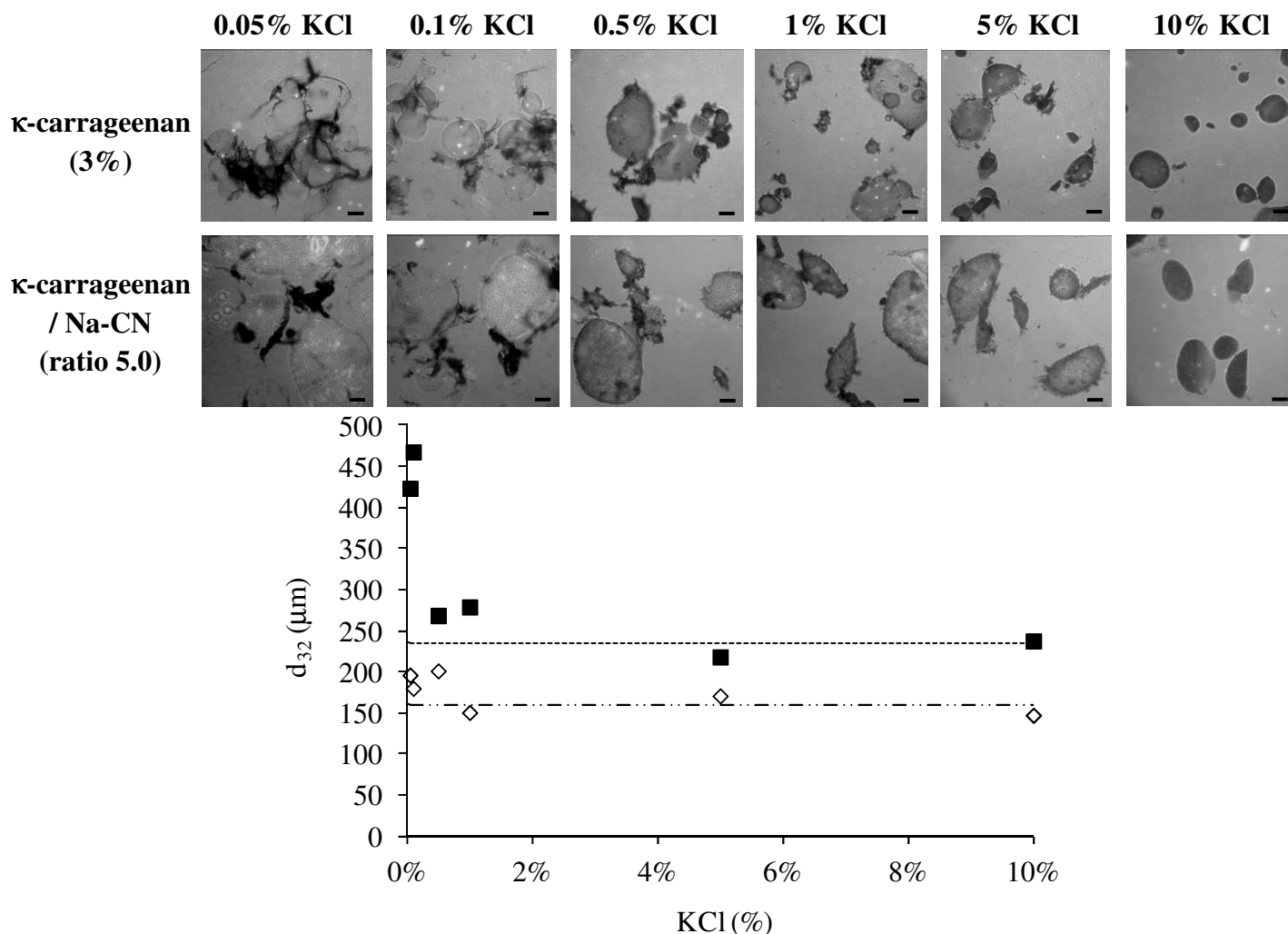
Figure 3.7. Micrographs and mean particle diameter (d_{32}) of the microgels dispersed in different salt solutions after 1 hour of incubation. Scale bar = 100 μm. Microgels of 3% κ-carrageenan ($\diamond$) dispersed in KCl solutions and (− − −) before dilution; microgels of κ-carrageenan/Na-CN ratio of 5.0 (■) dispersed in KCl solutions and (· · · ·) before dilution.

3.3.4. Evaluation of the rheology of the microgel suspensions

Figure 3.8 illustrates the flow curves of the microgels dispersed in 10% KCl solutions. The curves of the pure microgel (κ-carrageenan) suspensions fitted well the power law model, while those of the mixed microgels (κ-carrageenan – sodium caseinate)

were best fitted to the Herschel-Bulkley (HB) model (results not shown). The yield stress (σ_o) observed in the mixed suspensions indicated greater interaction between the microgels, probably leading to the formation of an interconnected structure (CHANNELL & ZUKOSKI, 1997). In addition, most of the samples did not show thixotropy, this behavior only being observed for the more concentrated suspensions (60%) of more irregular microgels (higher AR). Some curves could not be fitted to any rheological model (Figure 3.8), even after three sweeps of stress-shear rate performed to eliminate time dependence, and presented an overshoot characteristic of more complex structures. A particle network probably formed and reformed during the application of shear, which only occurred for the more concentrated suspensions of mixed microgels, especially with intermediate κ-carrageenan/Na-CN ratios. This can be explained by the morphology of the microgels (larger diameter and mainly irregular shape) (Table 3.3) and also by the interaction between protein and/or polysaccharide, favored at a ratio of 1.0.

The values for apparent viscosity at 50 s^{-1} were evaluated (Figure 3.9) in order to compare the behavior of the suspensions at a shear rate typical of chewing (STEFFE, 1996). In general, the suspensions of mixed microgels were more viscous than those composed of pure microgels, which could be mostly related to the shape of the particles, leading to a greater complexity of the interactions. Suspensions of irregular particles are frequently more viscous than those composed of spherical particles with the same volume fraction, which can be explained by the greater exclusion volume shown by non spherical particles, since they tend to rotate around an orbit when dispersed in solution (LINDSTRÖM & UESAKA, 2008).
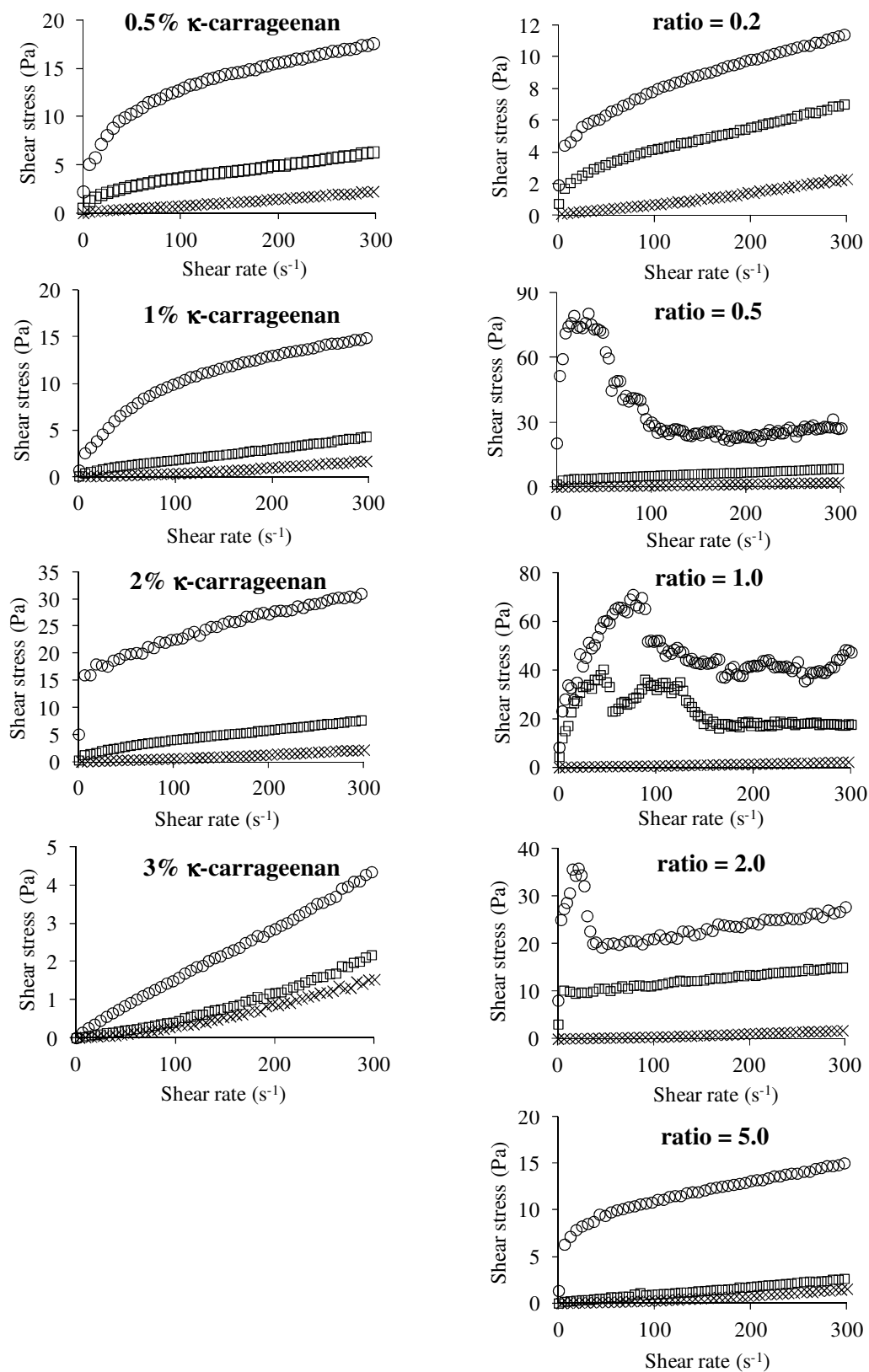
Figure 3.8. Flow curves of κ-carrageenan and κ-carrageenan/Na-CN microgel suspensions after elimination of time dependence. Volume fraction: (×) 20%, (□) 40% and (○) 60%.

An increase in volume fraction led to a reduction in the flow behavior index (increase in shear thinning behavior) (Figure 3.8) and an increase in suspension viscosity for all the systems studied (Figure 3.9). It is observed that the increase in shear rate in the dispersions with lower volume fraction led to greater interaction between the particles, causing an increase in dispersion viscosity or a shear-thickening behavior. As the volume fraction increased, higher shear rates led to orientation of the molecules in the direction of the flow and to breakage of the aggregates (BARNES et al., 1989) or a shear-thinning behavior. The influence of volume fraction on the rheological behavior of different suspensions was smaller for the systems containing 3% κ-carrageenan. This probably occurred because these microgels were more spherical (Table 3.3) than the others. On the other hand, the mixed microgel with a κ-carrageenan/Na-CN ratio of 1.0 was the system most influenced by the volume fraction (Figure 3.8), which can be explained by the combination of the irregular shape (aspect ratio >>1) (WOLF et al., 2001) and great diameter (Table 3.3), as well as by the electrostatic (repulsive or attractive) interactions between the caseinate and κ-carrageenan.
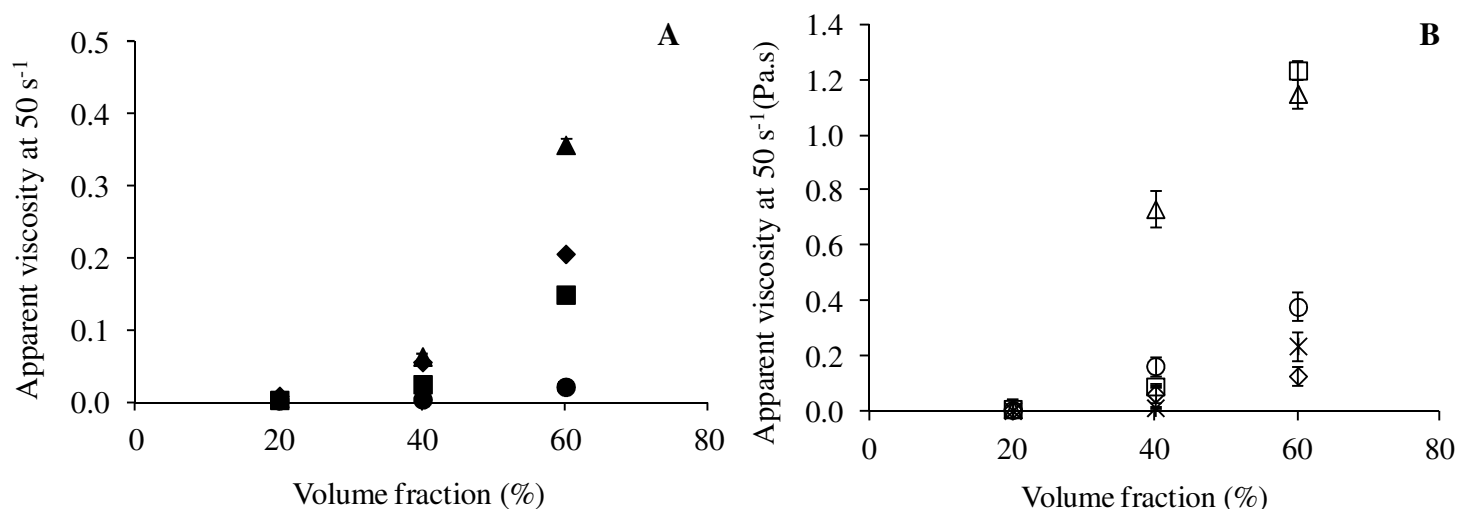
Figure 3.9. Apparent viscosity of κ-carrageenan and κ-carrageenan/Na-CN microgel suspensions at 50 s^{-1}. A) Pure microgels: (◆) 0.5%, (■) 1%, (▲) 2% and (●) 3% κ-carrageenan; and B) mixed microgels: (◇) 0.2, (□) 0.5, (△) 1.0, (○) 2.0 and (✳) 5.0 κ-carrageenan/Na-CN ratio.

3.4. CONCLUSIONS

This work evaluated the production of κ-carrageenan and κ-carrageenan – Na-CN microgels by extrusion, using potassium chloride for gelation. The results showed that an increase in air flow rate and decrease in feed flow rate and apparent viscosity promoted the formation of the smallest microgels, which was verified by the increase of some dimensionless numbers (Re$_{λl}$ and We$_l$). However, the aspect ratio of the particles was mainly influenced by the apparent viscosity and surface tension of the solutions, which was confirmed by the evaluation of Ohnesorge number (Oh). The biopolymer composition also influenced the microgel morphology, the mixed microgels (κ-carrageenan / Na-CN) being larger than the pure ones (κ-carrageenan), probably due to incompatibility between the

protein and polysaccharide and the slower gelation of mixed solutions. The microgels were very unstable when dispersed in water, but they maintained their shape when diluted in solutions with a high salt content (10% KCl). The wide range in size (d_{32} between ~84 μm and ~235 μm) and shape (AR between 1.33 and 1.9) of the microgels led to different rheological behavior of their suspensions, from shear thinning to shear thickening with the presence (or not) of yield stress, depending on the volume fraction of the particles.

3.5. ACKNOWLEDGMENTS

3.6. REFERENCES

ADAMS, S.; FRITH, W. J.; STOKES, J. R. Influence of particle modulus on the rheological properties of agar microgel suspensions. **Journal of Rheology**, v. 48, n. 6, p. 1195-1213, 2004.

ALISEDA, A.; HOPFINGER, E. J.; LASHERAS, J. C.; KREMER, D. M.; BERCHIELLI, A.; CONNOLLY, E. K. Atomization of viscous and non-newtonian liquids by a coaxial, high-speed gas jet. Experiments and droplet size modeling. **International Journal of Multiphase Flow**, v. 34, n. 2, p. 161-175, 2008.

ANNAKA, M.; OGATA, Y.; NAKAHIRA, T. Swelling behavior of covalently cross-linked gellan gels. **Journal of Physical Chemistry B**, v. 104, n. 29, p. 6755-6760, 2000.

ARLTOFT, D.; IPSEN, R.; MADSEN, F.; DE VRIES, J. Interactions between carrageenans and milk proteins: A microstructural and rheological study. **Biomacromolecules**, v. 8, n. 2, p. 729-736, 2007.

BARNES, H. A.; HUTTON, J. F.; WALTERS, K. **An introduction to rheology**. Elsevier Science Publishers: Amsterdam, 1989.

BELYAKOVA, L. E.; ANTIPOVA, A. S.; SEMENOVA, M. G.; DICKINSON, E.; MERINO, L. M.; TSAPKINA, E. N. Effect of sucrose on molecular and interaction parameters of sodium caseinate in aqueous solution: relationship to protein gelation. **Colloids and Surfaces B: Biointerfaces**, v. 31, n. 1-4, p. 31–46, 2003.

BLANDINO, A.; MACIAS, M.; CANTERO, D. Formation of calcium alginate gel capsules: Influence of sodium alginate and $CaCl_2$ concentration on gelation kinetics. **Journal of Bioscience and Bioengineering**, v. 88, n. 6, p. 686-689, 1999.

BOURRIOT, S.; GARNIER, C.; DOUBLIER, J. -L. Micellar-casein - κ-carrageenan mixtures. I. Phase separation and ultrastructure. **Carbohydrate Polymers**, v. 40, n. 2, p. 145-157, 1999.

BUREY, P.; BHANDARI, B. R.; HOWES, T.; GIDLEY, M. J. Hydrocolloid gel particles: formation, characterization, and application. **Critical Reviews in Food Science and Nutrition**, v. 48, n. 5, p. 361-377, 2008.

CHAN, E. –S.; LEE, B. –B.; RAVINDRA, P.; PONCELET, D. Prediction models for shape and size of ca-alginate macrobeads produced through extrusion-dripping method. **Journal of Colloid and Interface Science**, v. 338, n. 1, p. 63-72, 2009.

CHANNELL, G. M.; ZUKOSKI, C. F. Shear and compressive rheology of aggregated alumina suspensions. **AIChE Journal**, v. 43, n. 7, p. 1700-1708, 1997.

DALGLEISH, D. G.; MORRIS, E. R. Interactions between carrageenans and casein micelles: electrophoretic and hydrodynamic properties of the particles. **Food Hydrocolloids**, v. 2, n. 4, p. 311-320, 1988.

DE RUITER, G. A.; RUDOLPH, B. Carrageenan biotechnology. **Trends in Food Science & Technology**, v. 8, n. 12, p. 389-395, 1997.

ELLIS, A.; JACQUIER, J. C. Manufacture of food grade κ-carrageenan microspheres. **Journal of Food Engineering**, v. 94, n. 3-4, p. 316-320, 2009.

ELLIS, A.; KEPPELER, S.; JACQUIER, J. C. Responsiveness of κ-carrageenan microgels to cationic surfactants and neutral salts. **Carbohydrate Polymers**, v. 78, n. 3, p. 384-388, 2009.

HERRERO, E. P.; MARTÍN DEL VALLE, E. M.; GALÁN, M. A. Development of a new technology for the production of microcapsules based in atomization processes. **Chemical Engineering Journal**, v. 117, n. 2, p. 137-142, 2006.

HUNIK, J. H.; TRAMPER, J. Large-scale production of κ-carrageenan droplets for gel-bead production: theoretical and practical limitations of size and production rate. **Biotechnology Progress**, v. 9, n. 2, p. 186-192, 1993.

IMESON, A. P. Carrageenan. In: **Handbook of Hydrocolloids**. Phillips, G. O.; Williams, P. A. (Eds.), CRC Press: Boca Raton, 2000.

KEPPELER, S.; ELLIS, A.; JACQUIER, J. C. Cross-linked carrageenan beads for controlled release delivery systems. **Carbohydrate Polymers**, v. 78, n. 4, p. 973-977, 2009.

LAI, V. M. F.; WONG, P. A. –L.; LII, C. -Y. Effects of cation properties on sol-gel transition and gel properties of κ-carrageenan. **Journal of Food Science**, v. 65, n. 8, p. 1332-1337, 2000.

LANGENDORFF, V.; CUVELIER, G.; LAUNAY, B.; PARKER, A. Gelation and flocculation of casein micelle/carrageenan mixtures. **Food Hydrocolloids**, v. 11, n. 1, p. 35-40, 1997.

LEFEBVRE, A. H. **Atomization and sprays**. Taylor & Francis: New York, 1989.

LINDSTRÖM, S. B.; UESAKA, T. Simulation of semidilute suspensions of non-Brownian fibers in shear flow. **Journal of Chemical Physics**, v. 128, n. 2, p. 024901-1-024901-14, 2008.

MARTIN, A. H.; GOFF, H. D.; SMITH, A.; DALGLEISH, D. G. Immobilization of casein micelles for probing their structure and interactions with polysaccharides using scanning electron microscopy (SEM). **Food Hydrocolloids**, v. 20, n. 6, p. 817-824, 2006.

MCCLEMENTS, D. J. **Food emulsions: principles, practice and techniques**. CRC Press: New York, 2005.

MEUNIER, V.; NICOLAI, T.; DURAND, D. Structure of aggregating κ-carrageenan fractions studied by light scattering. **International Journal of Biological Macromolecules**, v. 28, n. 2, p. 157-165, 2001.

MOE, S. T.; SKJAK-BRAEK, G.; ELGSAETER, A.; SMIDSROED, O. Swelling of covalently crosslinked alginate gels: Influence of ionic solutes and nonpolar solvents. **Macromolecules**, v. 26, n. 14, p. 3589-3597, 1993.

MORRIS, E. R.; REES, D. A.; ROBINSON, G. Cation-specific aggregation of carrageenan helices: Domain model of polymer gel structure. **Journal of Molecular Biology**, v. 138, n. 2, p. 349-362, 1980.

NONO, M.; NICOLAI, T.; DURAND, D. Gel formation of mixtures of κ-carrageenan and sodium caseinate. **Food Hydrocolloids**, v. 25, n. 4, p. 750-757, 2011.

NÚÑEZ-SANTIAGO, M. C.; TECANTE, A. Rheological and calorimetric study of the sol-gel transition of κ-carrageenan. **Carbohydrate Polymers**, v. 69, n. 4, p. 763-773, 2007.

OAKENFULL, D.; MIYOSHI, E.; NISHINARI, K.; SCOTT, A. Rheological and thermal properties of milk gels formed with κ-carrageenan. I. Sodium caseinate. **Food Hydrocolloids**, v. 13, n. 6, p. 525-533, 1999.

PABST, W.; BERTHOLD, C.; GREGOROVÁ, E. Size and shape characterization of polydisperse short-fiber systems. **Journal of European Ceramic Society**, v. 26, n. 7, p. 1121-1130, 2006.

PONCELET, D.; LENCKI, R.; BEAULIEU, C.; HALLE, J. P.; NEUFELD, R. J.; FOURNIER, A. Production of alginate beads by emulsification/internal gelation. I. Methodology. **Applied Microbiology and Biotechnology**, v, 38, n. 1, p. 39-45, 1992.

REIS, C. P.; NEUFELD, R. J.; VILELA, S.; RIBEIRO, A. J.; VEIGA, F. Review and current status of emulsion/dispersion technology using an internal gelation process for the design of alginate particles. **Journal of Microencapsulation**, v. 23, n. 3, p. 245-257, 2006.

RIBEIRO, K. O.; RODRIGUES, M. I.; SABADINI, E.; CUNHA, R. L. Mechanical properties of acid sodium caseinate-κ-carrageenan gels: effect of co-solute addition. **Food Hydrocolloids**, v. 18, n. 1, p. 71-79, 2004.

RIZK, N. K.; LEFEBVRE, A. H. The influence of liquid film thickness on airblast atomization. **Journal of Engineering for Power**, v. 102, n. 7, p. 706-710, 1980.

SABADINI, E.; HUBINGER, M. D.; CUNHA, R. L. Stress relaxation of acid-induced milk gels. **Food and Bioprocess Technology**, p. 0342-4, 2010.

ŞEN, M.; ERBOZ, E. N. Determination of critical gelation conditions of κ-carrageenan by viscosimetric and FT-IR analyses. **Food Research International**, v. 43, n. 5, p. 1361-1364, 2010.

SMRDEL, P.; BOGATAJ, M.; ZEGA, A.; PLANINSEK, O.; MRHAR, A. Shape optimization and characterization of polysaccharide beads prepared by ionotropic gelation. **Journal of Microencapsulation**, v. 25, n. 2, p. 90-105, 2008.

STEFFE, J. F. **Rheological methods in food process engineering**. Freeman Press: East Lansing, 1996.

VARGA, C. M.; LASHERAS, J. C.; HOPFINGER, E. J. Initial breakup of a small-diameter liquid jet by a high-speed gas stream. **Journal of Fluid Mechanics**, v. 497, p. 405-434, 2003.

WOLF, B.; FRITH, W. J.; SINGLETON, S.; TASSIERI, M.; NORTON, I. T. Shear behavior of biopolymer suspensions with spheroidal and cylindrical particles. **Rheological Acta**, v. 40, p. 238-247, 2001.

ZHANG, J.; LI, X.; ZHANG, D.; XIU, Z. Theoretical and experimental investigations on the size of alginate microspheres prepared by dropping and spraying. **Journal of Microencapsulation**, v. 24, n. 4, p. 303-322, 2007.

CAPÍTULO 4. Produção de emulsões estabilizadas por complexos eletrostáticos Na-CN − κ-carragena

Stabilization of multilayered emulsions by sodium caseinate and κ-carrageenan

Perrechil, F. A. and Cunha, R. L.∗

Department of Food Engineering, Faculty of Food Engineering, University of Campinas

(UNICAMP), 13083-862 – Campinas, SP, Brazil.

∗ Corresponding author: Tel: +55-19-35214047; fax: +55-19-35214027;

e-mail: rosiane@fea.unicamp.br

ABSTRACT

The influence of κ-carrageenan concentration and pH on the stability, microstructure, droplet surface coverage, ζ-potential and rheological measurements of oil-in-water multilayered emulsions was studied. In a first step, the effect of concentration of sodium caseinate in the primary emulsion was evaluated. The emulsion composed by 20% (v/v) soybean oil and 0.5% (w/v) sodium caseinate was chosen to prepare the multilayered emulsions (or secondary emulsions) due to its high stability, good oil droplet coverage and low amount of free protein in solution. Secondary emulsions were then prepared by the mixture of primary emulsion with κ-carrageenan solutions with different concentrations. Emulsions were evaluated at pH 7 and 3.5. At pH 7, there was little adsorption of κ-carrageenan onto the droplet surface and depletion flocculation was observed when polysaccharide concentration exceeded 0.5% (w/v). At pH 3.5, a mixed κ-carrageenan – Na-CN second layer was formed around the protein-covered droplets and emulsions

showed bridging flocculation at lower polysaccharide concentrations (0.05 – 0.25% w/v) and oil droplets were completely covered from 0.5% (w/v) κ-carrageenan. Stable multilayered emulsions could be formed the highest κ-carrageenan concentration (1% w/v) in both pH values (7.0 and 3.5), which was attributed to the increase of the continuous phase viscosity, maintaining the emulsions kinetically stable. Thus, stable emulsions were successfully produced by using protein-polysaccharide interfacial complexes and the oil droplet diameter, zeta potential and rheological properties of these emulsions were not affected by pH changes.

Keywords: emulsion; protein; polysaccharide; bridging flocculation; depletion flocculation.

4.1. INTRODUCTION

Proteins extracted from a variety of natural sources have been extensively used due to their emulsifying properties (MCCLEMENTS, 2004) and because of the growing interest in the use natural emulsifiers (GARTI, 1999; GU et al., 2004; SURH et al., 2006). Nevertheless, the protein-stabilized emulsions are highly sensitive to environmental conditions, such as the pH, ionic strength and temperature (GU et al., 2004; PALLANDRE et al., 2007). For example, milk proteins provide good stability for emulsions at neutral pH due to a combination of electrostatic and steric stabilization mechanisms (DICKINSON et al., 1998). However, those emulsions become unstable when the pH is adjusted close to the isoelectric point of the adsorbed proteins because of the reduction in electrostatic repulsion between the droplets (MCCLEMENTS, 2005).

Many studies have demonstrated that the stability of emulsions to environmental conditions can be improved by the formation of protein-polysaccharide complexes through covalent bonding (KATO et al., 1992; OLIVER et al., 2006; O´REGAN & MULVIHILL, 2010) or electrostatic interactions (GU et al., 2004; GU et al., 2005; SURH et al., 2006; GUZEY & MCCLEMENTS, 2006; PALLANDRE et al., 2007). In the latter, multilayered interfacial membranes are formed around the droplets by the addition of a polysaccharide to an emulsion stabilized by an oppositely charged protein, being called layer-by-layer electrostatic deposition technique (GU et al., 2004; GU et al., 2005; SURH et al., 2006; PALLANDRE et al., 2007; GUZEY & MCCLEMENTS, 2006). A number of investigations have been done to produce multilayered emulsions using several proteins and polysaccharides, but to our knowledge there are no studies about emulsions stabilized by multilayered membranes composed by sodium caseinate and κ-carrageenan.

Sodium caseinate is an ingredient widely used due to its functional properties, which include emulsification, water and fat-binding, thickening and gelation (KINSELLA, 1984). This ingredient is a mixture of four caseins (α_{s1}-, α_{s2}-, β-, and κ-) that in aqueous solutions forms complexes and aggregates with a wide range of molecular weights (SINGH et al., 2003). κ-Carrageenan is a polysaccharide with a structure composed of repeating D-galactose and 3,6-anhydrogalactose (3,6 AG) units, both sulfated and non-sulfated, joined by alternating α-(1,3) and β-(1,4) glycosidic links (DE RUITER & RUDOLPH, 1997; IMESON, 2000). Even though it has long been known that κ-carrageenan can form complexes with casein micelles at neutral pH (LANGENDORFF et al., 1997; MARTIN et al., 2006; ARLTOFT et al., 2007), this phenomenon was not verified for κ-carrageenan and

sodium caseinate when the pH was just above the isoelectric point of protein (SINGH et al., 2003; MENA-CASANOVA et al., 2011).

Depending on the concentration of the ingredients in the emulsions, protein-coated droplets may be destabilized by bridging or depletion flocculation (GU et al., 2004). Bridging flocculation occurs when the polymer concentration is not enough to completely saturate the droplet surfaces, making the polymer chains able to adsorb onto the surfaces of two droplets (BERLI et al., 2002). On the other hand, in depletion flocculation, the presence of nonadsorbed molecules, such as the biopolymers, in the continuous phase of an emulsion causes an increase in the attractive forces between the droplets due to an osmotic effect associated with the exclusion of colloidal particles from a narrow region surrounding each droplet (MCCLEMENTS, 2005).

Thus, the objective of this work was to investigate the influence of pH and κ-carrageenan concentration on sodium caseinate-stabilized emulsions in order to improve the emulsion stability by interfacial complexation. For this purpose, mean droplet diameter, microstructure, droplet surface coverage, ζ-potential and rheological properties were evaluated.

4.2. MATERIAL AND METHODS

4.2.1. Materials

The ingredients used to prepare the emulsions were casein (Sigma-Aldrich Co., USA), κ-carrageenan gently supplied by CP Kelco (USA) and soybean oil (Bunge Alimentos S.A., Brazil).

4.2.2. Preparation of stock solutions

The sodium caseinate (Na-CN) stock solution (10% w/v) was prepared by dispersing casein in deionized water for 3 hours using a magnetic stirrer. The pH of the solution was constantly adjusted to 7.0 using 10 M NaOH. The polysaccharide stock solution (3% w/v) was prepared by dissolving κ-carrageenan powder in deionized water, followed by heat treatment at 90°C for 60 min under magnetic stirring and subsequent cooling to room temperature. The pH of κ-carrageenan solution was adjusted to 7.0 using HCl. The two solutions were then diluted at defined concentrations (section 4.2.3) in order to prepare the emulsions.

4.2.3. Preparation of emulsions

Primary oil-in-water (O/W) emulsions were prepared at 25°C by pre-mixing the soybean oil with a Na-CN aqueous solution using an Ultra Turrax model T18 (IKA, Germany) for 4 min at 14,000 rpm, followed by homogenization at 30 MPa / 5 MPa using a Panda 2K NS1001L double-stage homogenizer (Niro Soavi, Italy). The Na-CN concentration in the final emulsions varied between 0.25% and 3% (w/v), while the oil concentration was fixed at 20% (v/v).

Secondary O/W emulsions were prepared by mixing the primary emulsion containing 0.5% (w/v) Na-CN into κ-carrageenan solutions with different concentrations using magnetic stirring for 1 hour. The multilayered emulsions showed final composition of 10% (v/v) soybean oil, 0.25% (w/v) sodium caseinate and 0.05 – 1% (w/v) κ-carrageenan. The pH of part of these emulsions was adjusted to the value of 3.5 using 2 M HCl. Sodium azide (0.02% w/v) was added to all emulsions in order to prevent microbial growth.

4.2.4. Creaming stability measurements

Immediately after emulsion preparation, each sample was transferred into a 50 mL graduate cylindrical glass tube (internal diameter = 25 mm, height = 200 mm), sealed with a plastic cap and stored at room temperature during 7 days. The emulsion stability during storage was measured by checking the height of the serum layer (H) at the bottom of tube. The creaming index (CI) was reported as CI (%) = (H/H$_o$) × 100, where H$_o$ represents the initial height of the emulsion (KEOWMANEECHAI & MCCLEMENTS, 2002).

4.2.5. Optical microscopy

The microstructure of all emulsions was evaluated in the freshly prepared samples. For this, the emulsions were poured onto microscope slides, covered with glass cover slips and observed using a Scope.A1 microscope (Carl Zeiss, Germany) with a 100 × oil-immersion objective lens.

4.2.6. Confocal scanning laser microscopy (CSLM)

Fluorescein-5-isothiocyanate (FITC) had been used for the covalent labeling of κ-carrageenan, following the method described by Heilig et al. (2009). 20 mL dimethyl sulfoxide (DMSO) and 80 µL pyridine were mixed with 1 g κ-carrageenan and stirred at room temperature for 30 minutes. After the addition of 0.1 g FITC and 40 µL dibutyltin dilaurate, the mixture was incubated for 3 h in a 95°C water bath and, finally, cooled down to room temperature. The resulting gel was then minced, washed with ethanol 99.6% and dried at 65°C. The covalently labeled κ-carrageenan powder was dissolved and used to prepare the polysaccharide solution. Sodium caseinate solution was stained using a

fluorescent dye Rhodamine B. The protein and polysaccharide labeled solutions were then used to prepare the emulsions as described in the section 4.2.3. Samples were examined using a Zeiss LSM 780-NLO confocal on an Axio Observer Z.1 microscope (Carl Zeiss AG, Germany) with a 40 × objective. Images were collected using 488 and 543 nm laser lines for excitation of FITC and Rhodamine B fluorophores, respectively, with pinholes set to 1 airy unit for each channel, 1024×1024 image format.

4.2.7. Particle size analysis

Emulsions were diluted to a droplet concentration of approximately 0.005 wt % using deionized water and placed into the measurement chamber of the laser diffraction instrument (Mastersizer 2000, Malvern Instruments Ltd., UK). The size of oil droplets was determined as the volume-surface mean diameter ($d_{32} = \Sigma n_i d_i^3 / \Sigma n_i d_i^2$), where n_i is the number of droplets of diameter d_i. The particle size measurements were reported as the average and standard deviation of measurements made on freshly prepared samples, with three readings made per sample.

4.2.8. Chemical analyses of separated phases

The protein concentration of separated phases was determined by using the Kjeldahl method (AOAC, 1996), the water content was measured using gravimetric analysis and the polysaccharide concentration was measured using the phenol/sulfuric acid method (DUBOIS et al., 1956). The oil concentration was calculated by difference.

4.2.9. Determination of surface protein and polysaccharide concentrations

The surface concentration of protein and polysaccharide in the oil-in-water emulsions were determined using the method of Tangsuphoom and Coupland (2009) slightly modified. Emulsions were centrifuged at 14,000 × g for 40 min at 20°C. The cream phase was removed, resuspended in deionized water and centrifuged again under the same conditions. The resulting cream phase was carefully collected and filtered through Whatman # 1 filter paper. The protein and polysaccharide concentrations were determined as described in the section 4.2.8. Surface concentration of sodium caseinate and κ-carrageenan was calculated from the protein / polysaccharide content of the centrifuged cream phase (c) and the specific surface area of droplets (a) (Equation 4.1).

$$\Gamma = \frac{c}{a\phi} = \frac{c d_{32}}{6\phi} \tag{4.1}$$

where Γ is the surface polysaccharide (or protein) concentration (mg.m^{-2}), d_{32} is the volume-surface mean droplet diameter (µm), c is polysaccharide (or protein) concentration of the centrifuged cream phase (mg.mL^{-1} on wet basis), a is the specific surface area of the oil droplets (m^2/mL) and ϕ is the droplet volume fraction.

The concentration of non-adsorbed protein (C_{free}) was calculated from a mass balance of the protein of emulsion after centrifugation (Equation 4.2).

$$C_{free} = \frac{C_T \cdot V_T - C \cdot V}{V_s} \tag{4.2}$$

where C_T is the protein concentration in the initial emulsion (%), V_T is the volume of the initial emulsion (mL), V is the volume of the centrifuged cream phase (mL) and V_s is the volume of the serum phase after centrifugation (mL).

4.2.10. ζ-Potential measurements

To determine the electrical charge on the surface of oil droplets, freshly prepared emulsions were diluted to a droplet concentration of approximately 0.01 wt % using buffer solution (with the same pH as the sample being analysed) and placed into the measurement chamber of a microelectrophoresis instrument (Nano ZS Zetasizer, Malvern Instruments, UK). The measurements were made in quintuplicate.

The curve of ζ-potential versus polysaccharide concentration of the secondary emulsions can be fitted to a model (Equation 4.3) and used to determine the critical polysaccharide concentration to saturate the surface of droplets (PALLANDRE et al., 2007).

$$\frac{\zeta(c) - \zeta_{sat}}{\zeta_0 - \zeta_{sat}} = exp\left(-\frac{3c}{c_{sat}}\right) \tag{4.3}$$

where $\zeta(c)$ is the ζ-potential of the emulsion droplets covered with polysaccharide at concentration c (mV), ζ_0 is the ζ-potential in the absence of polysaccharide (mV), ζ_{sat} is the ζ-potential when the droplets are saturated with polysaccharide (mV) and c_{sat} is minimum amount of polysaccharide required to completely cover the surface of droplets (%).

In addition, the surface concentration at saturation (Γ_{sat}) can be calculated using Equation 4.4 (PALLANDRE et al., 2007).

$$\Gamma_{sat} = \frac{c_{sat}d_{32}}{6\phi} \tag{4.4}$$

4.2.11. Rheological measurements

The rheological measurements were carried out using a Physica MCR301 modular compact rheometer (Anton Paar, Austria). A 4 cm rough plate-plate geometry was used to analyze the O/W emulsions. Flow curves were obtained by an up-down-up step program

using a different shear stress range for each sample, in which the maximum shear rate value was 300 s^{-1}. Shear stress versus shear rate curves were fitted to power law model. All measurements were made in the freshly prepared emulsions in triplicate at 25°C.

4.3. RESULTS AND DISCUSSION

4.3.1. Primary Na-CN stabilized emulsions

The influence of Na-CN concentration on the mean droplet diameter (d_{32}) and the creaming index (CI) is shown in Figure 4.1. In a general way, the increase of protein concentration led a decrease of oil droplets up to 0.75% Na-CN and, above this protein concentration, the oil droplets maintained similar values of mean diameter. Similar results were reported by Srinivasan et al. (2000), that verified the decrease of d_{32} as the Na-CN concentration was increased from 0.5% to 1% and no further change in the droplet diameter with additional increase in caseinate concentration for a 30% (v/v) oil-in-water emulsions. Regarding the creaming index, emulsions containing lower amount of sodium caseinate (0.25 – 1% w/v) were very stable, with no phase separation after 7 days of storage (Figure 4.1). At 1.5% (w/v) Na-CN, an important creaming process took place, resulting in a CI of 75%. The instability of emulsions containing high concentrations of sodium caseinate has been attributed to depletion flocculation, which is mainly dependent on the amount of unadsorbed protein (DICKINSON & GOLDING, 1997). However, an additional increase of the protein concentration (2% until 3% w/v Na-CN) led to a reduction in the creaming index from 68.1 to 64.4%. This fact can be attributed to the formation of a network structure at higher Na-CN concentrations. The strength of the attractive depletion interaction is considerably stronger at these conditions, leading to a more restricted floc movement and the lower rate of reorganization (DICKINSON et al., 1997).

Na-CN (%)	CI (%)
0.25	0.0
0.5	0.0
0.75	0.0
1.0	0.0
1.5	75.0
2.0	68.1
2.5	66.0
3.0	64.4
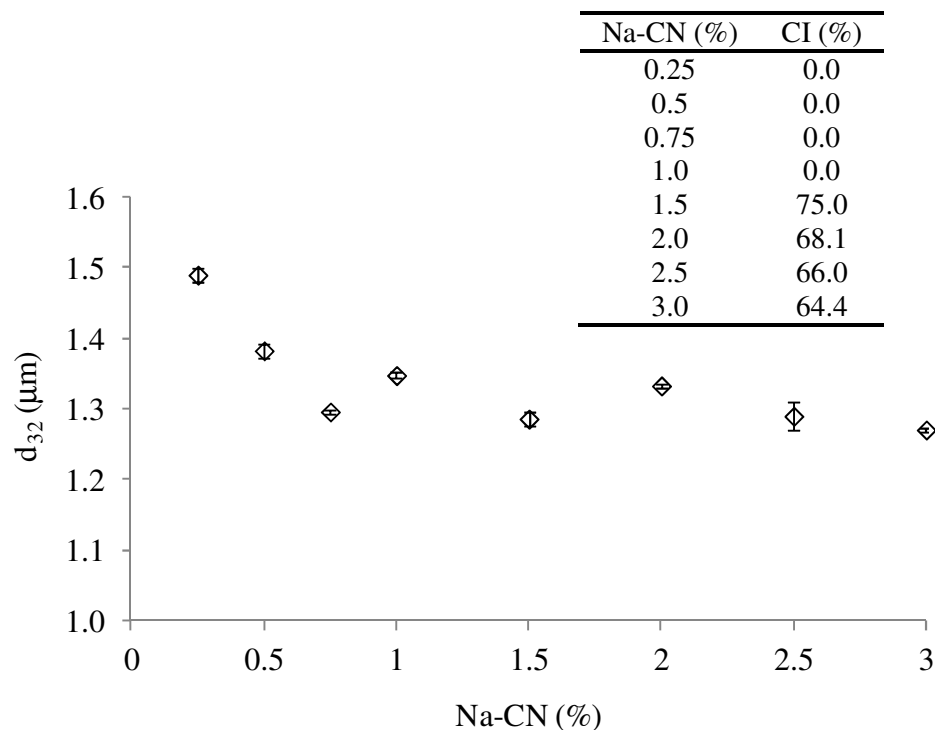
Figure 4.1. Influence of sodium caseinate concentration on the mean droplet diameter (d_{32}) and creaming index (CI) of oil-in-water emulsions.

In order to evaluate the depletion flocculation process in these emulsions, the protein surface concentration (Γ) and the concentration of unadsorbed protein (C_{free}) were quantified (Figure 4.2A). Protein surface concentration increased gradually with caseinate concentration up to 3% (w/v), as previously reported in other studies (SRINIVASAN et al., 1996; DICKINSON & GOLDING, 1997; SRINIVASAN et al., 1999). A surface concentration plateau at about 1 $mg.m^{-2}$ was observed for emulsions containing 0.5-1% (w/v) Na-CN. Srinivasan et al. (1996) attributed the plateau in their data to the saturated monolayer coverage of adsorbed casein molecules. The further increase in the protein surface concentration was attributed to the formation of a protein secondary layer at the interface.

The increase of the sodium caseinate content in the emulsions also led to an increase of the unadsorbed protein concentration (Figure 4.2A). Stable emulsions (Na-CN concentration up to 1% w/v) showed C_{free} between ~0.25 and 1.3% (Figure 4.2A), while higher concentrations of protein led to $C_{free} > $ ~2%, which was probably a concentration high enough to promote the depletion flocculation. The evaluation of Γ/C_{free} ratio (Figure 4.2B) showed three regions: 1) a plateau from 0.25% to 0.5% (w/v) Na-CN, 2) a region from 0.5% (w/v) to 1% (w/v) Na-CN of decrease of the Γ/C_{free} ratio and 3) a second plateau from 1.5% (w/v) Na-CN. The first region was attributed to the formation of protein monolayer around the droplets, the second one represented the saturation of monolayer and the third region can be related to the formation of the protein secondary layer at the interface. These data confirmed that the oil droplets were completely covered from 0.5% w/v Na-CN.
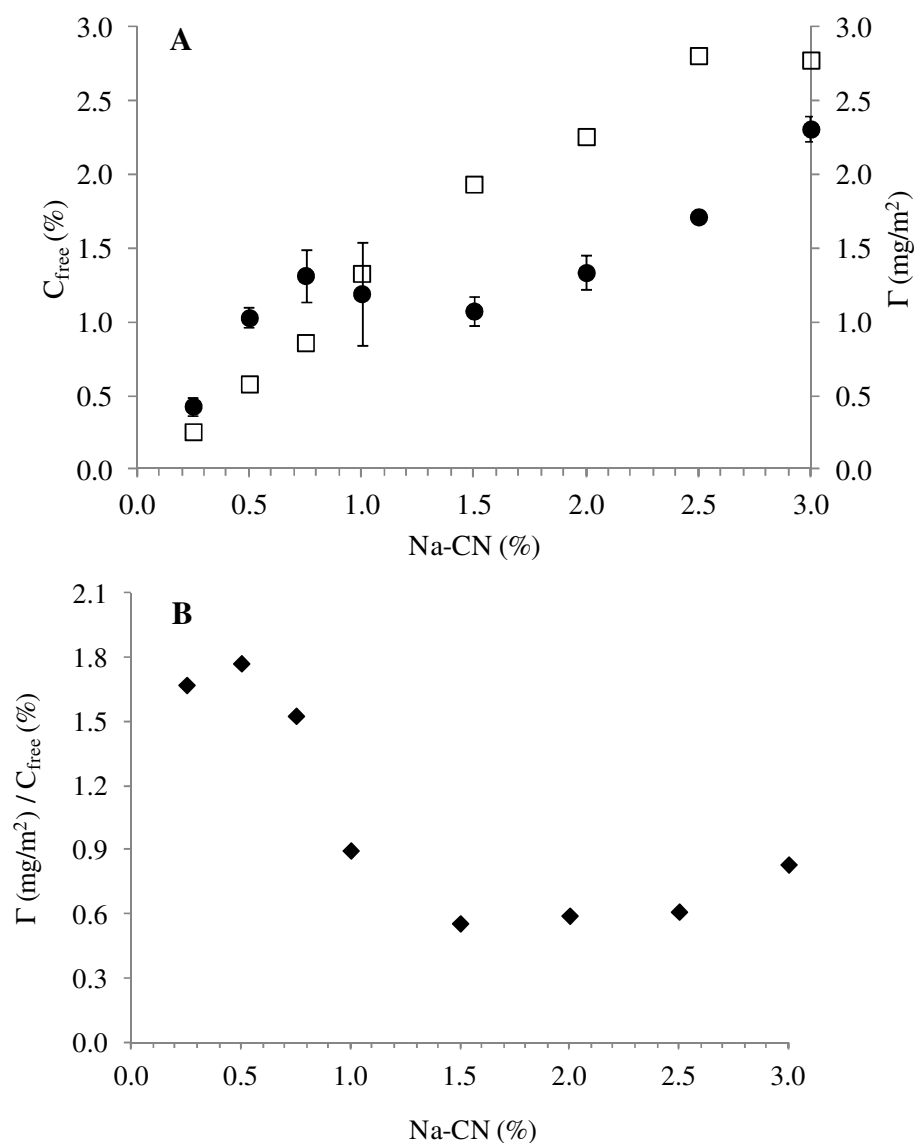
Figure 4.2. A) (●) Protein surface concentration (Γ) and (□) unadsorbed protein concentration (C_{free}) of O/W emulsions stabilized by sodium caseinate and B) ratio between Γ and C_{free}.

The primary emulsion containing 0.5% (w/v) Na-CN was very stable (Figure 4.1), its oil droplet surface was completely covered with protein and there was a rather low

amount of sodium caseinate free in the aqueous phase (Figure 4.2). Based on these results, this sample was chosen to produce the secondary emulsions containing κ-carrageenan.

4.3.2. Secondary Na-CN - κ-carrageenan emulsions

Figure 4.3 shows the visual appearance of secondary emulsions containing 0.25% (w/v) Na-CN and different amounts of κ-carrageenan at pH 7 and 3.5, produced from the mixture between the primary emulsion containing 0.5% (w/v) Na-CN and the κ-carrageenan solutions. At pH 7, the addition of low κ-carrageenan concentrations (0.05% and 0.1% w/v) caused the destabilization of the primary emulsion and generation of a cream top phase and a turbid serum bottom phase. Further increase of κ-carrageenan concentration to 0.25% (w/v) led to the formation of a translucent serum layer, indicating the increase of the instability of this emulsion (CHO & MCCLEMENTS, 2009). The translucent phase was attributed to the fast creaming of flocculated droplets (GU et al., 2004), resulting in a serum phase depleted of oil. These results were confirmed by the chemical composition of the separated phases (Table 4.1). In this case, the strength of the depletion attraction between the droplets increases with higher amount of polysaccharide in solution. In addition, κ-carrageenan and sodium caseinate tends to phase separate at neutral pH due to repulsive interactions between them (SINGH et al., 2003), especially at higher biopolymer concentrations. Nevertheless, stable emulsions were produced above 0.5% (w/v) κ-carrageenan, which can be attributed to the increase of viscosity of the continuous phase at higher κ-carrageenan concentrations, maintaining the emulsions kinetically stable. At lower κ-carrageenan concentrations (0.05% - 0.25% w/v), the viscosity of continuous phase was not sufficient to slow down the droplet movement, resulting in phase separation.

At pH 3.5, the addition of low amount of κ-carrageenan (0.05% and 0.1% w/v) also led to the destabilization of emulsions. However, the further addition of polysaccharide led to a decrease of the phase separation, resulting in a kinetically stable system at 1% (w/v) κ-carrageenan. The evaluation of chemical composition (Table 4.1) showed that the serum phase of unstable emulsions was oil free, indicating that the oil droplets were extensively flocculated at these conditions. In this case, probably there were insufficient polysaccharide molecules to completely cover the caseinate-coated droplets at low κ-carrageenan concentration, resulting in a bridging flocculation (PALLANDRE et al., 2007). With the increase of κ-carrageenan concentration, the flocculation was reduced due to the increased amount of polysaccharide adsorbed onto the droplet surfaces and the molecules free in solution caused an increase of viscosity.
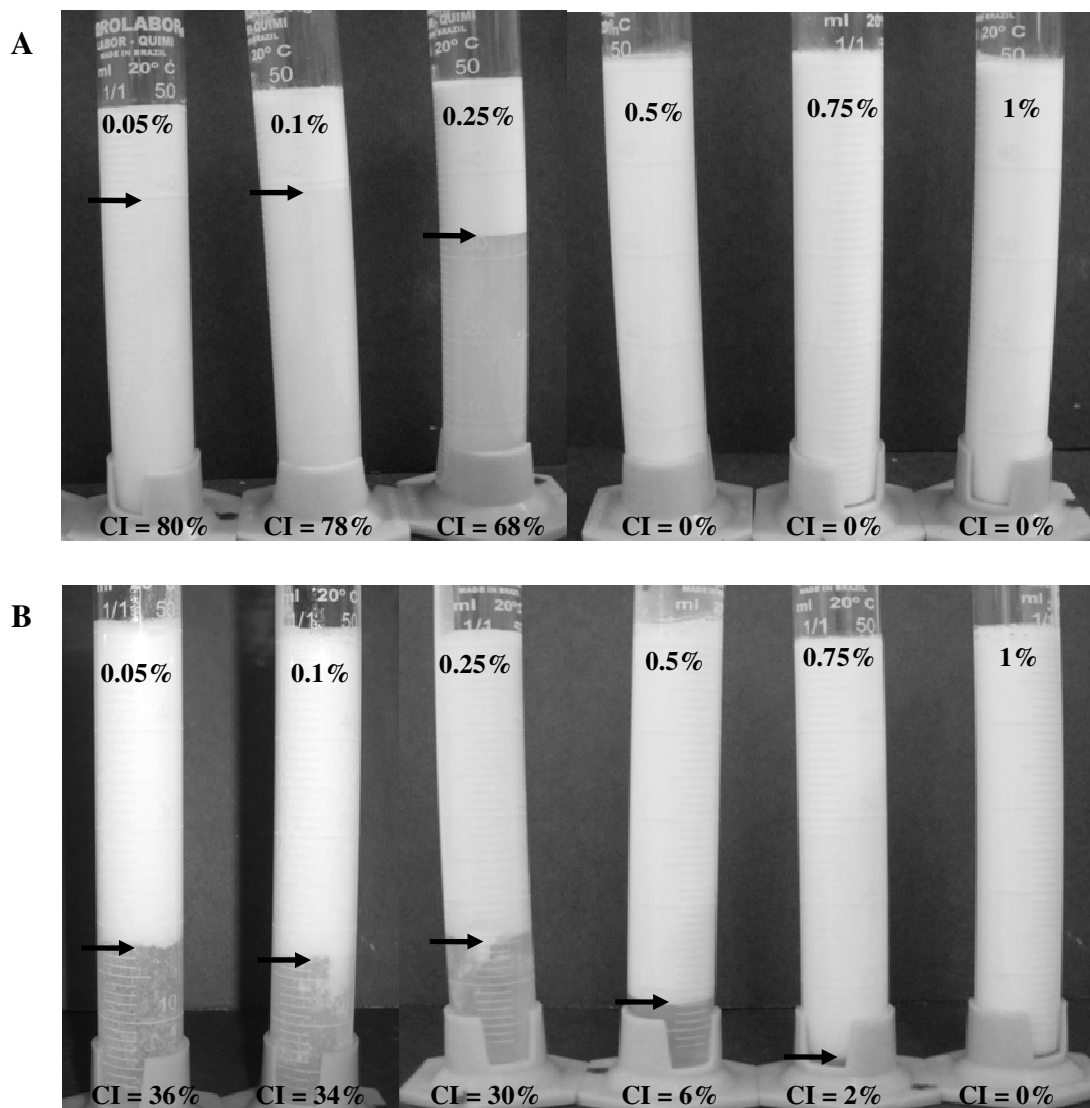
Figure 4.3. Visual appearance and creaming index (CI) of secondary oil-in-water emulsions containing 0.25% (w/v) Na-CN and different concentrations of κ-carrageenan after 7 days of storage. A) pH 7 and B) pH 3.5.

Table 4.1. Chemical composition of the separated phases of emulsions containing 0.25% (w/v) Na-CN, 10% (v/v) oil and different κ-carrageenan concentrations at pH 7 and 3.5

| | κ-carrageenan | Cream phase | | | Serum phase | | |
| | | PR | PS | Oil | PR | PS | Oil |
	(%)	(% w/w)	(% w/w)	(% w/w)	(% w/w)	(% w/w)	(% w/w)
	0.05%	0.56 ± 0.02	0.03 ± 0.00	42.3	0.22 ± 0.04	0.13 ± 0.01	2.4
pH 7	0.1%	0.58 ± 0.09	0.02 ± 0.00	41.8	0.18 ± 0.04	0.14 ± 0.02	0.8
	0.25%	0.60 ± 0.03	0.63 ± 0.02	33.3	0.16 ± 0.01	0.27 ± 0.01	0.06
	0.05%	0.29 ± 0.01	0.07 ± 0.01	15.6	0.07 ± 0.01	0.01 ±0.00	0.0
	0.1%	0.29 ± 0.03	0.13±0.01	15.2	0.11 ±0.01	0.05 ±0.01	0.0
pH 3.5	0.25%	0.31 ± 0.09	0.23 ±0.00	14.4	0.19 ±0.02	0.30 ± 0.02	0.0
	0.5%	0.36 ± 0.11	0.51 ±0.02	10.5	0.20 ±0.06	0.41 ± 0.03	0.0

PR = protein and PS = polysaccharide.

The evaluation of mean droplet diameter showed d_{32} around 1.6 µm for all emulsions produced at pH 7 (Figure 4.4A). On the other hand, the emulsions at pH 3.5 showed a marked reduction of d_{32} (from ~160 µm to 1.6 µm) with the increase of κ-carrageenan concentration (Figure 4.4B) due to the dissolution of droplet aggregates. The comparison of the mean droplet diameters at both pH values showed that d_{32} at pH 3.5 was greater than the one at pH 7 for most polysaccharide concentrations. However, d_{32} was very similar for samples with 1% (w/v) κ-carrageenan, which were stable emulsions.

A

B
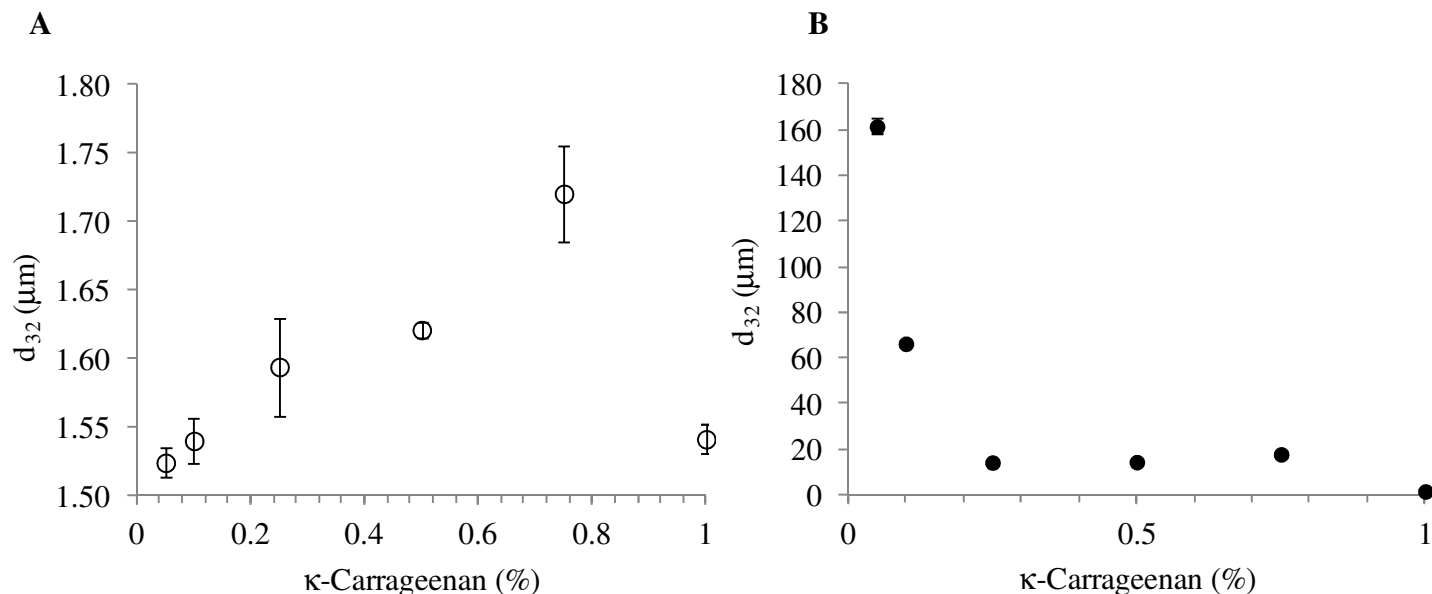
Figure 4.4. Mean droplet diameter (d_{32}) of O/W secondary emulsions containing 0.25% Na-CN and different concentration of κ-carrageenan (0.05%, 0.1%, 0.25%, 0.5%, 0.75% and 1%) at pH A) 7 and B) 3.5.

Figure 4.5 shows the confocal microscopy of emulsions containing 1% (w/v) κ-carrageenan at pH 7 (Figure 4.5A) and 3.5 (Figure 4.5B). In these images, the red areas indicate the presence of protein, while the green areas represent the polysaccharide. Sodium caseinate remained around the oil droplets for both emulsions, but it seemed to be more aggregated for emulsions at pH 3.5, which can be explained by the zeta potential of the pure protein at different pH values (ζ-potential at pH 7 = -39.1 mV and ζ-potential at pH 3.5 = + 25.8 mV). κ-Carrageenan was also concentrated around some droplets and the excess was homogeneously distributed in the continuous phase.
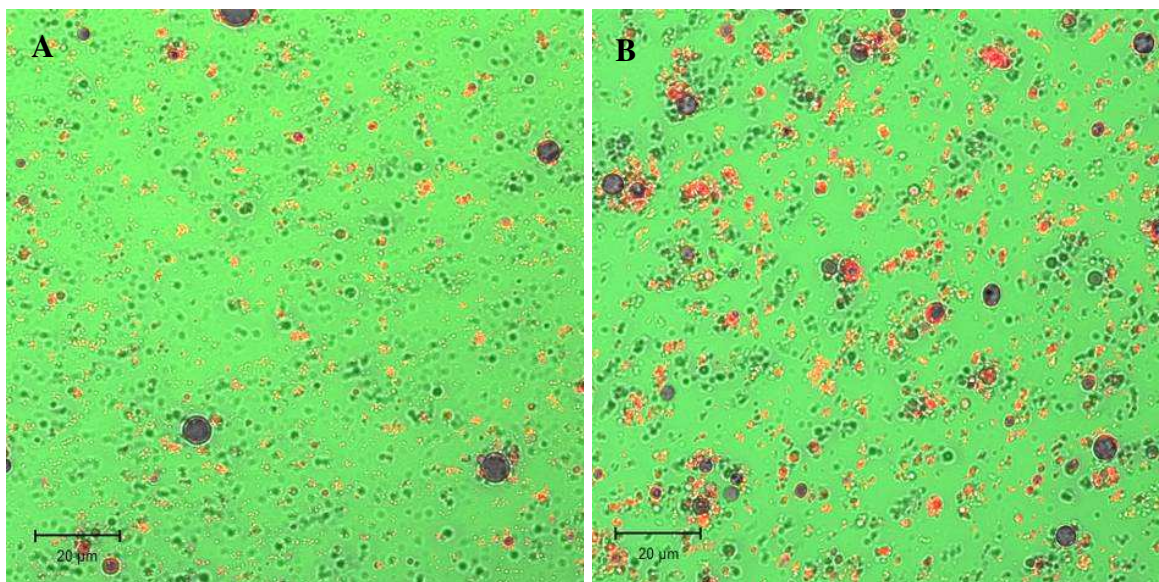
Figure 4.5. Confocal image of emulsions composed by 10% (v/v) soybean oil, 0.25% (w/v) Na-CN stained using Rhodamine B and 1% (w/v) κ-carrageenan stained by FITC at A) pH 7 and B) pH 3.5. Scale bar = 20 µm.

In order to evaluate the effect of κ-carrageenan on the coverage of oil droplet surfaces, the protein (Γ_{prot}) and polysaccharide (Γ_{polys}) surface concentrations were determined (Table 4.2). At pH 7, the addition of 0.05% (w/v) polysaccharide did not affect the value of Γ_{prot} (compare to Figure 4.2A). The further increase of κ-carrageenan concentration up to 0.5% (w/v) promoted the increase of Γ_{prot}, which can be explained by the incompatibility between the biopolymers, i.e., the protein in solution tended to migrate towards the oil surface. The decrease of Γ_{prot} above 0.5% (w/v) κ-carrageenan probably occurred due to the experimental difficulties that can be demonstrated by the standard deviation values (Table 4.2). Thus, there was a tendency to decrease the polysaccharide surface concentration in relation to protein surface concentration ($\Gamma_{polys}/ \Gamma_{prot}$), indicating the increase of free polysaccharide in solution favoring the depletion flocculation. At pH

3.5, the increase of κ-carrageenan concentration led to an increase of Γ_{polys} and $\Gamma_{polys}/\Gamma_{prot}$ (Table 4.2), indicating the increase of droplet coverage and the decrease of bridging flocculation. However, a direct comparison of the results obtained at the two different pH values (Table 4.2) reveals a significant increase of Γ_{prot} and Γ_{polys} for emulsions at pH 3.5 and low polysaccharide content. This behaviour suggests that a mixed protein-polysaccharide second layer was formed. This is typically the case of interfaces formed by complex coacervates or charged soluble complexes. The formation of soluble complexes was previously reported between whey proteins and λ-carrageenan (WEINBRECK et al., 2004) and between Na-CN and arabic gum (YE et al., 2006). Figure 4.6 shows that the emulsions containing polysaccharides had a negative zeta potential. Therefore, the soluble aggregates formed in the aqueous phase would be interacting with the Na-CN monolayer resulting in a mixed second layer. The proposed mechanism was based on the following thoughts. Carrageenan is one of the most negatively charged polysaccharide and, due to its high molecular weight, has a rather low diffusion coefficient. By adding the primary emulsion to the carrageenan solution one can infer that carrageenan molecules would first complex with the free Na-CN in solution rather than with the protein adsorbed at interface. Fewer patches may be available for complexation on the absorbed CN molecules due to restriction in their conformations at the interface when anchored to the droplet surface (JOURDAIN et al., 2008).

Table 4.2. Protein (Γ_{prot}) and polysaccharide (Γ_{polys}) surface concentration of multilayered emulsions containing sodium caseinate and κ-carrageenan

κ-Carrageenan (%)	pH 7			pH 3.5		
	Γ_{prot} (mg/m^2)	Γ_{polys} (mg/m^2)	$\Gamma_{polys}/\Gamma_{prot}$	Γ_{prot} (mg/m^2)	Γ_{polys} (mg/m^2)	$\Gamma_{polys}/\Gamma_{prot}$
0.05	0.96 ± 0.01	1.60 ± 0.52	1.68	4.48 ± 0.05	5.52 ± 0.47	1.23
0.1	1.34 ± 0.31	1.95 ± 0.15	1.45	3.38 ± 0.69	4.78 ± 0.05	1.41
0.25	3.20 ± 0.33	1.89 ± 0.34	0.59	2.19 ± 0.25	4.40 ± 0.06	2.01
0.5	7.05 ± 1.52	2.95 ± 0.19	0.42	3.39 ± 0.28	7.33 ± 0.11	2.16
0.75	5.74 ± 1.63	1.99 ± 0.29	0.35	2.82 ± 0.78	7.24 ± 0.24	2.57
1.0	2.25 ± 0.10	3.49 ± 1.18	1.55	2.79 ± 0.09	7.11 ± 0.34	2.55

The adsorption of κ-carrageenan to the Na-CN-coated droplets was also monitored using ζ-potential measurements (Figure 4.6). In the absence of κ-carrageenan, the ζ-potential of the droplets at pH 7 and 3.5 was -21.0 mV and +25.8 mV, respectively. That occurred because the sodium caseinate used to stabilize the droplets had a net positive charge below the isoelectric point (pI ~4.6) and a negative charge above the pI (SURH et al., 2006). Emulsions containing κ-carrageenan showed negatively charged droplets at both pH conditions. The increase of κ-carrageenan content led to even greater overall negative electrical charge. This change in the ζ-potential suggests the adsorption of polysaccharide to the oil droplets primarily coated by protein (CHO & MCCLEMENTS, 2009), especially at pH 3.5, when the sodium caseinate and κ-carrageenan have opposite charges.

Values of ζ_{sat} = -32.8 mV, c_{sat} = 0.39 % κ-carrageenan and Γ_{sat} = 10.7 mg/m^2 were obtained through Equations 4.3 and 4.4 for emulsions at pH 3.5. Comparing ζ_{sat} with ζ-potential obtained experimentally it is possible to conclude that the oil surfaces were

completely covered from ~0.5% (w/v) κ-carrageenan, when Γ_{polys} was approximately constant, although Γ_{sat} was little higher than Γ_{polys} experimentally obtained. The model proposed by Pallandre et al. (2007) could not be employed for emulsions at pH 7 because there was a small adsorption of polysaccharide to the protein-coated droplets since both are negatively charged. Thus, the ζ-potential values showed little variation with addition of polysaccharide because most of the κ-carrageenan added to the emulsion remained free in the continuous phase, confirming the assumption of depletion flocculation at higher polysaccharide concentrations.
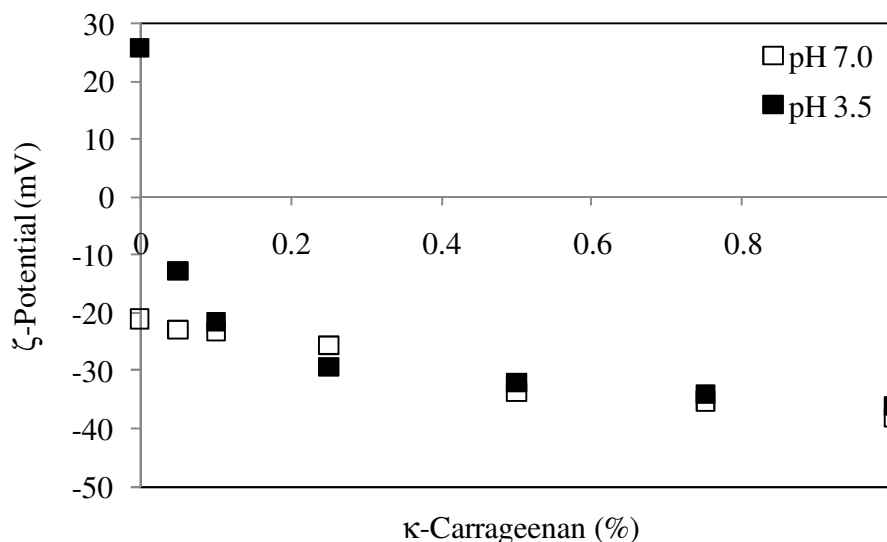
Figure 4.6. Influence of κ-carrageenan concentration on the ζ-potential of O/W emulsions stabilized by sodium caseinate at pH 7 and pH 3.5.

Figure 4.7 shows the effect of κ-carrageenan concentration on the rheological properties of O/W emulsions stabilized by sodium caseinate. Emulsion with low polysaccharide concentration (0.05% w/v) at pH 7 showed behavior close to the Newtonian (n = 0.92) and the increase of κ-carrageenan concentration turned the emulsions more

pseudoplastic (Figure 4.7A). On the other hand, emulsions at pH 3.5 with low κ-carrageenan concentration (0.05 and 0.1% w/v) could not be fitted to any rheological model and showed an overshoot characteristic of more complex structures (results not shown). This can be explained by the high attraction of protein-coated droplets at pH close to pI resulting in a droplet network similar to emulsions without κ-carrageenan at pH 3.7 (PERRECHIL & CUNHA, 2010). The increase of polysaccharide concentration at pH 3.5 led to an increase in the flow behavior index (n) from ~0.6 (0.25% w/v κ-carrageenan) to ~0.8 (0.5-1% w/v κ-carrageenan) (Figure 4.7A). Apparent viscosity at 100 s^{-1} of emulsions at pH 7 increased with κ-carrageenan concentration due to the higher polysaccharide free in solution and depletion flocculation. On the other hand, emulsions became less viscous at pH 3.5 up to 0.5% (w/v) κ-carrageenan, which can be explained by the dissolution of droplet aggregates, followed by a slight increase of η_{100s}^{-1} from 0.5% to 1% (w/v) κ-carrageenan due to the presence of free polysaccharide in solution, since the droplet surface was saturated at 0.5% (w/v) κ-carrageenan. Emulsions containing 0.5, 0.75 and 1% (w/v) κ-carrageenan showed the same flow behavior index and apparent viscosity independently on the pH value.

In summary, sodium caseinate and κ-carrageenan were both negatively charged and incompatible at pH 7, resulting in weak adsorption of polysaccharide onto the protein-coated oil droplets. Thus, polysaccharide remained in the continuous phase, promoting the depletion flocculation process and the increase of emulsion viscosity. The competition between these two processes determined the degree of emulsion stability. On the other hand, sodium caseinate and κ-carrageenan were oppositely charged at pH 3.5, which favored the adsorption of κ-carrageenan onto the Na-CN-coated oil droplets. At low

polysaccharide content, the interfaces were not saturated and the emulsions were unstable due to bridging flocculation. As the content of κ-carrageenan increased, the oil droplets became completely coated resulting in electrostatic and steric repulsion between them. The further addition of polysaccharide increased the amount of κ-carrageenan free in the aqueous phase, promoting the increase of emulsion viscosity.
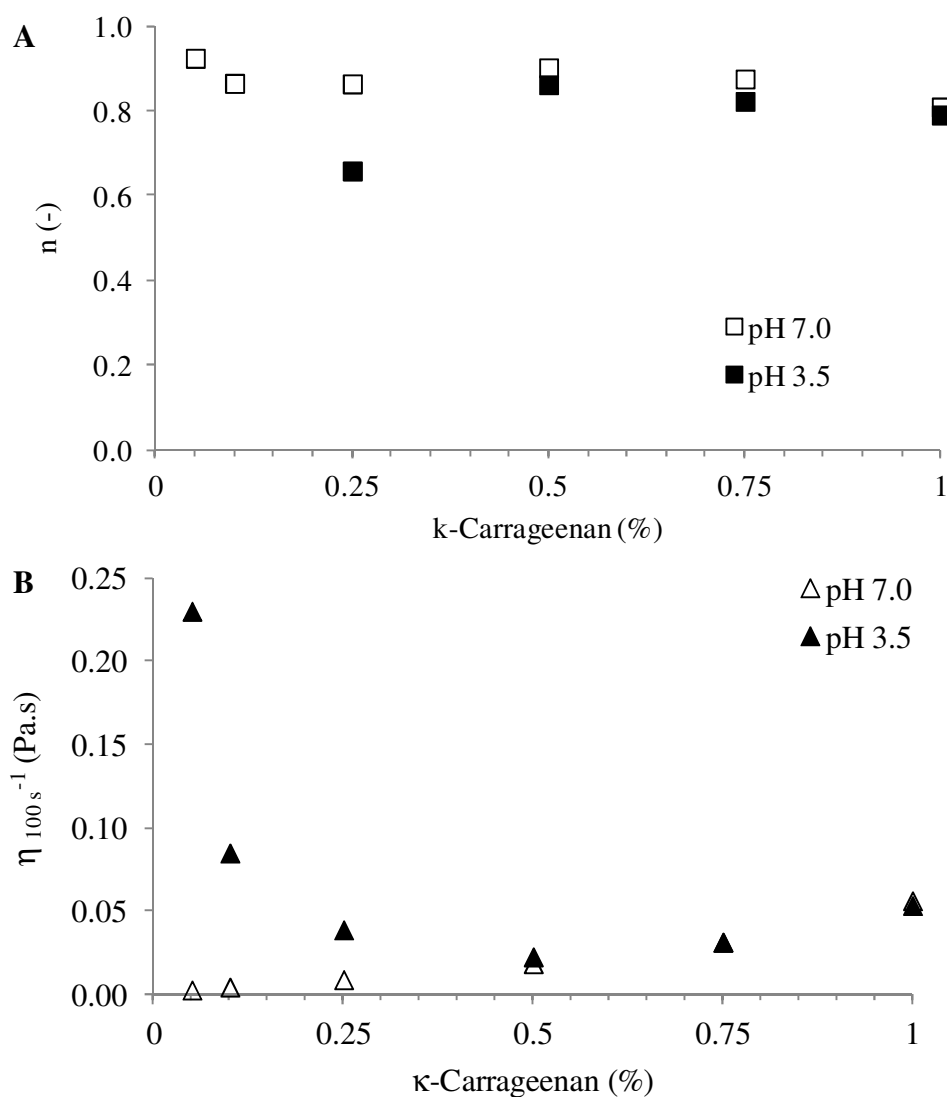
Figure 4.7. Rheological behavior of O/W emulsions stabilized by sodium caseinate and κ-carrageenan at pH 7 and pH 3.5. A) Flow behavior index (n) and B) apparent viscosity at 100 s^{-1} (η_{100s}^{-1}).

4.4. CONCLUSIONS

The addition of low amount of κ-carrageenan led to unstable emulsions, independent on the pH of system. Nevertheless, the increase of κ-carrageenan concentration promoted the stabilization of emulsions at both pH values 7 and 3.5 due to the increase of the viscosity of the continuous phase that slowed down the movement of flocs and droplets. However, the κ-carrageenan was weakly adsorbed onto the droplet surfaces at pH 7 and the increase of polysaccharide content promoted the depletion flocculation. On the other hand, a strong adsorption of κ-carrageenan and protein was verified at pH 3.5. At this condition, emulsions showed bridging flocculation at lower polysaccharide concentration and the formation of a mixed protein-polysaccharide layer around the Na-CN-coated droplets with further addition of κ-carrageenan, which collaborated to improve the stability of these systems. In addition, the aggregation of protein at pH 3.5 probably contributed to the destabilization of emulsions when compared to those at pH 7. Multilayered emulsion containing 1% (w/v) κ-carrageenan was highly stable and showed similar values of d_{32}, ζ-potential and rheological properties for both pH values. Thus, it can be concluded that the production of sodium caseinate:κ-carrageenan electrostatic complexes can improve the stability of emulsions against the environmental stresses, like pH values around the isoelectric point of protein.

4.5. ACKNOWLEDGEMENTS

4.6. REFERENCES

AOAC. **Official Method of Analysis** (16th ed.). Association of Official Analytical Chemists: Washington, 1996.

ARLTOFT, D.; IPSEN, R.; MADSEN, F.; DE VRIES, J. Interactions between carrageenans and milk proteins: A microstructural and rheological study. **Biomacromolecules**, v. 8, n. 2, p. 729-736, 2007.

BERLI, C. L. A.; QUEMADA, D.; PARKER, A. Modelling the viscosity of depletion flocculated emulsions. **Colloids and Surfaces A: Physicochemical and Engineering Aspects**, v. 203, p. 11-20, 2002.

CHO, Y. -H.; MCCLEMENTS, D. J. Theoretical stability maps for guiding preparation of emulsions stabilized by protein-polysaccharide interfacial complexes. **Langmuir**, v. 25, n. 12, p. 6649-6657, 2009.

DE RUITER, G. A.; RUDOLPH, B. Carrageenan biotechnology. **Trends in Food Science & Technology**, v. 8, n. 12, p. 389-395, 1997.

DICKINSON, E.; GOLDING, M. Depletion flocculation of emulsions containing unadsorbed sodium caseinate. **Food Hydrocolloids**, v. 11, n. 1, p. 13-18, 1997.

DICKINSON, E.; GOLDING, M.; POVEY, M. J. W. Creaming and flocculation of oil-in-water emulsions containing sodium caseinate. **Journal of Colloid and Interface Science**, v. 185, n. 2, p. 515-529, 1997.

DICKINSON, E.; SEMENOVA, M. G.; ANTIPOVA, A. S. Salt stability of casein emulsions. **Food Hydrocolloids**, v. 12, n. 2, p. 227-235, 1998.

DUBOIS, M.; GILLES, K. A.; HAMILTON, J. K.; REBERS, P. A.; SMITH, F. Colorimetric method for determination of sugar and related substances. **Analytical Chemistry**, v. 28, n. 3, p. 350-356, 1956.

GARTI, N. What can nature offer from an emulsifier point of view: trends and progress? **Colloids and Surfaces A: Physicochemical and Engineering Aspects**, v. 152, n. 1, p. 125–146, 1999.

GU, Y. S.; DECKER, E. A.; MCCLEMENTS, D. J. Influence of pH and ι-carrageenan concentration on physicochemical properties and stability of β-lactoglobulin-stabilized oil-in-water emulsions. **Journal of Agricultural and Food Chemistry**, v. 52, n. 11, p. 3626-3632, 2004.

GU, Y. S.; DECKER, E. A.; MCCLEMENTS, D. J. Influence of pH and carrageenan type on properties of β-lactoglobulin stabilized oil-in-water emulsions. **Food Hydrocolloids**, v. 19, n. 1, p. 83-91, 2005.

GUZEY, D.; MCCLEMENTS, D. J. Formation, stability and properties of multilayer emulsions for application in the food industry. **Advances in Colloid and Interface Science**, v. 128-130, p. 227-248, 2006.

HEILIG, A.; GÖGGERLE, A.; HINRICHS, J. Multiphase visualization of fat containing β-lactoglobulin - κ-carrageenan gels by confocal scanning laser microscopy, using a novel dye, V03-01136, for fat staining. **LWT – Food Science and Technology**, v. 42, n. 2, p. 646-653, 2009.

IMESON, A. P. **Carrageenan**. In: Handbook of Hydrocolloids. Phillips, G. O.; Williams, P. A. (Eds.), CRC Press: Boca Raton, 2000.

JOURDAIN, L.; LESER, M. E.; SCHMITT, C.; MICHEL, M.; DICKINSON, E. Stability of emulsions containing sodium caseinate and dextran sulfate: Relationship to complexation in solution. **Food Hydrocolloids**, v. 22, n. 4, p. 647-659, 2008.

KATO, A.; MIFURU, R.; MATSUDOMI, N.; KOBAYASHI, K. Functional casein-polysaccharide conjugates prepared by controlled dry heating. **Bioscience, Biotechnology, and Biochemistry**, v. 56, n. 4, p. 567-571, 1992.

KEOWMANEECHAI, E., MCCLEMENTS, D. J. Influence of EDTA and citrate on physicochemical properties of whey protein-stabilized oil-in-water emulsions containing $CaCl_2$. **Journal of Agricultural and Food Chemistry**, v. 50, n. 24, p. 7145-7153, 2002.

KINSELLA, J. E. Milk proteins: physicochemical and functional properties. **Critical Reviews in Food Science and Nutrition**, v. 21, n. 3, p. 197-262, 1984.

LANGENDORFF, V.; CUVELIER, G.; LAUNAY, B.; PARKER, A. Gelation and flocculation of casein micelle/carrageenan mixtures. **Food Hydrocolloids**, v. 11, n. 1, p. 35-40, 1997.

MARTIN, A. H.; GOFF, H. D.; SMITH, A.; DALGLEISH, D. G. Immobilization of casein micelles for probing their structure and interactions with polysaccharides using scanning electron microscopy (SEM). **Food Hydrocolloids**, v. 20, n. 6, p. 817-824, 2006.

MCCLEMENTS, D. J. **Food emulsions: principles, practice and techniques**. CRC Press: New York, 2005.

MCCLEMENTS, D. J. Protein-stabilized emulsions. **Current Opinion in Colloid & Interface Science**, v. 9, n. 5, p. 305-313, 2004.

MENA-CASANOVA, E.; TOTOSAUS, A. Improvement of emulsifying properties of milk proteins with κ or λ carrageenan: effect of pH and ionic strength. **International Journal of Food Science and Technology**, v. 46, n. 3, p. 535-541, 2011.

O'REGAN, J.; MULVIHILL, D. M. Heat stability and freeze–thaw stability of oil-in-water emulsions stabilized by sodium caseinate–maltodextrin conjugates. **Food Chemistry**, v. 119, n. 1, p. 182–190, 2010.

OLIVER, C. M.; MELTON, L. D.; STANLEY, R. A. Creating proteins with a novel functionality via the Maillard Reaction: A review. **Critical Reviews in food Science and Nutrition**, v. 46, n. 4, p. 337-350, 2006.

PALLANDRE, S.; DECKER, E. A.; MCCLEMENTS, D. J. Improvement of stability of oil-in-water emulsions containing caseinate-coated droplet by addition of sodium alginate. **Journal of Food Science**, v. 72, n. 9, p. E518-E524, 2007.

PERRECHIL, F. A.; CUNHA, R. L. Oil-in-water emulsions stabilized by sodium caseinate: Influence of pH, high-pressure homogenization and locust bean gum addition. **Journal of Food Engineering**, v. 97, n. 4, p. 441-448, 2010.

SINGH, H.; TAMEHANA, M.; HEMAR, Y.; MUNRO, P. A. Interfacial compositions, microstructures and properties of oil-in-water emulsions formed with mixtures of milk proteins and κ-carrageenan: 1. Sodium caseinate. **Food Hydrocolloids**, v. 17, n.4, p. 539-548, 2003.

SRINIVASAN, M.; SINGH, H.; MUNRO, P. A. Adsorption behaviour of sodium and calcium caseinates in oil-in-water emulsions. **International Dairy Journal**, v. 9, n. 3-6, p. 337-341, 1999.

SRINIVASAN, M.; SINGH, H.; MUNRO, P. A. Sodium caseinate-stabilized emulsions: factors affecting coverage and composition of surface proteins. **Journal of Agriculture and Food Chemistry**, v. 44, n. 12, p. 3807-3811, 1996.

SRINIVASAN, M.; SINGH, H.; MUNRO, P. A. The effect of sodium chloride on the formation and stability of sodium caseinate emulsions. **Food Hydrocolloids**, v. 14, n. 5, p. 497-507, 2000.

SURH, J.; DECKER, E. A.; MCCLEMENTS, D. J. Influence of pH and pectin type on properties and stability of sodium-caseinate stabilized oil-in-water emulsions. **Food Hydrocolloids**, v. 20, n. 5, p. 607-618, 2006.

TANGSUPHOOM, N.; COUPLAND, J. N. Effect of surface-active stabilizers on the surface properties of coconut milk emulsions. **Food Hydrocolloids**, v. 23, n. 7, p. 1801-1809, 2009.

WEINBRECK, F.; NIEUWENHUIJSE, H; ROBIJN, G. W.; DE KRUIF, C. G. Complexation of whey proteins with carrageenan. **Journal of Agricultural and Food Chemistry**, v. 52, n. 11, p. 3550-3555, 2004.

YE, A. Q.; FLANAGAN, J.; SINGH, H. Formation of stable nanoparticles via electrostatic complexation between sodium caseinate and gum arabic. **Biopolymers**, v. 82, n. 2, p. 121-133, 2006.

CAPÍTULO 5.   Desenvolvimento de microesferas de Na-CN – κ-carragena para encapsulação de compostos hidrofóbicos

Development of Na-CN - κ-carrageenan microbeads for encapsulation of lipophilic compounds

Perrechil, F. A.; Vilela, J. A. P.; Guerreiro, L. M. R. and Cunha, R. L.∗

Department of Food Engineering, Faculty of Food Engineering, University of Campinas (UNICAMP), 13083-862 – Campinas, SP, Brazil.

∗ Corresponding author: Tel: +55-19-35214047; fax: +55-19-35214027;

e-mail: rosiane@fea.unicamp.br

ABSTRACT

Ionotropic gelation of emulsions composed by sodium caseinate and κ-carrageenan at pH 7 and 3.5 was evaluated to encapsulate soybean oil. The influence of some process variables of extrusion process (nozzle diameter of fluid exit and collecting distance) on the production of microbeads was studied, as well as the stability of these microbeads. The fluid nozzle diameter showed little influence on the shape of microbeads, with a slight tendency to decrease the microbead diameter with the increase of fluid nozzle diameter. On the other hand, the collecting distance strongly influenced the shape of microbeads and they became more spherical (aspect ratio was reduced from ~2.0 to ~1.4) as the collecting distance was increased from 10 cm to 50 cm. The pH of emulsions did not affect the aspect ratio of microbeads, but the diameter was greater for microbeads produced at pH 3.5. This difference was attributed to the kind of interactions between κ-carrageenan and sodium caseinate at these distinct pHs. While the protein was predominant at the external surface

and the gelled polysaccharide in the internal region of microbeads at pH 7, a thicker double-layer of protein-polysaccharide was observed at pH 3.5. The microbeads were highly unstable when dispersed in deionized water, sugar solutions and low concentrations of salt, releasing the encapsulated oil. However, no release of oil from microbeads was observed when they were dispersed in ethanol or potassium chloride solutions with concentration above 0.75%, although they have modified their shape when dispersed in ethanol. In general, the obtained results demonstrated the viability of the extrusion process to produce biopolymers-based microbeads and the potential application of these systems.

Keywords: extrusion; ionic gelation; microscopy; particle size distribution; emulsion

5.1. INTRODUCTION

Microbeads have been largely employed for the encapsulation of hydrophilic and amphiphilic compounds such as peptides (CHANDY et al., 1998), enzymes (AZARNIA et al., 2008), proteins (VANDENBERG et al., 2001) and probiotics (ALBERTINI et al., 2010; CORBO et al., 2011). Polysaccharides are the ingredients commonly used to prepare the microbeads due to their good biocompatibility, biodegradability, low toxicity, abundance in nature and low cost (KAIHARA et al., 2011; KAREWICZ et al., 2011). There has been growing interest in the development of delivery systems to encapsulate lipophilic components, such as vitamins, oils, flavors, colors and nutraceuticals, for high moisture applications (MATALANIS et al., 2011). For this purpose, encapsulation systems with amphiphilic properties should be employed (COLINET et al., 2010).

Oils are generally encapsulated by the spray-drying method, using carbohydrates, proteins and gums as wall materials (CHAN, 2011). However, most of products show high water activity, which would cause the dissolution of the dried microcapsules. In this

context, the gelled beads have the advantage of being used in hydrated media without breaking down (BUREY et al., 2008). Among the methods used to prepare the microbeads, the extrusion technique followed by an ionotropic gelation is extensively used, since it is considered simple (CORBO et al., 2011). In this case, droplets are formed by the use of a syringe or an atomizer (pressure nozzle) and collected in a hardening solution containing a gelling agent (HUNIK & TRAMPER, 1993, BLANDINO et al., 1999).

The first step of oil encapsulation process normally includes the emulsification of the oil into the encapsulation material and the emulsion stability has a significant influence on the encapsulation efficiency (CHAN, 2011). The stability of emulsions can be improved by the addition of emulsifiers, such as the proteins, or by the application of high-pressure homogenization. In addition, the high pressure homogenization can produce emulsions with smaller oil droplets (JAFARI et al., 2008), which can also increase the retention of the encapsulated oil (SOOTTITANTAWAT et al., 2003).

Thus, the purpose of this work was to study the process parameters involved in the production of microbeads by the extrusion of emulsions composed by soybean oil, sodium caseinate and κ-carrageenan at pH 7 and 3.5 into potassium chloride solution, in order to obtain potential encapsulation matrices for hydrophobic components. The morphology and stability of microbeads in different media were examined, evaluating the possible application of these particles.

5.2. MATERIAL AND METHODS

5.2.1. Material

The ingredients used to prepare the systems were κ-carrageenan, gently supplied by CPKelco (Atlanta, USA), casein (Sigma-Aldrich Co., St. Louis, USA), soybean oil (Bunge Alimentos S.A., Brazil) and potassium chloride P.A. (Labsynth, Diadema, Brazil). All other reagents were of analytical grade.

5.2.2. Preparation of stock solutions

The sodium caseinate (Na-CN) stock solution (10% w/v) was prepared by dispersing casein in deionized water for 3 hours using a magnetic stirrer. The pH of the solution was constantly adjusted to 7 using 10 M NaOH. Polysaccharide stock solution (3% w/v) was prepared by dissolving the κ-carrageenan powder in deionized water, followed by heat treatment at 90°C for 60 min with magnetic stirring and subsequent cooling to room temperature. The pH of κ-carrageenan solution was adjusted to 7 using HCl. The two solutions were then diluted in order to prepare the emulsions.

5.2.3. Preparation of emulsions

A primary oil-in-water (O/W) emulsion was prepared at 25°C by pre-mixing the soybean oil with a Na-CN aqueous solution using an Ultra Turrax model T18 (IKA, Germany) for 4 min at 14,000 rpm, followed by homogenization at 30 MPa / 5 MPa using a Panda 2K NS1001L double-stage homogenizer (Niro Soavi, Italy). The Na-CN and oil concentrations in the final emulsions were fixed at 0.5% (w/v) and 20% (v/v), respectively. Secondary O/W emulsions were prepared at room temperature by mixing the primary

emulsion into κ-carrageenan solutions using magnetic stirring for 1 hour. The final composition of secondary emulsions was 10% (v/v) soybean oil, 0.25% (w/v) sodium caseinate and 0.05 – 1.5% (w/v) κ-carrageenan. These emulsions were maintained at pH 7 and part of them was adjusted to pH 3.5 using HCl.

5.2.4. Visual phase diagrams

Visual phase diagrams of emulsions with different κ-carrageenan concentration versus KCl were made to establish the appropriate concentrations of salt and polysaccharide for gel formation. The mixtures were prepared by mixing 4 mL of each emulsion with 4 mL of each KCl solution. These mixtures were stirred at room temperature and the gel formation was evaluated after 24 hours of storage based on visual examinations. From these data it was possible to construct the sol-gel transition diagrams and to set up some of the conditions for microbead preparation.

5.2.5. Microbeads

5.2.5.1. Production of microbeads

Microbeads were prepared by the extrusion of secondary emulsions through an atomizer nozzle (0.7, 1.0 or 1.2 mm diameter) into a KCl solution (concentration determined from the visual phase diagrams) at room temperature. The height from the atomizer nozzle to the KCl solution (H) (Figure 5.1A) varied between 10 and 50 cm. The feed flow rate was fixed at the minimum capacity of the peristaltic pump (0.2 L/h), while the compressed air flow rate at the nozzle was fixed at the maximum value possible (0.12 m^3/h) avoiding the splash of the salt solution out of the container (the parameters were

based on the study presented in Chapter 3). The gelled particles were maintained in the salt

solution for 30 minutes (CHAN et al., 2009) and then filtered through a sieve with opening

of 0.053 mm. The microbeads were stored at 10°C and their microstructure and stability

were evaluated.
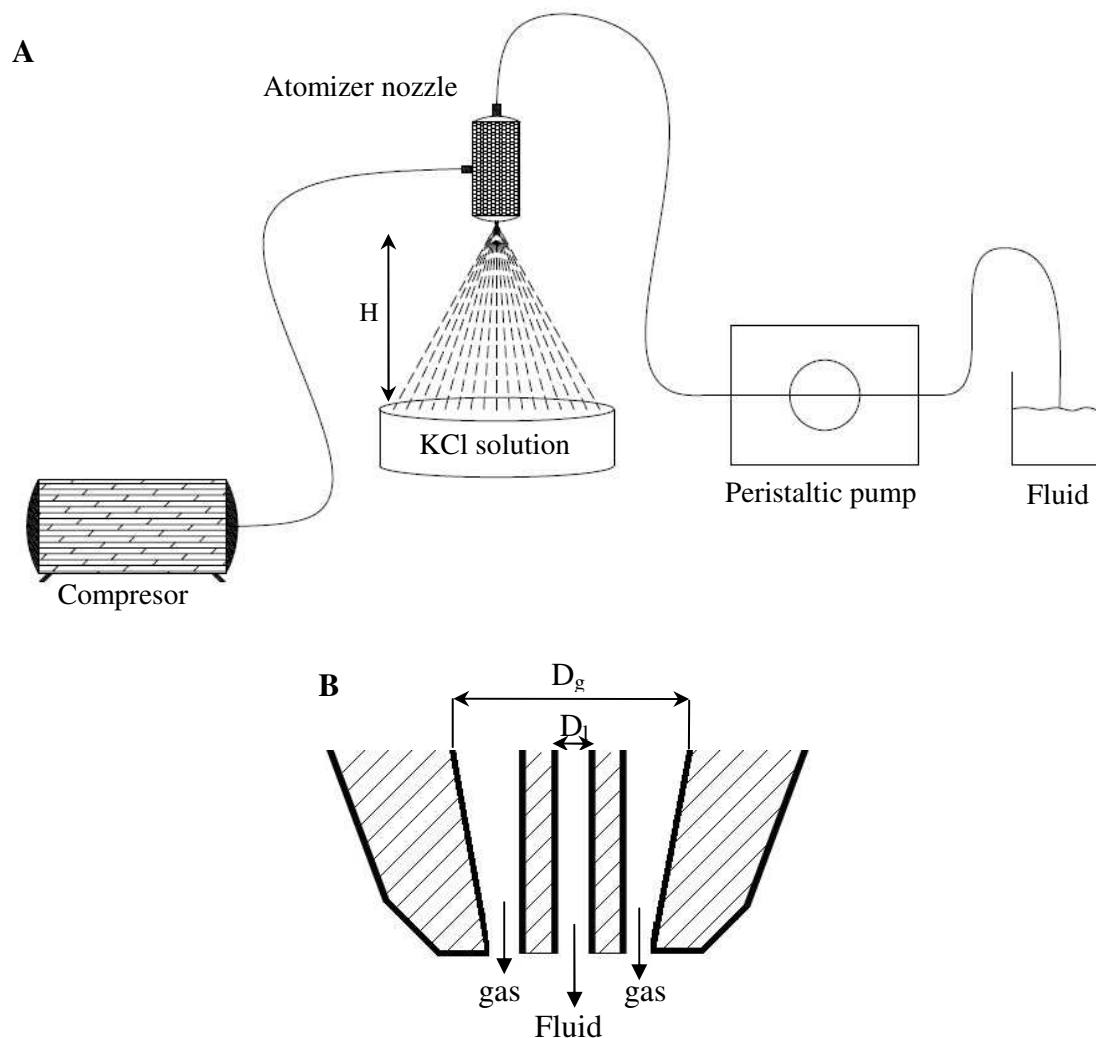
Figure 5.1. A) Extrusion formation of microgels and B) atomizer nozzle. H = height from

the atomizer nozzle to the salt solution, D_l = diameter of the fluid nozzle exit and D_g =

diameter of gas nozzle exit.

The configuration of the atomizer nozzle used in this work is schematically shown in Figure 5.1B. It consists of a round liquid jet surrounded by a co-flowing annular gas stream. The diameter of the liquid jet was D_l = 0.7, 1.0 or 1.2 mm and the gas nozzle exit diameter was D_g = 2.5, 3.08 or 3.35 mm, respectively.

The atomization process can be evaluated by some dimensionless parameters, such as the Reynolds numbers of the gas (Re_g) and the liquid layers ($Re_{\lambda l}$), Weber number (We) and Ohnesorge number (Oh), described in the Equations 5.1, 5.2, 5.3 and 5.4, respectively.

$$Re_g = \frac{v_g b_g}{v_g} \tag{5.1}$$

$$Re_{\lambda l} = \frac{(v_c - v_l)\lambda_l}{v_l} \tag{5.2}$$

where v_l and v_g are kinematic viscosities (ratio between the liquid dynamic viscosity and its density) of the liquid and gas (m^2/s), respectively, v_l and v_g are the liquid and gas velocities (m/s), respectively, v_c is the velocity of the waves produced in the exit of the nozzle

$(v_c = \frac{\sqrt{\rho_l}v_l + \sqrt{\rho_g}v_g}{\sqrt{\rho_l} + \sqrt{\rho_g}})$ and λ_l is the wavelength $(\lambda_l \approx \frac{2Cb_g}{\sqrt{Re_g}}\frac{\sqrt{\rho_l}}{\sqrt{\rho_g}})$, where C is the

coefficient of proportionality that depends on the nozzle design, ρ_l is the liquid density (kg/m^3), ρ_g is the gas density (kg/m^3) and b_g is the thickness of the gas layer ($b_g = (D_g - D_l)/2$).

$$We_l = \frac{\rho_g\left(v_g - v_l\right)^2 D_l}{\sigma} \tag{5.3}$$

where σ is the surface tension (N/m).

$$Oh = \frac{\eta_l}{\sqrt{\rho_l \sigma D_l}} \tag{5.4}$$

The Weber number defines the ratio between the destabilizing dynamic pressure forces exerted by the gas on the liquid and the confining forces associated with the surface tension (VARGA et al., 2003). Thus, the increase of We tends favor the disruption of liquid, leading to smaller droplets. The Ohnesorge number relates the liquid viscosity and the surface tension and can be associated to the sphericity of particles.

5.2.6. Microbead evaluation

5.2.6.1. Optical microscopy

The morphology of the microbeads was evaluated by optical microscopy using a Scope.A1 microscope (Carl Zeiss, Germany) with a 10× objective lens. For this, the microgels were poured onto microscope slides and carefully covered with glass cover slips. At least 10 images were obtained for each sample.

The shape of the microbeads was determined from image analysis. Measurements of the maximum (F_{max}) and minimum (F_{min}) Feret diameters were carried out for each particle, with a total of 400 particles per sample. The aspect ratio (AR) was obtained from the relation between F_{max} and F_{min} (Equation 5.5).

$$AR = \frac{F_{max}}{F_{min}} \tag{5.5}$$

5.2.6.2. Confocal scanning laser microscopy (CSLM)

Fluorescein-5-isothiocyanate (FITC) was used for the covalent labeling of κ-carrageenan, following the method described by Heilig et al. (2009). 20 mL DMSO and 80 µL pyridine were mixed with 1 g κ-carrageenan and stirred at room temperature for 30 minutes. After the addition of 0.1 g FITC and 40 µL dibutyltin dilaurate, the mixture was

incubated for 3 h in a 95°C water bath and, finally, cooled down to room temperature. The resulting gel was then minced, washed with ethanol 99.6% and dried at 65°C. The covalently labeled κ-carrageenan powder was then dissolved as described in the section 5.2.2 to prepare the polysaccharide solution. Sodium caseinate solution was labeled with Rhodamine B by the addition of the fluorescent dye directly to the protein solution. The protein and polysaccharide labeled solutions were used to prepare the emulsions and microbeads for confocal analysis as detailed in sections 5.2.3 and 5.2.5.1.

Samples were examined using a Zeiss LSM 780-NLO confocal on an Axio Observer Z.1 microscope (Carl Zeiss AG, Germany) using a 40 × objective. Images were collected using 488 and 543 nm laser lines for excitation of FITC and Rhodamine B fluorophores, respectively, with pinholes set to 1 airy unit for each channel, 1024×1024 image format. Images were taken along the height of the samples.

5.2.6.3. Particle size analysis

Particle size analysis was carried out in 0.4% (w/v) KCl solution (particle concentration of ~0.005% wt) using a Malvern Mastersizer 2000 (Malvern Instruments Ltd., UK). The size of particles was determined as the volume-surface mean diameter ($d_{32} = \Sigma n_i d_i^3 / \Sigma n_i d_i^2$), where n_i is the number of microbeads of diameter d_i. The particle size measurements were reported as the average and standard deviation of measurements made on microbeads, with three readings made per sample.

5.2.6.4. Evaluation of microbead stability

Microbeads composed by 1.5% (w/v) κ-carrageenan were used to evaluate their stability in different media. Suspensions were prepared by dispersing the microbeads directly in the measurement chamber of the laser diffraction instrument (Mastersizer 2000, Malvern Instruments Ltd., UK) in the concentration of approximately of 0.005% (w/w). Deionized water, ethanol, sucrose solutions (0.5 – 15% w/v) and potassium chloride solutions (concentrations between 0.2% and 7.5% w/v) were used as suspension media. In addition, the microstructure of the microbeads in these different media was monitored through observation of suspensions in the optical Scope.A1 microscope (Carl Zeiss, Germany) with a 10× objective lens.

5.3. RESULTS AND DISCUSSION

5.3.1. Visual phase diagrams

Visual phase diagrams were constructed from the mixture between KCl solutions with double-layer emulsions composed by 10% (v/v) soybean oil, 0.25% (w/v) Na-CN and different κ-carrageenan concentrations at pH 7 and 3.5 (Figures 5.2A and 5.2B). The phase diagrams were separated into three regions (liquid, weak gel and strong gel) based on visual examinations. In both diagrams, the gel formation occurred from a critical value of κ-carrageenan of 0.25% (w/v) and a KCl concentration above 0.1% (w/v). The exception was the emulsion containing 1.5% (w/v) κ-carrageenan at pH 3.5, which formed gel already at 0.1% (w/v) KCl. Below the critical salt concentration, κ-carrageenan was in the disordered state (random coil conformation) and above this KCl concentration, κ-carrageenan was in the ordered conformation (helix) and the helical chains were aggregated into a three-

dimensional network (NÚÑEZ-SANTIAGO et al., 2011). At 1.5% κ-carrageenan and pH 3.5, the cations presented in the polysaccharide were probably sufficient to promote the coil to helix transition at room temperature.

Stronger gels were only produced using κ-carrageenan concentration above 0.5% (w/v) and KCl concentrations between 0.2 and 0.5%. In such conditions the polysaccharide junction zones were probably saturated with potassium ions. Pure κ-carrageenan aqueous systems also showed strong gel formation at concentration above 0.5% (w/v) (Chapter 3). However, the systems without oil formed three-dimensional networks at higher KCl concentrations (Chapter 3), probably because the addition of oil decreased the number of junction zones that can be formed between the polysaccharide chains. At higher KCl concentrations (> 0.6% w/v), weak gels or liquid systems were produced depending on the κ-carrageenan concentration (Figure 5.2), which can be explained by the disordered aggregation of polysaccharide molecules with expulsion of water (syneresis), preventing the formation of a three-dimensional network (Chapter 3).

The comparison between the phase diagrams constructed at different pH values showed that stronger gels were formed for lower κ-carrageenan concentrations at pH 3.5 (Figure 5.2B) when compared to the systems at pH 7, which can be explained by the higher interaction between the positive protein and the negative charged polysaccharide below the isoelectric point. KCl concentration of 0.4% (w/v) was chosen for the production of microbeads, since strong gels were produced for majority of the systems at this salt level.
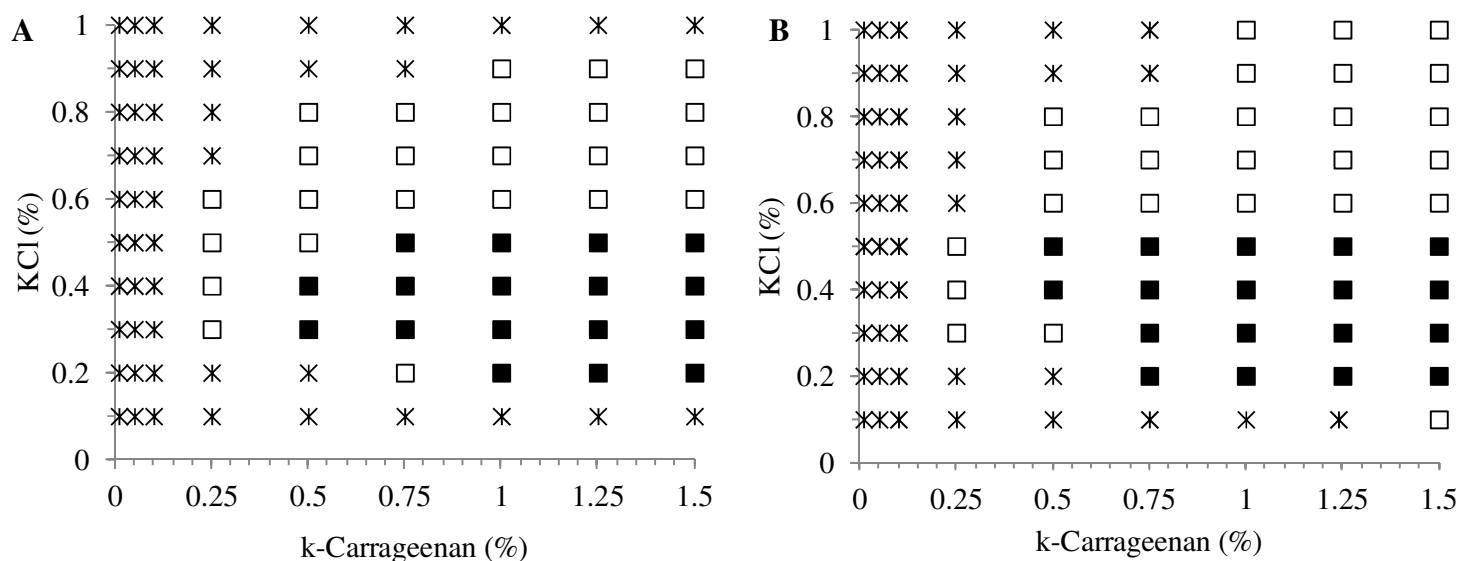
Figure 5.2. Visual phase diagram of O/W emulsions containing 0.25% (w/v) Na-CN and different κ-carrageenan concentration / KCl systems at room temperature and (A) pH 7 and (B) pH 3.5. (■) Strong gels, (□) weak gels and (✳) liquid.

5.3.2. Effect of process variables on the microbead production

5.3.2.1. Effect of nozzle diameter

In order to evaluate the influence of the diameter of fluid nozzle exit on the final morphology of microbeads, emulsions composed by 0.25% (w/v) Na-CN, 1% (w/v) κ-carrageenan and 10% (v/v) soybean oil at pH 7 and 3.5 were atomized in 0.4% (w/v) KCl solution at fixed compressed air flow rate (0.12 m^3/h), feed flow rate (0.2 L/h) and collecting distance (50 cm). Figure 5.3 shows the particle size distribution and microscopic images of the microbeads produced using different fluid nozzle diameters (D$_l$ = 0.7, 1.0 or 1.2 mm). The microscopic images show that microbeads were produced for all fluid nozzle diameters, with the oil encapsulated in the gelled matrix and some free oil droplets in solution. The free oil droplets were mainly observed at the smaller fluid nozzles (0.7 and

1.0 mm), probably because the shear rate was greater at these conditions (Table 5.1), leading to a destabilization of emulsions during the atomization process.

These results also showed that the morphology of microbeads was not very sensitive to the fluid nozzle diameter, showing little difference between the aspect ratios. At each pH, all microbeads showed very similar particle size distribution. The evaluation of d_{32} showed the tendency that bigger nozzles produced smaller microbeads (Figure 5.3). Comparing the microbeads produced at pH 7 and 3.5 it was verified that the microbeads produced at pH 3.5 were greater than those produced at pH 7, which can be explained by the interactions between the protein and polysaccharide under these different pH values that will be discussed in the section 5.3.3. Nevertheless, the aspect ratio was not influenced by the pH of emulsion.

D$_l$ = 0.7 mm   D$_l$ = 1.0 mm   D$_l$ = 1.2 mm

pH 7

d$_{32}$ = 93.7 ± 1.1μm   **d$_{32}$ = 85.0 ± 1.7 μm**   **d$_{32}$ = 86.0 ± 0.7 μm**
AR = 1.35 ± 0.08   **AR = 1.48 ± 0.02**   **AR = 1.42 ± 0.06**

pH 3.5

d$_{32}$ = 158.8 ± 4.4 μm   **d$_{32}$ = 120.8 ± 6.3 μm**   **d$_{32}$ = 107.4 ± 0.7 μm**
AR = 1.50 ± 0.08   **AR = 1.50 ± 0.14**   **AR = 1.40 ± 0.12**
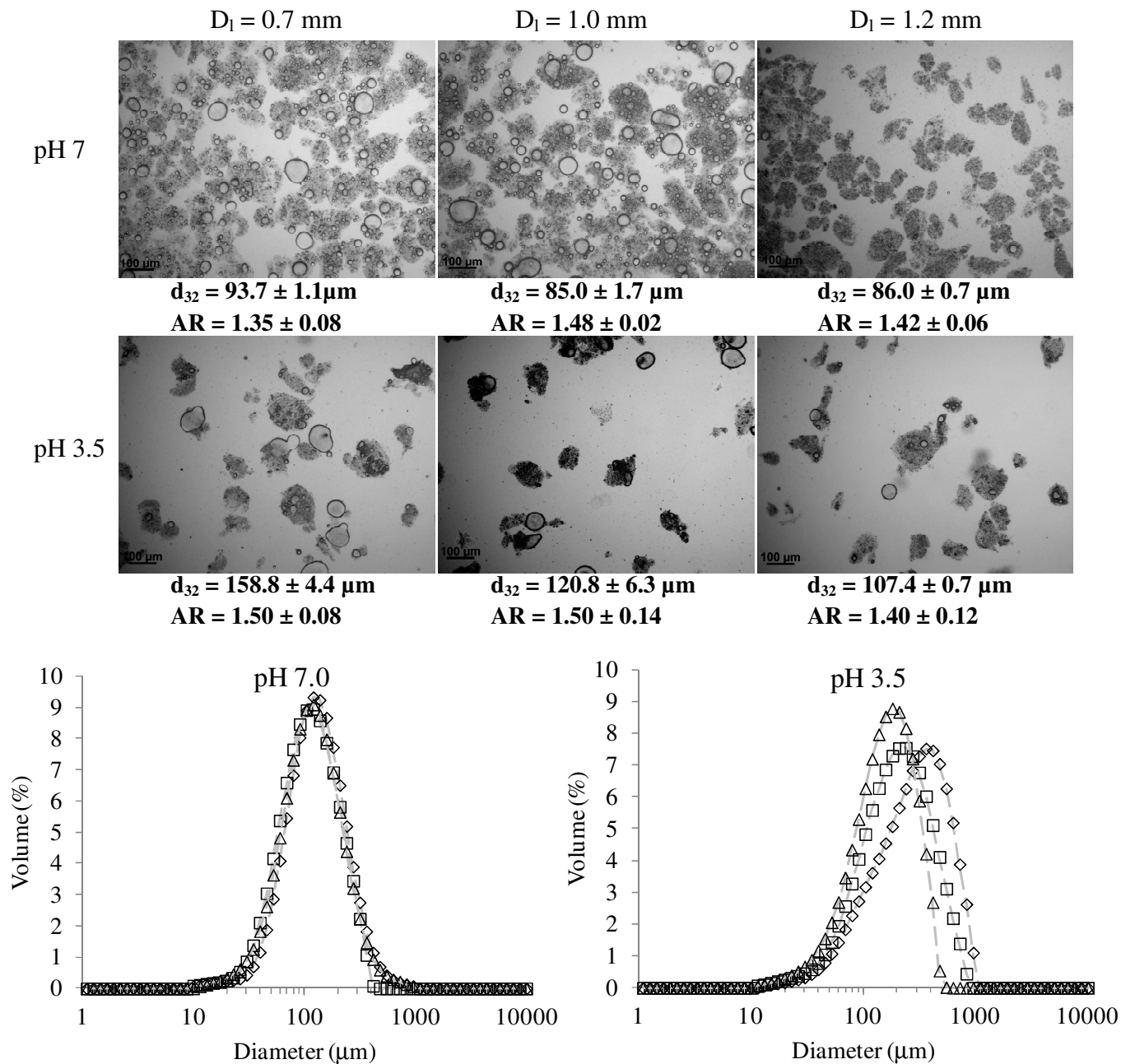
Figure 5.3. Particle size distribution and microstructure of microbeads composed by 10% (v/v) soybean oil, 0.25% (w/v) Na-CN and 1% (w/v) κ-carrageenan at pH 7 and 3.5 produced using collecting distance of 50 cm and different fluid nozzle diameters (D$_l$): (—◇—) 0.7 mm, (—□—) 1.0 mm and (—△—) 1.2 mm. Scale bar = 100 μm.

The production of microbeads using different nozzle diameters could be evaluated using dimensionless parameters (Table 5.1), which are mainly dependent on the gas boundary layer thickness at the nozzle exit (ALISEDA et al., 2008). The increase of fluid nozzle diameter was accompanied by the increase of gas exit area (gas boundary layer) due to the increase of nozzle diameter of gas exit (D_g) (Table 5.1). Thus, there was a decrease of the Reynolds number of the gas (Re_g) and, consequently, of the Reynolds number of liquid layer ($Re_{\lambda l}$) and Weber number (We_l). $Re_{\lambda l}$ was higher than 10 in all experiments, which was the condition necessary to the droplet breakup (ALISEDA et al., 2008). The reduction of We_l with the increase of nozzle diameter (Table 5.1) indicated the tendency to produce larger particles (ALISEDA et al., 2008). Nevertheless, the experimental results showed an opposite tendency, which could be attributed to the destabilization of the emulsions during the atomization at smaller nozzles (0.7 and 1.0 mm). Unstable emulsions with large oil droplets difficult the formation of very reduced particles. The Ohnesorge number did not vary with the fluid nozzle diameter and with the pH value (Table 5.1), confirming that the aspect ratio was not affected by these variables.

Based on these results, the fluid nozzle exit with 1.2 mm of diameter was chosen to produce the microbeads in the next steps of this work.

Table 5.1. Shear rate and dimensionless parameters of the experiments at different nozzle diameters

	Nozzle diameter (mm)	Gas exit area (mm^2)	$\dot{\gamma}$ (s^{-1})	Re$_g$	Re$_{\lambda l}$	Oh	We$_l$
	0.7	3.02	7646	9373	182.6	0.09	329.4
pH 7	1.0	3.85	4551	6576	129.7	0.09	236.8
	1.2	4.98	2625	5897	103.2	0.10	155.3
	0.7	3.02	7646	9373	185.7	0.09	329.4
pH 3.5	1.0	3.85	4551	6576	138.2	0.09	236.8
	1.2	4.98	2625	5897	115.4	0.09	155.3

5.3.2.2. Effect of collecting distance

The effect of the distance between the atomizer nozzle and the salt solution (H) was evaluated by varying H from 10 to 50 cm and using fixed fluid nozzle diameter (D_l = 1.2 mm) and κ-carrageenan concentration (1% w/v) at pH 7 and 3.5 (Figure 5.4). The particles produced at lower height (10 cm) showed a non-spherical shape and a lot of surface oil droplets dispersed in the gelling medium. The microbeads became more spherical as the collecting distance increased from 10 to 50 cm, as can be observed by their microstructures and by the reduction of aspect ratio from ~2.0 to ~1.4 for both pH values (Figure 5.4). The size of microbeads also tended to decrease with the increase of collecting distance, especially for emulsions at pH 3.5, whose d_{32} decreased from 138.7 µm to 107.4 µm. During the extrusion process, a minimum distance between the nozzle and the salt solution is necessary to promote the complete break up process and the rearrangement of the shape of the liquid drop (ALISEDA et al., 2008; CHAN et al., 2009). Chan et al. (2009) observed that spherical beads of alginate were produced at collecting distances between 10 and 100

cm using dripping method, but below this range, beads were tear-shaped. In addition, Aliseda et al. (2008) verified a decrease of mean droplet diameter with the increase of distance for extrusion of different fluids (water and mixtures containing glycerol and water), with completion atomization from 5 cm. A higher distance was necessary to complete the atomization in the present work (50 cm), probably because the emulsions had a lower surface tension (~ 57 mN/m) than the water or glycerol solutions (72 mN/m and 65 mN/m, respectively), needing more time for the droplet to achieve the spherical shape.

At short distance, the irregular shape and larger d_{32} of microbeads were associated to the incomplete break up process and the presence of free oil droplets was a consequence of the strong impact between droplets and salt solution, promoting the destabilization of the emulsions. Since the droplet velocity decreased during falling due to the thrust and friction force, the impact with salt solution tended to decrease at higher collecting distances. However, at distances higher than 50 cm, droplets could be deformed due to the coalescence of droplets during their falling (ALISEDA et al., 2008).

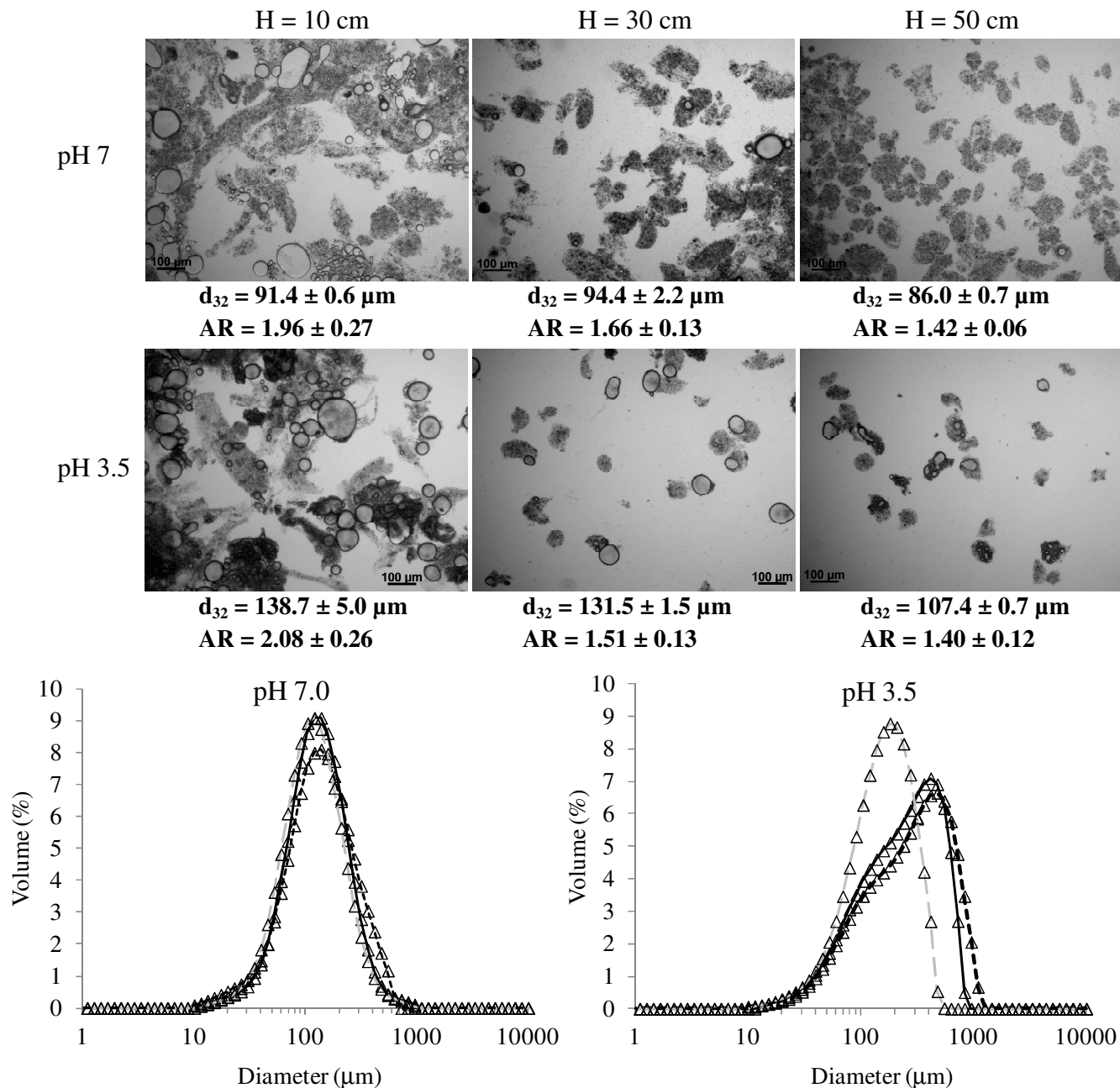|	H = 10 cm	H = 30 cm	H = 50 cm
pH 7	$d_{32} = 91.4 \pm 0.6$ μm AR = 1.96 ± 0.27	$d_{32} = 94.4 \pm 2.2$ μm AR = 1.66 ± 0.13	$d_{32} = 86.0 \pm 0.7$ μm AR = 1.42 ± 0.06
pH 3.5	$d_{32} = 138.7 \pm 5.0$ μm AR = 2.08 ± 0.26	$d_{32} = 131.5 \pm 1.5$ μm AR = 1.51 ± 0.13	$d_{32} = 107.4 \pm 0.7$ μm AR = 1.40 ± 0.12

Figure 5.4. Microstructure and particle size distribution of microbeads composed by 10% (v/v) soybean oil, 0.25% (w/v) Na-CN and 1% (w/v) κ-carrageenan at pH 7 and 3.5 produced using fluid nozzle diameter of 1.2 mm and different collecting distances: (−△−) 10 cm, (─△─) 30 cm and (─△─) 50 cm. Scale bar = 100 μm.

The comparison between microbeads produced at different pH showed again that particles produced at pH 3.5 were larger but had similar aspect ratio. From these results, the collecting distance of 50 cm was chosen to produce the microbeads in the following steps of this study.

5.3.3. Interaction between Na-CN and κ-carrageenan in the microbeads

Figure 5.5 shows the confocal microscopy of microbeads composed by 10% (v/v) soybean oil, 0.25% (w/v) Na-CN and 1.5% (w/v) κ-carrageenan at pH 7 and 3.5 produced at the conditions chosen in the section 5.3.2 (fluid nozzle diameter of 1.2 mm and collecting distance of 50 cm). In these images, sodium caseinate appears as red color, while the green areas indicate the presence of κ-carrageenan. The pictures revealed that different structures of microbeads were produced at distinct pH values. While the microbead at pH 3.5 showed the external surface composed by polysaccharide (Figure 5.5B), the confocal microscopy at pH 7 indicated the predominant presence of protein at the external surface of microbeads (Figure 5.5A).

At pH 7, protein and polysaccharide were both negatively charged (Figure 5.6A), resulting in an electrostatic repulsion between them. Thus, the protein was concentrated at the surface of oil droplets, while the polysaccharide was mainly free in the aqueous phase. During the atomization process, the Na-CN-coated oil droplets probably migrated to the air-liquid interface due to the lower surface tension of protein (Figure 5.6C). As the particles come into contact with the salt solution, part of protein was dissolved, releasing the oil and, simultaneously, potassium ions entered into the particles, promoting the gelation of polysaccharide (Figure 5.6E). On the other hand, when the pH was reduced

below the isoelectric point (pI ~4.6), the protein became positively charged (ζ-potential ~ +25 mV at pH 3.5) favoring its electrostatic interaction with the polysaccharide (ζ-potential = -55 mV) (Figure 5.6B). In this case, κ-carrageenan was adsorbed onto the Na-CN coated oil droplets, resulting in the formation of a double layer (Figure 5.6D). When the particles came into contact with the salt, the potassium ions promoted the gelation of polysaccharide, producing the microbeads (Figure 5.6F). However, as the κ-carrageenan was linked to the sodium caseinate at the oil surface, there was lower amount of free polysaccharide in solution and the gelation of polysaccharide tended to be slower when compared to the microbeads at pH 7. Thus, there was a higher dissolution of microbeads before gelation, which was responsible for their larger diameter at pH 3.5 when compared to the particle at pH 7 (sections 5.3.2.1. and 5.3.2.2.).
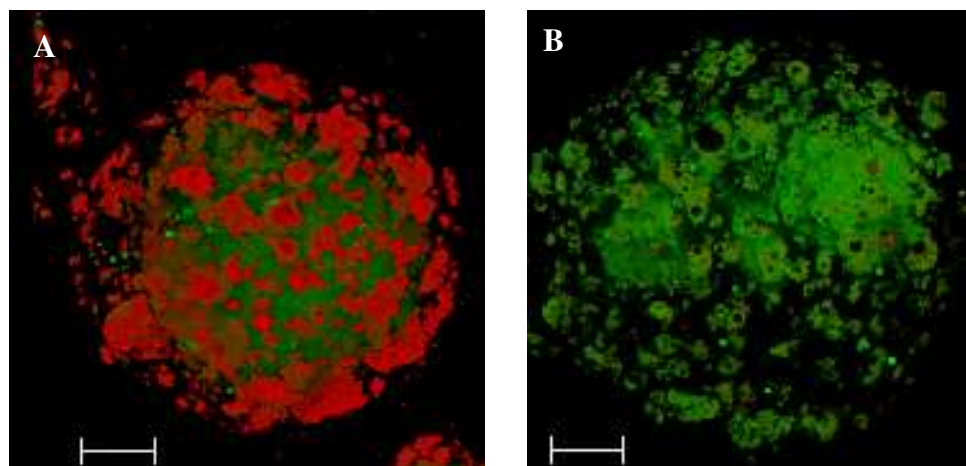
Figure 5.5. Confocal microscopy of microbeads composed by 10% (v/v) soybean oil, 0.25% (w/v) sodium caseinate and 1.5% (w/v) κ-carrageenan produced at A) pH 7 and B) pH 3.5. Scale bar = 20 µm.

pH 7   **pH 3.5**

A   Na-CN   **B**

Charge distribution

κ-carrageenan

C   **D**

Before gelation

K⁺   K⁺

E   **F**

After gelation

Figure 5.6. Charge distribution (A and B) and schematic representation of κ-carrageenan and sodium caseinate at droplets before gelation (C and D) and microbeads after gelation (E and F) at pH 7 and 3.5.

5.3.4. Stability of microbeads

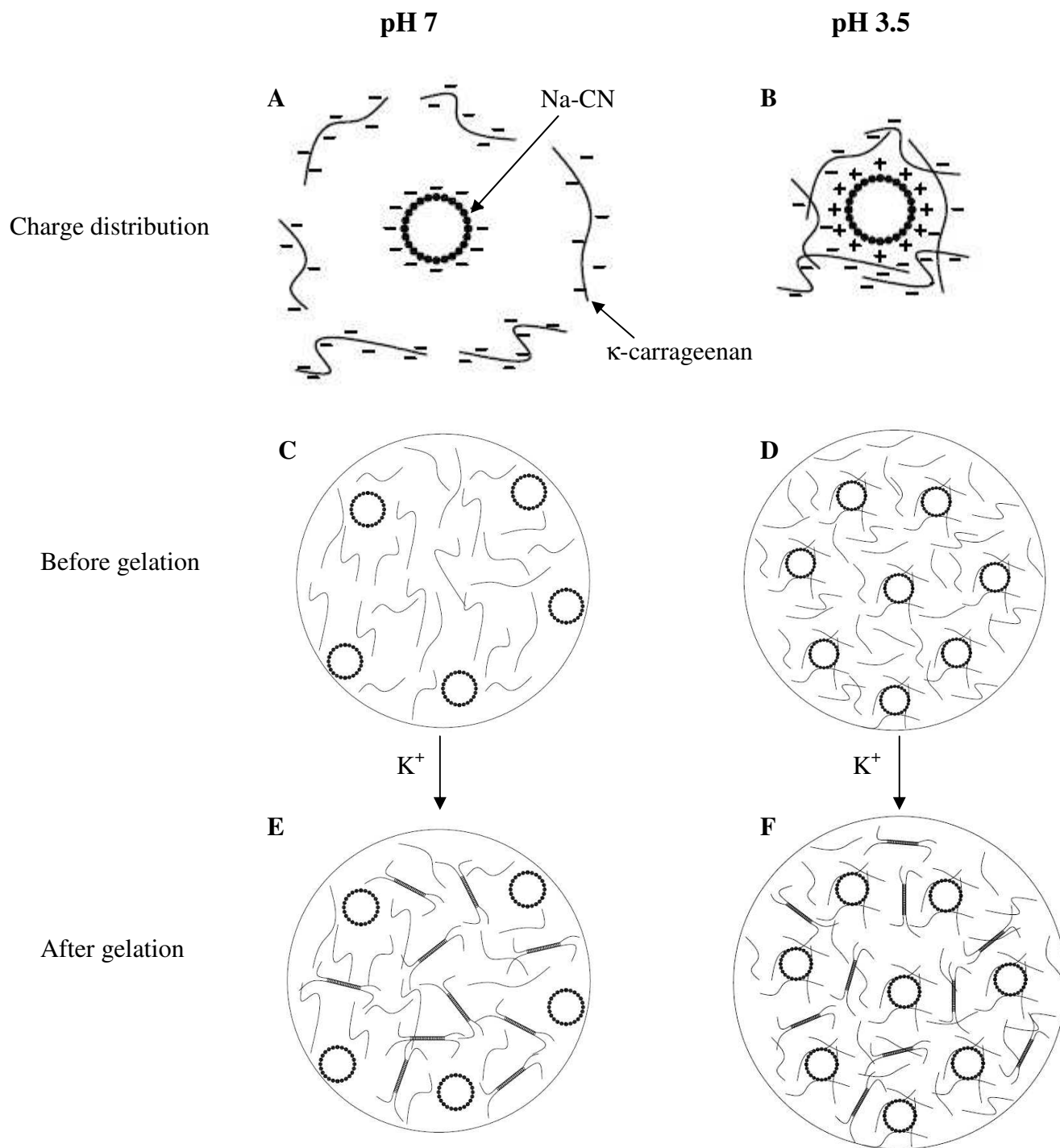The stability of microbeads was evaluated in different media (ethanol, deionized water, sucrose solution and salt solutions) in order to determine their potential incorporation in products without releasing the encapsulated oil during the storage of the products. The dielectric constant (ε) and water activity (a_w) of these media are shown in Table 5.2.

Table 5.2. Dielectric constant (ε) and water activity (a_w) of the dispersion media

Solution	Dielectric constant (ε)	Water activity (a_w)
Ethanol	24.3	–
Deionized water	78.5	1
Sucrose solution		
1%	78.3	0.999
5%	77.4	0.996
7.5%	76.8	0.994
10%	76.2	0.992
15%	74.9	0.988
KCl solution		
0.2%	78.3	0.999
0.75%	77.5	0.996
1.9%	76.0	0.992
3.7%	73.5	0.984
7.5%	68.5	0.968

5.3.4.1. Stability in ethanol

The stability of microbeads at pH 7 and 3.5 was evaluated in ethanol as shown in Figure 5.7. Microbeads at the gelling bath (standard) showed spherical shape and a

monomodal particle size distribution for both pH values. The particle size distribution of standard microbeads was determined using 0.4% KCl (0.05 M) solution as dispersion medium. The comparison between particle size distribution of microbeads dispersed in ethanol and the standard microbeads showed small differences, with a tendency to decrease the mean particle diameter with dispersion in ethanol. The evaluation of mean particle diameter (d_{32}) confirmed the collapse of particles when dispersed in ethanol, since they were significantly smaller than the standard ones. The evaluation of microscopic images showed that the oil droplets were not released from microbeads, which had significant change of shape that could modify significantly the rheological behavior of the microbeads suspensions (ELLIS et al., 2009). In addition, the microscopy also showed that the particles tended to aggregate when they were at rest, which could not be observed in the particle size distribution due to the agitation during the laser diffraction analysis. The effect of ethanol on the microbeads can be explained by the lower dielectric constant of alcohol when compared to the other solvents (Table 5.2), which decrease the solvent polarity (RAGHAVAN et al., 2000). With this, there was an increase of particle-particle electrostatic interaction and a decrease in the particle-solvent interaction, resulting in their precipitation.
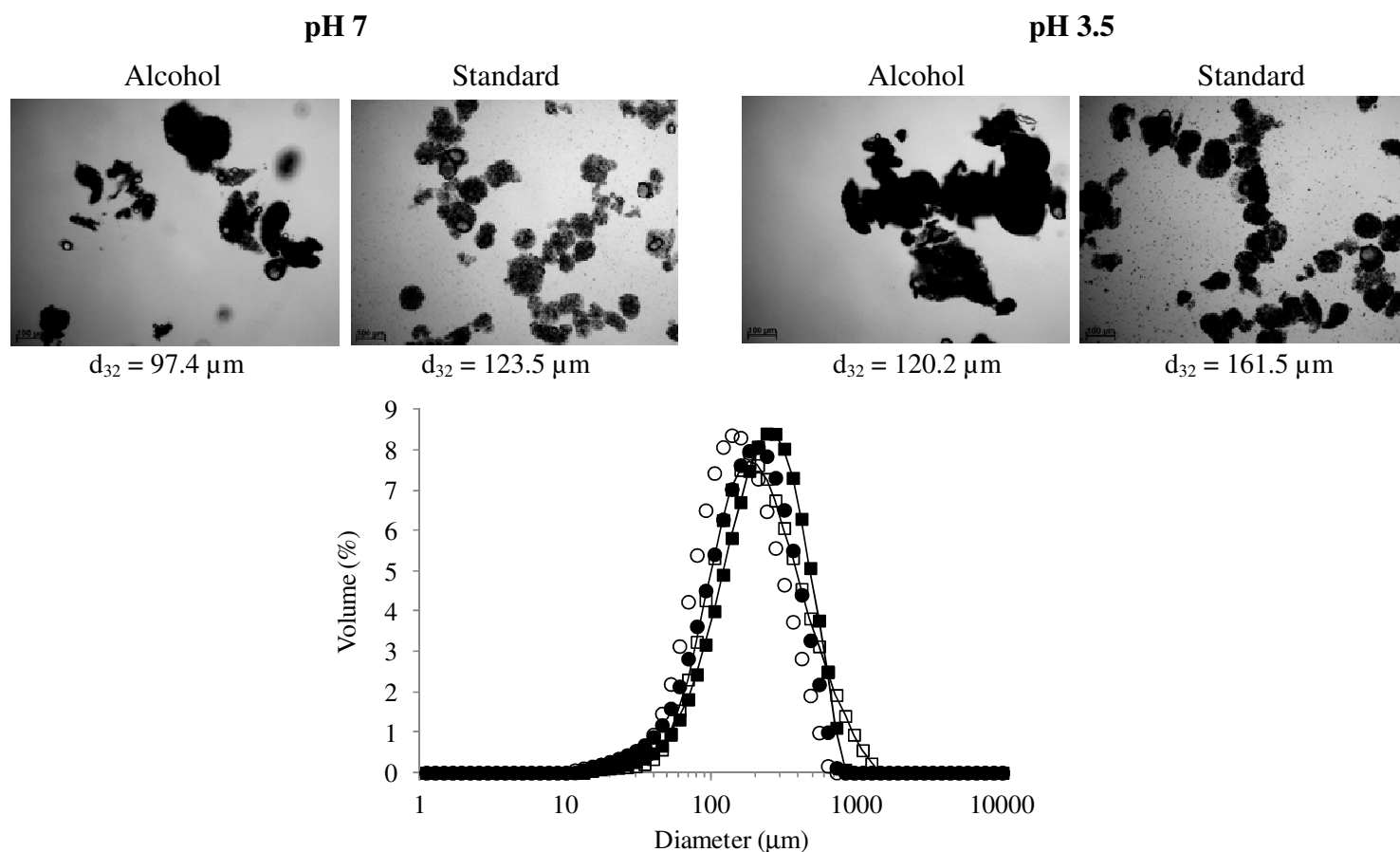
pH 7		pH 3.5	
Alcohol	Standard	Alcohol	Standard

$d_{32} = 97.4\ \mu m$　　$d_{32} = 123.5\ \mu m$　　　$d_{32} = 120.2\ \mu m$　　$d_{32} = 161.5\ \mu m$

Figure 5.7. Microstructure and particle size distribution of microbeads composed by 10% (v/v) soybean oil, 0.25% (w/v) Na-CN and 1.5% κ-carrageenan at pH 7 and 3.5 dispersed in ethanol. (—□—) pH 7 standard, (○) pH 7 in ethanol, (—■—) pH 3.5 standard and (●) pH 3.5 in ethanol. Scale bar = 100 µm.

5.3.4.2. Stability in aqueous solutions

Figure 5.8 shows the microstructure and particle size distribution of the two types of microbeads dispersed in deionized water. The dispersion in deionized water promoted the dissolution of a large amount of microbeads, releasing the oil droplets to the aqueous medium. However, the oil droplets did not show coalescence, indicating that the protein continued adsorbed onto the oil-water interface and only the polysaccharide network was

dissolved. The particle size distribution showed a bimodal distribution for microbeads dispersed in deionized water, differently from the standard microbeads. The values of the modes of bimodal distribution (Figure 5.8) indicated that the first peak (lower diameter range) corresponded to the free oil droplets (~1.9 µm), while the second peak referred to the remaining microbeads. In this case, the second peak was shifted to lower values of particle diameter in relation to the standard, indicating that microbeads were partially dissolved in the water. Microbeads produced at pH 3.5 seemed to be less unstable when dispersed in deionized water than those at pH 7, which was verified through the particle size distribution. The first peak was smaller (25% volume) than the second one (75% volume) for pH 3.5, while an opposite tendency was verified for pH 7 (60% volume in the first peak and 40% in the second one). In addition, the modes at pH 3.5 were higher than at pH 7, with the second mode closer to the mean diameter of standard particle. A possible explanation for this behavior relies on the position of the oil droplets, which were at the microbead surface for the pH 7 emulsions (Figure 5.5A) and, thus more prone to leak out by the dissolution of κ-carrageenan network in the core of the particle.

The high instability of microbeads in water can be explained by the migration of KCl to deionized water due to the difference in ion concentration, destabilizing the junction zones of κ-carrageenan and disintegrating the microbeads. This destabilization was different than that observed in microgels composed by κ-carrageenan and sodium caseinate without oil, in which their dispersion in deionized water led to a swelling and loss the shape (Chapter 3). It probably occurred because in the microbeads containing oil, the κ-carrageenan network was formed between the oil droplets, resulting in lower amount of

junction zones. Thus, the destabilization of junction zones led to disintegration of microbeads into small pieces.
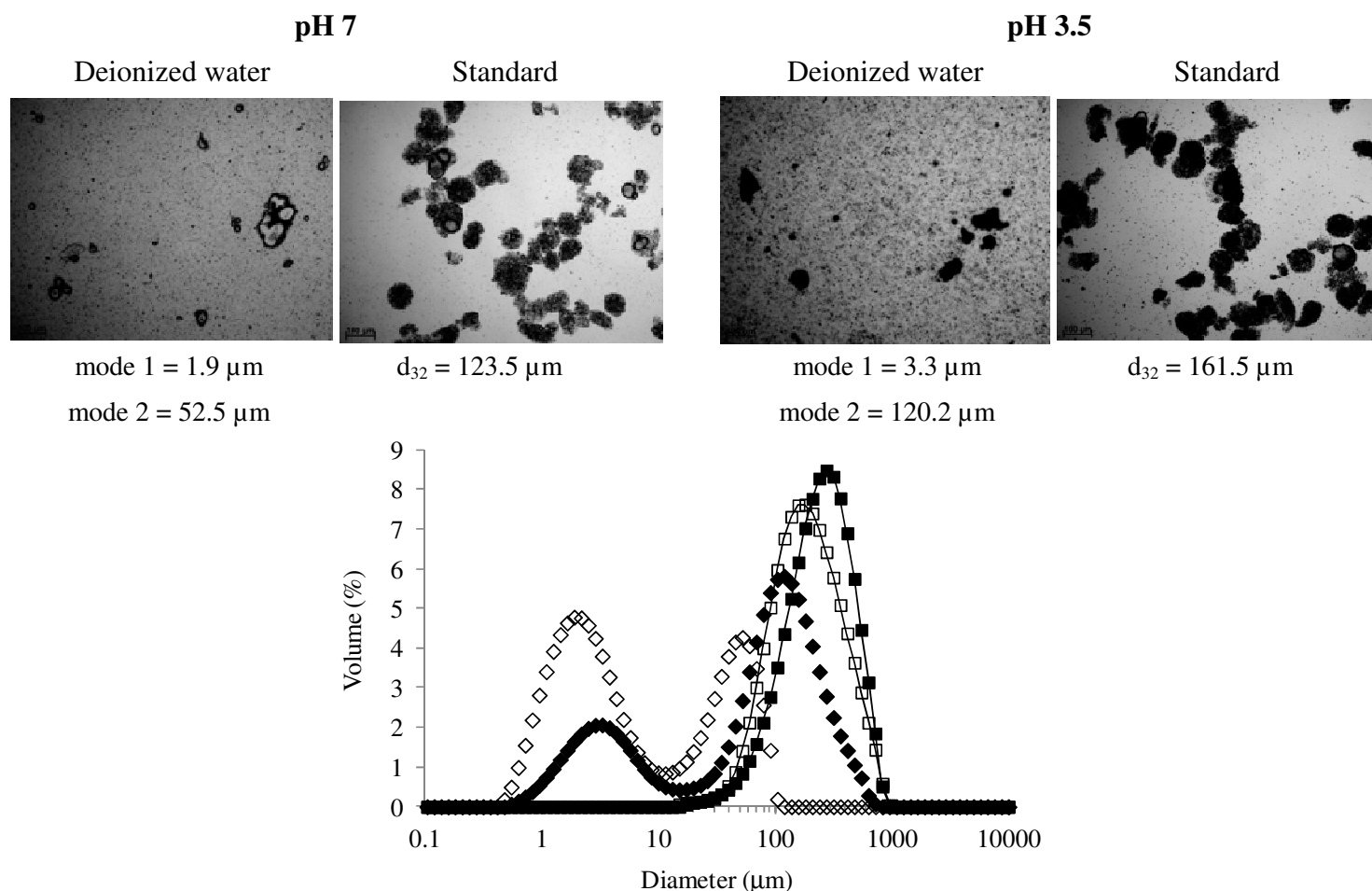

<div align="center">

pH 7   **pH 3.5**

Deionized water   Standard   Deionized water   Standard

mode 1 = 1.9 µm d_{32} = 123.5 µm   mode 1 = 3.3 µm d_{32} = 161.5 µm

mode 2 = 52.5 µm   mode 2 = 120.2 µm

</div>

Figure 5.8. Microstructure and particle size distribution of microbeads composed by 10% (v/v) soybean oil, 0.25% (w/v) Na-CN and 1.5% κ-carrageenan at pH 7 and 3.5 dispersed in deionized water. (—☐—) pH 7 standard, (◇) pH 7 in deionized water, (—■—) pH 3.5 standard and (◆) pH 3.5 in deionized water. Scale bar = 100 µm.

Figure 5.9 shows the stability of the microbeads in solutions with different sucrose concentrations. It is interesting to test the stability in these solutions since sucrose (or table sugar) is presented in a considerable amount of food products due to its sensorial

properties. The microstructures showed that the microbeads were destabilized in all sucrose concentrations, losing their shape and releasing the encapsulated oil. The particle size distribution showed that microbeads dispersed in sucrose solutions showed a bimodal distribution, which once more could be related to the free oil droplets (first peak) and the remaining microbeads (second peak).

For microbeads produced at pH 7, the importance of the first peak (mode = 2.51 µm) tended to decrease as the sucrose concentration was increased (volume from ~57% to ~41%), while the second one (mode = 60.2 µm) tended to increase (volume from ~43% to ~54%), indicating the improvement of the stability. Microbeads at pH 3.5 were less sensitive to the sucrose concentration, showing no differences in the first peak (mode = 3.3 µm and volume ~28%) and a small difference in the second peak (mode = 120.2 µm and volume between 71 and 72%). The sucrose stabilization effect could not be explained by the reduction of the water activity (a_w), since a_w was reduced from ~ 1 to ~0.988 by increasing sucrose concentration up to 15% (w/v) (Table 5.2). This result can be attributed to the capacity of sucrose to modify the structure of water surrounding the proteins, leading to the formation of Na-CN aggregates by hydrophobic interactions and, consequently, resulting in the protein stabilization (RIBEIRO et al., 2004).
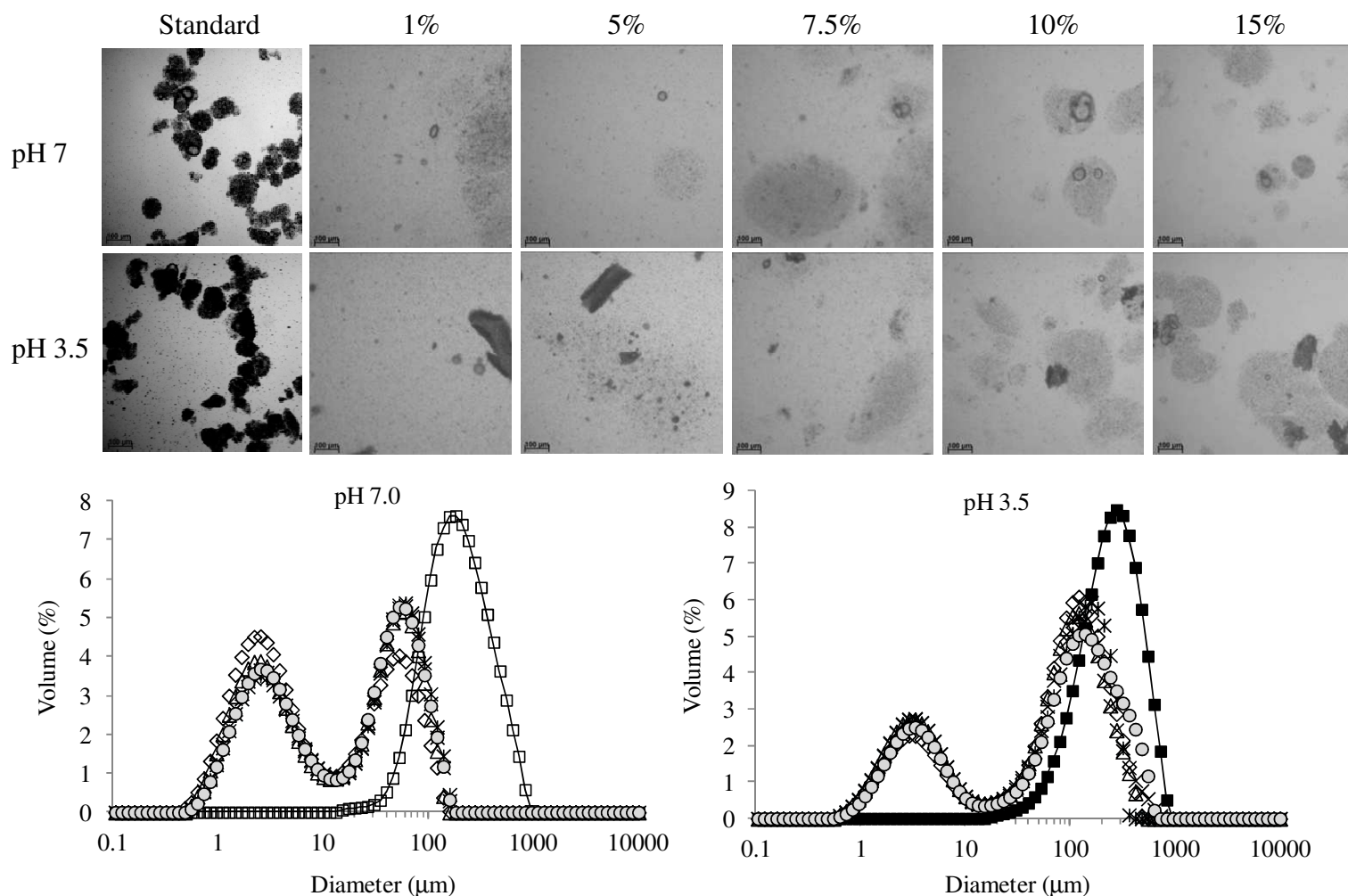
Figure 5.9. Microstructure and particle size distribution of microbeads composed by 10% (v/v) soybean oil, 0.25% (w/v) Na-CN and 1.5% κ-carrageenan at pH 7 and 3.5 dispersed in different sucrose solutions: (◇) 1%, (△) 5%, (✕) 7.5%, (✳) 10% and (◉) 15%. Standard: (⊟) pH 7 and (■) pH 3.5. Scale bar = 100 μm.

The stability of the microbeads in salt solutions was evaluated by their dispersion in potassium chloride solutions at different concentrations (between 0.2% and 7.5% w/v). At lower salt concentrations (0.2% and 0.75% w/v KCl) the microbeads lost their shape (Figure 5.10). The increase of KCl concentration (> 1.9% w/v) led to microbeads with

similar microstructures than those with no dilution (standard). However, despite these differences in the microstructure, the microbeads dispersed in all KCl solutions showed very similar particle size distribution (Figure 5.10).

The comparison between the mean particle diameters (d_{32}) indicated that the increase in KCl concentration from 0.2% to 0.75% (w/v) led to a slight increase in the diameter of the microbeads (Figure 5.11). This behavior was opposite than that verified for microgels composed by κ-carrageenan and sodium caseinate without oil (Chapter 3), where microgels swelled after dispersion in solutions with low KCl concentrations. In the case of particles containing the encapsulated oil, the κ-carrageenan network tended to disintegrate at the lowest KCl concentration (0.2% w/v) by the migration of salt to the water resulting in the release of oil droplets, as can be seen in Figure 5.10. Nevertheless, between 0.75% and 3.7% (w/v) KCl, the mean diameter of the microbeads was very similar to the standard, indicating that the KCl at these concentrations tended to stabilize the junctions zones of the κ-carrageenan chains because the microbeads were in osmotic equilibrium with the surrounding medium. At 7.5% (w/v) KCl, the microbeads tended to show a smaller diameter, probably because the water inside the microbeads tended to migrate to the medium containing high salt concentration in order to restore the osmotic equilibrium (ELLIS et al., 2009). Lower salt concentration was necessary to stabilize the microbeads (0.75% KCl) when compared to the microgels without oil that were stable only if dispersed in solutions containing 10% KCl (Chapter 3). As discussed earlier, this probably occurred due to the lower amount of junction zones present in the structure of microbeads.

Evaluating these results it is possible to conclude that the microbeads were very stable if dispersed in KCl solutions with concentration higher than 0.75%, maintaining their size and shape without release of the encapsulated oil.
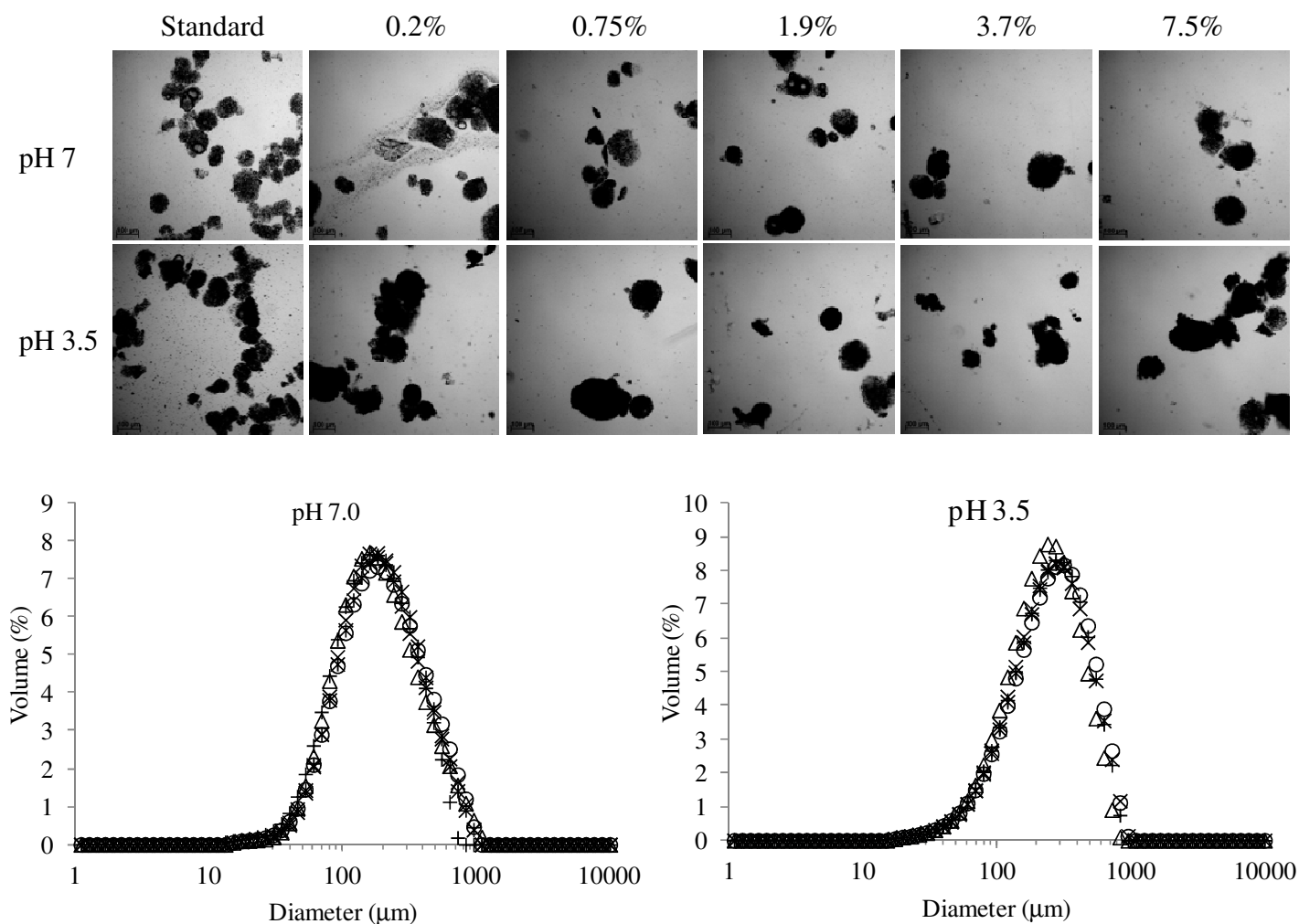

Figure 5.10. Microstructure and particle size distribution of microbeads composed by 10% (v/v) soybean oil, 0.25% (w/v) Na-CN and 1.5% (w/v) κ-carrageenan at pH 7 and 3.5 dispersed in KCl solutions with different concentrations: (△) 0.2%, (✕) 0.75%, (✳) 1.9%, (○) 3.7% and (＋) 7.5%.
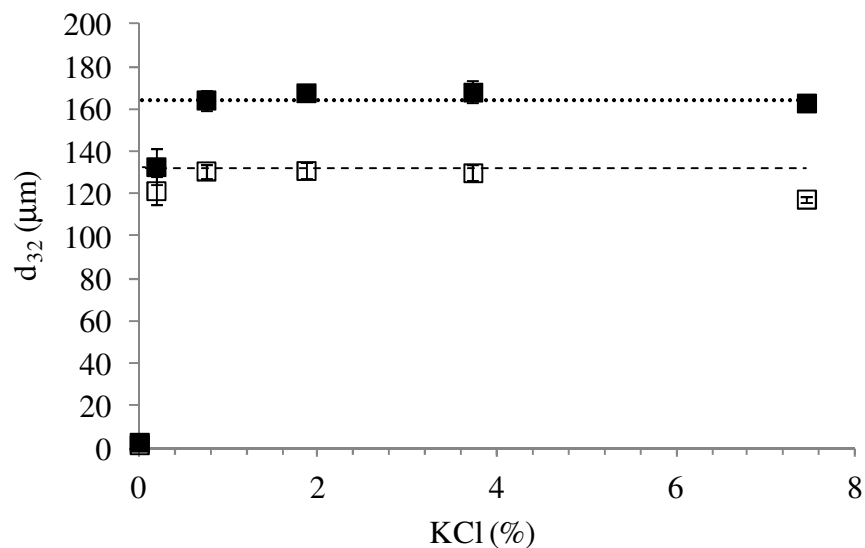
Figure 5.11. Mean particle diameter (d_{32}) of microbeads composed by 10% (v/v) soybean oil, 0.25% (w/v) Na-CN and 1.5% (w/v) κ-carrageenan at pH 7 and 3.5 in relation to the concentration of KCl solutions. (– – –) pH 7 standard, (□) pH 7 in KCl solution, (··········) pH 3.5 standard and (■) pH 3.5 in KCl solution.

5.4. CONCLUSIONS

Na-CN - κ-carrageenan microbeads were studied as a matrix for encapsulation of oil and hydrophobic components. The results showed that the smaller and more spherical microbeads were produced with the biggest fluid nozzle diameter (1.2 mm) and highest collecting distance (50 cm) tested. The pH of microbeads did not influence the shape of microbeads, but they were smaller when produced at pH 7. The microgels produced in both pH were very unstable when dispersed in deionized water and aqueous solutions of salt and sugar at low concentrations. The increase of sucrose and KCl concentrations tended to improve the microbead stability through different mechanisms. The beads were stable if dispersed in KCl concentration higher than 0.75%. When dispersed in ethanol, the

microbeads seemed to collapse losing their shape. Thus, the microbeads developed in this work can be applied in products containing high potassium chloride and alcoholic solutions without release the encapsulated oil.

5.5. ACKNOWLEDGEMENTS

5.6. REFERENCES

ALBERTINI, B.; VITALI, B.; PASSERINI, N.; CRUCIANI, F.; DI SABATINO, M.; RODRIGUEZ, L.; BRIGIDI, P. Development of microparticulate systems for intestinal delivery of *Lactobacillus acidophilus* and *Bifdobacterium lactis*. **European Journal of Pharmaceutical Sciences**, v. 40, n. 4, p. 359-366, 2010.

ALISEDA, A.; HOPFINGER, E. J.; LASHERAS, J. C.; KREMER, D. M.; BERCHIELLI, A.; CONNOLLY, E. K. Atomization of viscous and non-newtonian liquids by a coaxial, high-speed gas jet. Experiments and droplet size modeling. **International Journal of Multiphase Flow**, v. 34, n. 2, p. 161-175, 2008.

AZARNIA, S.; LEE, B. H.; ROBERT, N.; CHAMPAGNE, C. P. Microencapsulation of a recombinant aminopeptidase (PepN) from *Lactobacillus rhamnosus* S93 in chitosan-coated alginate beads. **Journal of Microencapsulation**, v. 25, n. 1, p. 46-58, 2008.

BLANDINO, A.; MACIAS, M.; CANTERO, D. Formation of calcium alginate gel capsules: Influence of sodium alginate and $CaCl_2$ concentration on gelation kinetics. **Journal of Bioscience and Bioengineering**, v. 88, n. 6, p. 686-689, 1999.

BUREY, P.; BHANDARI, B. R.; HOWES, T.; GIDLEY, M. J. Hydrocolloid gel particles: Formation, characterization, and application. **Critical Reviews in Food Science and Nutrition**, v. 48, n. 5, p. 361-377, 2008.

CHAN, E. –S. Preparation of Ca-alginate beads containing high oil content: Influence of process variables on encapsulation efficiency and bead properties. **Carbohydrate Polymers**, v. 84, n. 4, p. 1267-1275, 2011.

CHAN, E. –S.; LEE, B. –B.; RAVINDRA, P.; PONCELET, D. Prediction models for shape and size of ca-alginate macrobeads produced through extrusion-dripping method. **Journal of Colloid and Interface Science**, v. 338, n. 1, p. 63-72, 2009.

CHANDY, T.; MOORADIAN, D. L.; RAO, G. H. R. Chitosan/polyethylene glycol – alginate microcapsules for oral delivery of hirudin. **Journal of Applied Polymer Science**, v. 70, n. 11, p. 2143-2153, 1998.

COLINET, I.; DULONG, V.; MOCANU, G.; PICTON, L.; LE CERF, D. Effect of chitosan coating on the swelling and controlled release of a poorly water-soluble drug from an amphiphilic and pH-sensitive hydrogel. **International Journal of Biological Macromolecules**, v. 47, n. 2, p. 120-125, 2010.

CORBO, M. R.; BEVILACQUA, A.; SINIGAGLIA, M. Shelf life of alginate beads containing lactobacilli and bifidobacteria: characterisation of microspheres containing *Lactobacillus delbrueckii* subsp. *bulgaricus*. **International Journal of Food Science and Technology**, v. 46, n. 10, p. 2212-2217, 2011.

ELLIS, A.; KEPPELER, S.; JACQUIER, J. C. Responsiveness of κ-carrageenan microgels to cationic surfactants and neutral salts. **Carbohydrate Polymers**, v. 78, n. 3, p. 384-388, 2009.

HEILIG, A.; GÖGGERLE, A.; HINRICHS, J. Multiphase visualization of fat containing β-lactoglobulin - κ-carrageenan gels by confocal scanning laser microscopy, using a novel dye, V03-01136, for fat staining. **LWT – Food Science and Technology**, v. 42, n. 2, p. 646-653, 2009.

HUNIK, J. H.; TRAMPER, J. Large-scale production of κ-carrageenan droplets for gel-bead production: theoretical and practical limitations of size and production rate. **Biotechnology Progress**, v. 9, n. 2, p. 186-192, 1993.

JAFARI, S. M.; ASSADPOOR, E.; HE, Y.; BHANDARI, B. Re-coalescence of emulsion droplets during high-energy emulsification. **Food Hydrocolloids**, v. 22, n. 7, p. 1191-1202, 2008.

KAIHARA, S.; SUZUKI, Y.; FUJIMOTO, K. *In situ* systhesis of polysaccharide nanoparticle via polyion complex of caboxymethyl cellulose and chitosan. **Colloids and Surfaces B: Biointerfaces**, v. 85, n. 2, p. 343-348, 2011.

KAREWICZ, A.; ŁĘGOWIK, J.; NOWAKOWSKA, M. New bilayer-coated microbead system for controlled release of 5-aminosalicylic acid. **Polymer Bulletin**, v. 66, n. 3, p. 433-443, 2011.

MATALANIS, A.; JONES, O. G.; MCCLEMENTS, D. J. Structured biopolymer-based delivery systems for encapsulation, protection, and release of lipophilic compounds. **Food Hydrocolloids**, v. 25, n. 8, p. 1865-1880, 2011.

NÚÑEZ-SANTIAGO, M. C.; TECANTE, A.; GARNIER, C.; DOUBLIER, J. L. Rheology and microstructure of κ-carrageenan under different conformations induced by several concentrations of potassium ion. **Food Hydrocolloids**, v. 25, n. 1, p. 32-41, 2011.

RAGHAVAN, S. R.; WALLS, H. J.; KHAN, S. A. Rheology of silica dispersions in organic liquids: new evidence for salvation forces dictated by hydrogen bonding. **Langmuir**, v. 16, n. 21, p. 7920-7930, 2000.

RIBEIRO, K. O.; RODRIGUES, M. I.; SABADINI, E.; CUNHA, R. L. Mechanical properties of acid sodium caseinate - κ-carrageenan gels: effect of co-solute addition. **Food Hydrocolloids**, v. 18, n. 1, p. 71-79, 2004.

SOOTTITANTAWAT, A.; YOSHII, H.; FURUTA, T.; OHKAWARA, M.; LINKO, P. Microencapsulation by spray drying: Influence of emulsion size on the retention of volatile compounds. **Journal of Food Science**, v. 68, n. 7, p. 2256-2262, 2003.

VANDENBERG, G. W.; DROLET, C.; SCOTT, S. L.; DE LA NOÜE, J. Factors affecting protein release from alginate-chitosan coacervate microcapsules during production and gastric/intestinal simulation. **Journal of Controlled Release**, v. 77, n. 3, p. 297-307, 2001.

VARGA, C. M.; LASHERAS, J. C.; HOPFINGER, E. J. Initial breakup of a small-diameter liquid jet by a high-speed gas stream. **Journal of Fluid Mechanics**, v. 497, p. 405-434, 2003.

CAPÍTULO 6.   Encapsulação de triptofano em microesferas de Na-CN e κ-carragena

Encapsulation of tryptophan using microbeads of sodium caseinate and κ-carrageenan produced by the atomization

Perrechil, F. A. and Cunha, R. L.∗

Department of Food Engineering, Faculty of Food Engineering, University of Campinas

(UNICAMP), 13083-862 – Campinas, SP, Brazil.

∗ Corresponding author: Tel: +55-19-35214047; fax: +55-19-35214027;

e-mail: rosiane@fea.unicamp.br

ABSTRACT

Tryptophan was encapsulated in microbeads formed by ionotropic gelation of multilayered emulsion. Microbeads were produced from the extrusion of emulsions composed by soybean oil, sodium caseinate and κ-carrageenan at pH 7 and 3.5 into potassium chloride solution. The influence of κ-carrageenan concentration on the size and morphology of microbeads was studied. In addition, confocal microscopy, encapsulation efficiency, tryptophan release and rheological properties of microbeads suspensions in salt solution were evaluated. The morphology of microbeads was very influenced by the increase of κ-carrageenan concentration, tending to be greater and more spherical. The confocal microscopy illustrated the structural differences between microbeads produced at different pH (7 and 3.5) due to the electrostatic interactions between protein and polysaccharide. Despite these structural differences, microbeads with different pH showed similar results for encapsulation efficiency, tryptophan release and rheological properties of the

suspensions of microbeads in salt solution. Encapsulation efficiency was very low (~30%), but the encapsulated tryptophan showed low release in the salt solution (~0.01%). In addition, the rheological measurements indicated that the incorporation of microbeads exerted slight influence on the viscosity of aqueous solutions, mainly up to 40% volume fraction. Thus, these microbeads could be added to products as a delivery system without compromising their texture.

Keywords: ionic gelation; emulsion; confocal microscopy; rheology; encapsulation efficiency

6.1. INTRODUCTION

There has been a growing interest within the food industry in the development of food products that provide health benefits. Among the interesting components to incorporate in the products, tryptophan can be attractive because it is an essential amino acid that may act in the central nervous system as serotonin precursor. Studies revealed that a significant increase in brain tryptophan and brain serotonin (5-HT) can be accomplished by the intake of pure tryptophan from dietary, leading to the regulation of several physiological functions, such as mood, sleep and appetite (MARKUS et al., 2008). However, tryptophan can provide a bitter taste due to their hydrophobic side chains in the same way as other amino acids, such as valine, isoleucine, phenylalanine, leucine and tyrosine (NILSANG et al., 2005). One way to mask the bitter off-taste is through the encapsulation of these components. Delivery systems in the form of hydrogels that trap the molecules of interest within networks can be employed to protect and transport the bioactive compounds (CHEN et al., 2006) without modifying the sensorial and physicochemical properties of food products.

Recent advances in hydrogel microparticles have focused on finding more biocompatible, non-toxic material intended for pharmaceutical, biomedical or food applications (MUHAMAD et al., 2011). Hydrogels formed from polysaccharides, such as carrageenan, are good candidates for drug or bioactive delivery systems due to their nontoxicity and good gelling ability, thermo reversibility of the gel network and appropriate viscoelastic properties. The encapsulation of oil with bioactives can be an alternative for protecting hydrophobic compounds (CHAN, 2011), and an amphiphilic molecule or surfactant should be added to stabilize the oil-water interface.

The first step of this encapsulation process normally includes the emulsification of the oil into the encapsulation matrix material. In this case, the encapsulation efficiency is dependent on the emulsion stability (CHAN, 2011) and the partition coefficient of the bioactive compound. In addition, the biopolymeric matrices must be in the size of few micrometers and have a spherical shape in order to be incorporated in food systems without influencing their texture to do not compromise the consumer satisfaction (ELLIS & JACQUIER, 2009).

Thus, the purpose of this work was to evaluate the feasibility to encapsulate tryptophan in sodium caseinate - κ-carrageenan microbeads produced at pH 7 and 3.5 for application in products with high water content. The microbeads were produced by the extrusion of multilayered emulsions into a KCl solution. The influence of κ-carrageenan concentration on the microbead morphology, as well was the encapsulation efficiency, the tryptophan release in an aqueous solution and the rheology of microbead suspensions were studied.

6.2. MATERIAL AND METHODS

6.2.1. Material

The ingredients used to prepare the systems were κ-carrageenan, gently supplied by CPKelco (Atlanta, USA), casein (Sigma-Aldrich Co., St. Louis, USA), soybean oil (Bunge Alimentos S.A., Brazil), potassium chloride P.A. (Labsynth, Diadema, Brazil) and L-tryptophan (Sigma-Aldrich Co., St. Louis, USA). All other reagents were of analytical grade.

6.2.2. Preparation of stock solutions

The sodium caseinate (Na-CN) stock solution (10% w/v) was prepared by dispersing casein in deionized water for 3 hours using a magnetic stirrer. The pH of the solution was constantly adjusted to 7 using 10 M NaOH. κ-Carrageenan stock solution (3% w/v) was prepared by dissolving the powder in deionized water, followed by heat treatment at 90°C for 60 min with magnetic stirring and subsequent cooling to room temperature. The pH of κ-carrageenan solution was adjusted to 7 using HCl. The two solutions were then diluted in order to prepare the emulsions.

6.2.3. Preparation of primary emulsion

A primary oil-in-water (O/W) emulsion was prepared at 25°C by pre-mixing the soybean oil containing or not (unloaded) tryptophan with a Na-CN aqueous solution using an Ultra Turrax model T18 (IKA, Germany) for 4 min at 14,000 rpm, followed by homogenization at 30 MPa / 5 MPa using a Panda 2K NS1001L double-stage homogenizer

(Niro Soavi, Italy). The oil, Na-CN e tryptophan concentrations in the primary emulsions were fixed in 20% (v/v), 0.25% (w/v) and 0.5% (w/v), respectively.

6.2.4. Microbeads

6.2.4.1. Production of unloaded microbeads

Secondary (or multilayered) O/W emulsions were prepared by mixing the primary emulsion without tryptophan to solutions containing different concentrations of κ-carrageenan using magnetic stirring for 1 hour. The multilayered emulsions showed final composition of 10% (v/v) soybean oil, 0.25% (w/v) sodium caseinate and 0.5 – 1.5% (w/v) κ-carrageenan. Part of these emulsions was adjusted to pH 3.5 using HCl.

Unloaded (without tryptophan) microbeads were prepared by external gelation. Multilayered emulsions were extruded from an atomizer nozzle (1.2 mm diameter) into a 0.4% (w/v) KCl solution at room temperature. For the atomization process, the height from the atomizer nozzle to the KCl solution was fixed at 50 cm, the feed flow rate was fixed as the minimum (0.2 L/h), while the compressed air flow rate at the nozzle was fixed at the maximum as possible (0.12 m^3/h), avoiding the splash of the salt solution out of the container. The gelled particles were maintained in the salt solution for 30 minutes (CHAN et al., 2009) and then filtered through a sieve with opening of 0.053 mm. The microbeads were stored at 10°C and the microstructure and particle size distribution were evaluated.

6.2.4.2. Production of microbeads containing tryptophan

κ-Carrageenan solution (3% w/v) was mixed to the primary emulsion containing tryptophan (section 6.2.3) using magnetic stirring for 1 hour and the pH was kept at 7.0 or

adjusted to pH 3.5. The final composition of the secondary emulsions was 0.25% (w/v) tryptophan, 10% (w/v) soybean oil, 0.25% (w/v) Na-CN and 1.5% (w/v) κ-carrageenan. Such emulsions were extruded according to section 6.2.4.1, resulting in the microbeads containing the encapsulated tryptophan.

6.2.5. Evaluation of microbeads

6.2.5.1. Optical microscopy

The morphology of the microbeads was evaluated by optical microscopy using a Scope.A1 microscope (Carl Zeiss, Germany) with a 10× objective lens. For this, the microgels were poured onto microscope slides and carefully covered with glass cover slips. At least 10 images were obtained for each sample.

The shape of the microgels was determined from image analysis. Measurements of the maximum (F_{max}) and minimum (F_{min}) Feret diameters were carried out for each particle, with a total of 400 particles per sample. The aspect ratio (AR) was obtained from the relation between F_{max} and F_{min} (Equation 6.1).

$$AR = \frac{F_{max}}{F_{min}} \tag{6.1}$$

6.2.5.2. Particle size analysis

Particle size analysis was carried out using 0.4% (w/v) KCl solution as dispersion medium (particle concentration of ~0.005% wt) using a Malvern Mastersizer 2000 (Malvern Instruments Ltd., UK). The size of particles was determined as the volume-surface mean diameter ($d_{32} = \Sigma n_i d_i^3 / \Sigma n_i d_i^2$), where n_i is the number of microgel of diameter d_i. The particle size measurements were reported as the average and standard deviation of

measurements made on microbeads, with three readings made per sample. Particle size distribution was displayed in terms of volume fraction versus particle size.

6.2.5.3. Confocal scanning laser microscopy (CSLM)

Fluorescein-5-isothiocyanate (FITC) was used for the covalent labeling of κ-carrageenan, following the method described by Heilig et al. (2009). 20 mL DMSO and 80 µL pyridine were mixed with 1 g κ-carrageenan and stirred at room temperature for 30 minutes. After the addition of 0.1 g FITC and 40 µL dibutyltin dilaurate, the mixture was incubated for 3 h in a 95°C water bath and, finally, cooled down to room temperature. The resulting gel was then minced, washed with ethanol 99.6% and dried at 65°C. The covalently labeled κ-carrageenan powder was dissolved and used to prepare the polysaccharide solution. Sodium caseinate solution was stained using a fluorescent dye Rhodamine B. The protein and polysaccharide labeled solutions were then used to prepare the emulsions and microbeads for confocal analysis as described in the sections 6.2.3 and 6.2.4.2, respectively.

Samples were examined in a Zeiss LSM 780-NLO confocal on an Axio Observer Z.1 microscope (Carl Zeiss AG, Germany) using a 40 × objective. Images were collected using 488 and 543 nm laser lines for excitation of FITC and Rhodamine B fluorophores, respectively, with pinholes set to 1 airy unit for each channel, 1024×1024 image format. Images were taken in the middle of the height of the samples.

6.2.5.4. Determination of tryptophan solubility

The solubility of tryptophan in soybean oil was determined. For this, different concentrations of tryptophan (between 0.5 and 10% w/v) were dispersed in soybean oil using magnetic stirring and application of ultrasound during 30 minutes. After this, the solution were visually examined and the presence or not of a precipitate was checked.

6.2.5.5. Quantification of tryptophan

The tryptophan content was spectrophotometrically determined using the methodology described by Spies (1967). 9 mL of 21.2 N surfuric acid was mixed to 30 mg of p-dimethylaminobenzaldehyde and 1 mL of sample and placed in the dark at 25°C for 6 hours. Then, 0.1 mL of 0.045 % (w/v) sodium nitrite was added. After 30 minutes, absorbance was read at 590 nm using the spectrophotometer SQ-2800 (UNICO, USA). In order to quantify the amount of tryptophan, a calibration curve was constructed using solutions with known tryptophan concentrations between 10 and 80 µg/mL.

6.2.5.6. Encapsulation efficiency and release of tryptophan from microbeads

Encapsulation efficiency (EE%) was calculated from the relation between the encapsulated tryptophan and tryptophan initially added to the microbeads. The amount of encapsulated tryptophan was determined by the dissolution of 1g microbeads in 25 g deionized water using magnetic stirring during 1 h, followed by the quantification of tryptophan as described in the section 6.2.5.5.

The release measurements were carried out according to methodology described by Alvim and Grosso (2010), with modifications. For this, 0.4 g microbeads were dispersed in 5 mL of 0.75% KCl solution in several glass tubes. This dispersing medium was used to

maintain the microbeads stable in order to simulate the application of microbeads in a product with high water content. The tubes were covered and placed on a shaker at approximately 90 rpm and 20°C. After 5, 10, 20, 30, 60, 120, 180, 240 and 360 minutes, one tube of each sample was filtered and the liquid containing the released tryptophan was evaluated as described in the section 6.2.5.5. The release was expressed as a percentage of the released tryptophan determined in the filtrate by the total amount of tryptophan in the microbead.

6.2.5.7. Rheological measurements of the suspensions

The rheological properties of the suspensions (10%, 20%, 40% and 60% microbeads (w/w) dispersed in 0.75% (w/v) KCl solution were evaluated. A modular compact rheometer Physica MCR301 (Anton Paar, Austria) with a parallel plate geometry (50 mm) and 2 mm gap was used for the measurements. Flow curves were obtained by an up-down-up steps program with the shear rate varying between 0 and 300 s^{-1}. All measurements were performed in triplicate at 25°C.

6.3. RESULTS AND DISCUSSION

6.3.1. Characterization of unloaded microbeads

The effect of κ-carrageenan concentration on the microstructure and particle size distribution of microbeads containing 10% (v/v) soybean oil and 0.25% (w/v) Na-CN at pH 7.0 and 3.5 is shown in Figure 6.1. The microscopic images show that microbeads produced from extrusion of multilayered emulsions were composed by small oil droplets recovered by the gelled biopolymers. The increase of κ-carrageenan in the microbeads from 0.5% to

1.5% promoted the formation of bigger and more spherical microbeads for both pH values (Figure 6.1). The evaluation of particle size distribution showed a monomodal distribution for most of the systems, with exception of microbeads containing low κ-carrageenan concentrations (0.5% and 0.75% for pH 7 and 0.5% for pH 3.5) that showed bimodal distribution (Figure 6.1). For these samples, the mode of first peak was around 1 µm, which was correspondent to the mean diameter of oil droplets, indicating the destabilization of emulsions during the atomization process. For microbeads that showed monomodal distribution, the peak was shifted to lower values as the polysaccharide concentration was decreased for microbeads at pH 7.0 and were very similar distribution curves for systems at pH 3.5 (Figure 6.1).
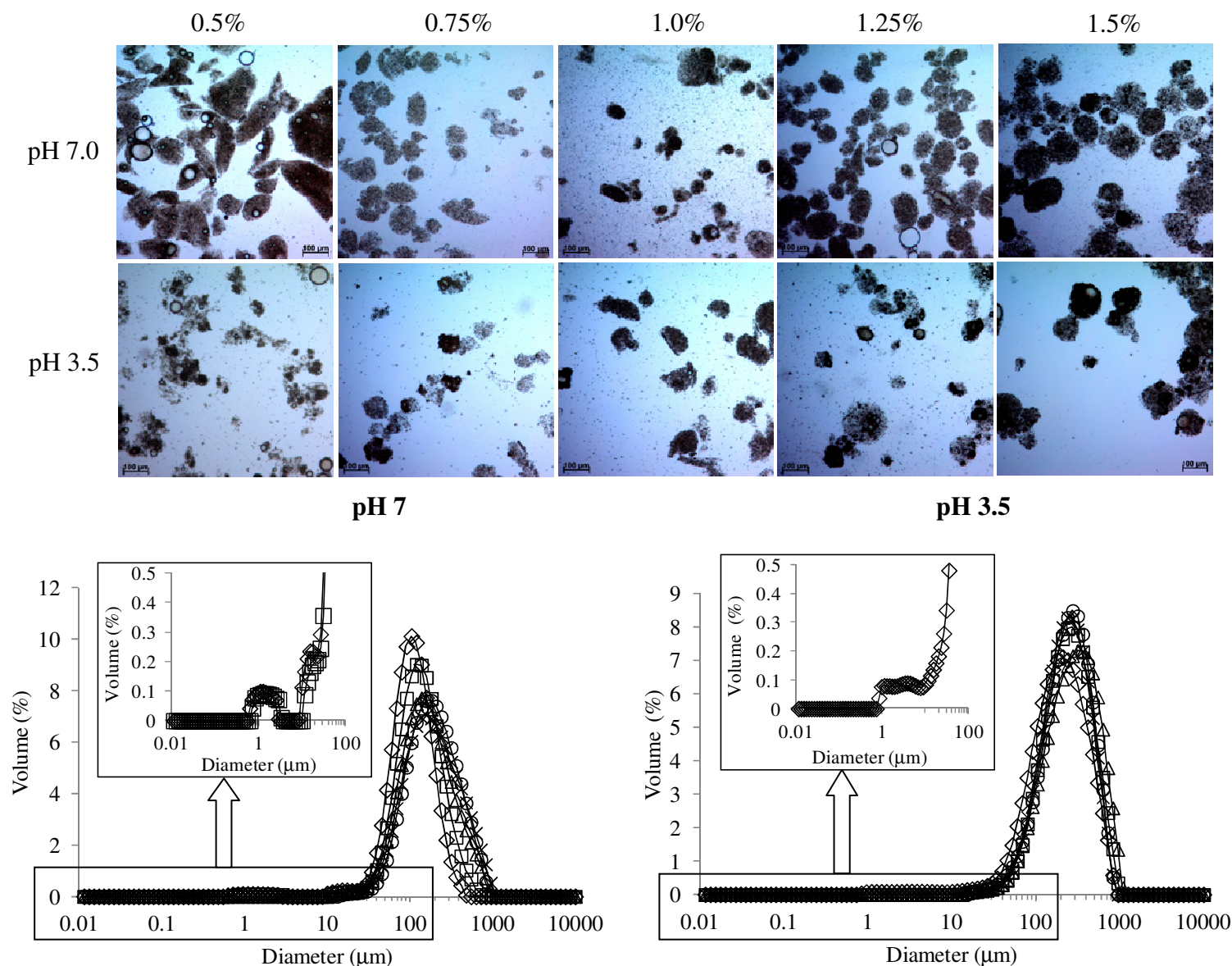
Figure 6.1. Microstructure of microbeads composed by 10% (v/v) soybean oil, 0.25% (w/v) Na-CN and different κ-carrageenan concentrations at pH 7 and 3.5. (—◇—) 0.5%, (—□—) 0.75%, (—△—) 1.0%, (—✕—) 1.25% and (—○—) 1.5% κ-carrageenan. Scale bar = 100 μm.

Table 6.1 shows the mean particle diameter (d_{32}) and the aspect ratio (AR) of the microbeads at pH 7 and 3.5. These results confirmed the tendency of microbeads to increase the particle diameter, especially at pH 7, and to reduce the aspect ratio with the

increase of polysaccharide concentration in both pH values. Systems with low κ-carrageenan concentration showed very reduced d_{32} due to the bimodal distribution (presence of free oil droplets). On the other hand, the increased size of microbeads at high polysaccharide concentrations could be related to the higher biopolymer density, which resulted in thicker films at the atomizer nozzle and consequently an increase in the particle diameter. The same effect was verified for microgels composed by κ-carrageenan and sodium caseinate without oil produced by the same process (Chapter 3). On the other hand, the more spherical shape could be associated with the higher surface tension (results not shown) and viscosity of the emulsions containing higher κ-carrageenan concentrations (Table 6.1). The comparison between the pH values showed that microbeads produced at pH 3.5 presented similar aspect ratio than those produced at pH 7 but, at pH 3.5, the microbeads showed higher particle diameters.

Table 6.1. Apparent viscosity at 300 s^{-1} (η_{300}) of emulsions used to prepare the microbeads, mean particle diameter (d_{32}) and aspect ratio of microbeads containing different κ-carrageenan concentrations at pH 7.0 and 3.5.

	η_{300} (mPa.s)		d_{32} (µm)		AR (-)	
κ-Carrageenan (%)	pH 7.0	pH 3.5	pH 7.0	pH 3.5	pH 7.0	pH 3.5
0.5	14.8 ± 0.2	10.7 ± 0.1	30.7 ± 0.2	25.3 ± 2.7	1.98 ± 0.17	1.54 ± 0.13
0.75	28.4 ± 1.1	14.0 ± 9.4	34.7 ± 0.1	159.9 ± 8.1	1.55 ± 0.08	1.42 ± 0.19
1.0	50.1 ± 1.2	37.5 ± 1.3	106.5 ± 2.8	176.1 ± 8.1	1.56 ± 0.12	1.50 ± 0.13
1.25	74.9 ± 1.6	52.5 ± 3.0	121.6 ± 2.9	157.5 ± 5.3	1.39 ± 0.04	1.33 ± 0.17
1.5	115.7 ± 2.1	123.5 ± 6.1	130.4 ± 2.9	160.9 ± 6.1	1.28 ± 0.12	1.24 ± 0.08

From these results, the microbeads composed by 1.5% (w/v) κ-carrageenan at pH 7 and pH 3.5 were chosen to the following steps of this work due to their more spherical shape (Figure 6.1 and Table 6.1), which would affect less the rheological properties of food products.

6.3.2. Microbeads containing tryptophan

6.3.2.1. Confocal microscopy

In order to evaluate the interactions between Na-CN and κ-carrageenan in the microbeads, particles containing 10% (v/v) soybean oil, 0.25% (w/v) Na-CN, 1.5% (w/v) κ-carrageenan and 0.25% (w/v) tryptophan were evaluated using confocal scanning laser microscopy (CSLM) (Figure 6.2). As Rhodamine B and FITC are specific dyes, Na-CN linked to Rhodamine B appear as red regions in the micrographs, while the green areas indicate the presence of κ-carrageenan. Figures 6.2A and 6.2D shows only the labeled polysaccharide (FITC-channel), Figures 6.2B and 6.2E illustrated the labeled protein (Rhodamine B-channel) and Figures 6.2C and 6.2F shows the overlapping images. These pictures revealed that the protein was mainly concentrated around the oil droplets for microbeads produced in both pH 7 and 3.5 (Figures 6.4B and 6.4E, respectively). However, the protein (Na-CN and probably tryptophan) were more concentrated at the external surface of microbeads at pH 7 (Figure 6.4C), while the κ-carrageenan was predominant in the microbead surface at pH 3.5 (Figure 6.4F). The position of biopolymers into the microbeads can be explained by the electrostatic interactions between Na-CN and κ-carrageenan (Chapter 5).

At pH 7, both protein and polysaccharide are negatively charged, resulting in an electrostatic repulsion and consequently a micro-phase separation. On the other hand, the negatively charged κ-carrageenan is attracted by the positively charged sodium caseinate at pH 3.5, resulting in a double layer around the oil droplets (GUZEY & MCCLEMENTS, 2006). During the atomization process of emulsion at pH 7, the Na-CN-coated oil droplets probably migrated to the air-liquid interface and, as the particles come into contact with the salt solution, part of protein was dissolved while the potassium ions promoted the gelation of polysaccharide simultaneously. On the other hand, when the particles at pH 3.5 came into contact with the salt, the potassium ions promoted the gelation of polysaccharide, producing the microbeads. As the κ-carrageenan was linked to the sodium caseinate at the oil surface, there was lower amount of free polysaccharide in solution and the gelation of polysaccharide tended to be slower when compared to the microbeads at pH 7. Thus, there was a higher dissolution of microbeads before gelation, which could be related to the higher microbead diameter at pH 3.5 when compared to that at pH 7.
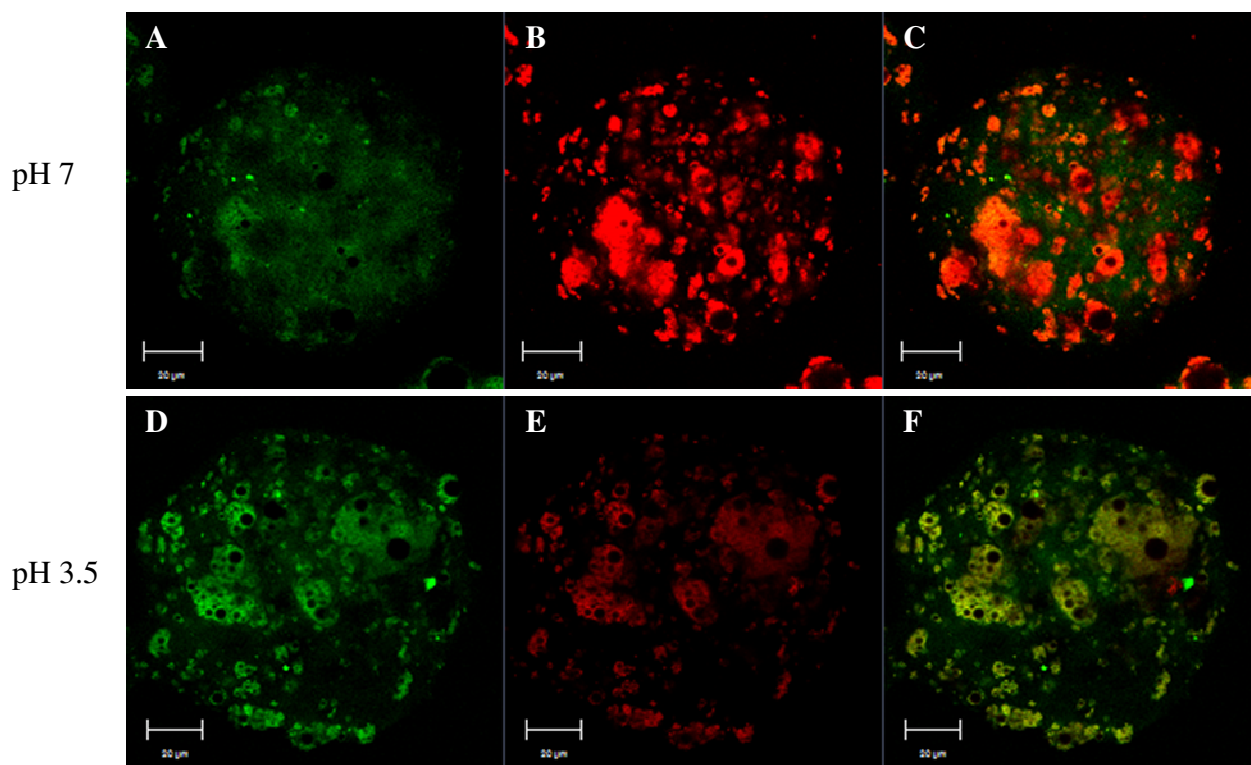
Figure 6.2. CSLM micrographs of microbeads composed by 10% (v/v) soybean oil, 0.25% (w/v) Na-CN and 1.5% (w/v) κ-carrageenan at pH 7: A) FITC-channel, B) Rhodamine B-channel and C) dual-channel (FITC + Rhodamine B); and at pH 3.5: D) FITC-channel, E) Rhodamine B-channel and F) dual-channel (FITC + Rhodamine B). Scale bar = 20 µm.

6.3.2.2. Encapsulation efficiency and release measurements of tryptophan

The solubility of tryptophan in soybean oil was determined in order to establish the affinity of this amino acid to the apolar phase. The dispersion of several tryptophan concentrations in oil (Figure 6.3) showed that this amino acid was completely dissolved only up to 0.5%, above this concentration it precipitated. During the production of emulsions, 2.5% (w/v) tryptophan was added to the oil phase. Thus, it can be considered that only 20% of initial amount of tryptophan was solubilized in the oil phase, while the others 80% were situated in the aqueous phase or the interface.
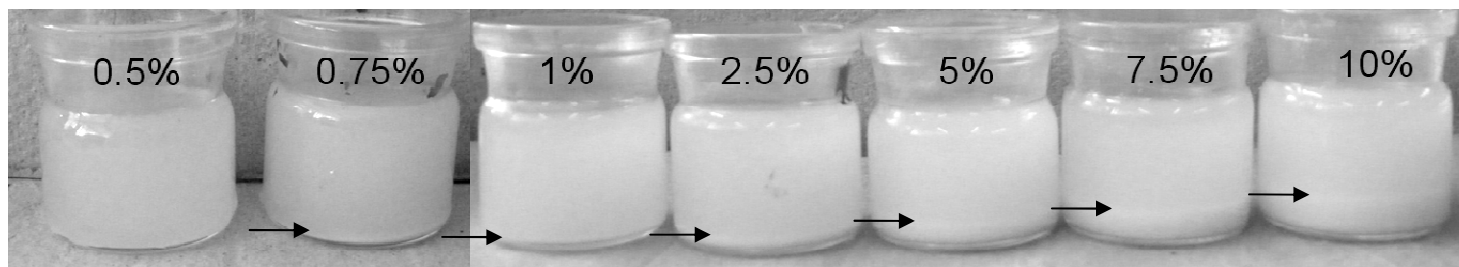
Figure 6.3. Dispersion of different concentrations of tryptophan in soybean oil

The tryptophan concentrations on the emulsions and microbeads composed by 1.5% (w/v) κ-carrageenan at pH 7 and 3.5 were determined using a calibration curve. The multilayered emulsions produced at both pH values showed very similar tryptophan concentration (~0.33 %) (Table 6.2). In the same way, the pH value did not affect the tryptophan concentration in the microbeads and both samples showed ~0.1% tryptophan in their composition (Table 6.2). Comparing the initial amount of tryptophan in the emulsions with that encapsulated in the microbeads it is possible to verify that a large amount of tryptophan was lost during the bead formation and the encapsulation efficiency was very low (EE ~29%). This low encapsulation efficiency can be explained by the large pore size of the gel matrix, which could not hinder the diffusion of low molecular weight compounds, such as the tryptophan, from microbeads during the hardening process with potassium chloride. During the production of microbeads, the tryptophan situated in the continuous aqueous phase probably leaked out to the hardening solution, while the remained was kept dispersed in the oil phase and oil-water interface, protected by the protein. Considering the partitioning coefficient (octanol versus water) of tryptophan, the encapsulation efficiency should have been even lower due to the higher affinity of this molecule to the water phase. Probably, the biopolymer layers at the interface contributed

for retaining the tryptophan in the oil phase. As the oil droplets were covered by the protein independent on the pH (Figure 6.2), it can explain the similar encapsulation efficiency of microbeads produced in different pH values. Azarnia et al. (2008) verified similar encapsulation efficiency (EE ~30%) for the encapsulation of recombinant aminopeptidase (PepN) in alginate beads produced by extrusion in $CaCl_2$ solution. This EE was improved (EE = 79 – 88%) by the addition of 0.1 – 0.2% chitosan to the salt solution, resulting in chitosan-coated alginate beads with smaller pores on the bead surface. Other works showed that the encapsulation efficiency can be improved by the complexation between two different polysaccharides, such as complexes alginate – guar gum (GEORGE & ABRAHAM, 2007) and tamarind seed polysaccharide – alginate (NAYAK & PAL, 2011). The combination of two polysaccharides probably led to the formation of a network with smaller pores that prevented the release of the encapsulated bioactive, which did not occur for the protein-polysaccharide complex.

Table 6.2. Concentration of tryptophan on the samples and encapsulation efficiency

	Sample	Tryptophan (%)	EE (%)
pH 7.0	Emulsion	0.328 ± 0.003	–
	Microbead	0.096 ± 0.004	29.13
pH 3.5	Emulsion	0.338 ± 0.018	–
	Microbead	0.100 ± 0.005	29.47

The release measurements of tryptophan from the microbeads were carried out as a function of time in a potassium chloride solution (0.75% w/v) in order to simulate their application in products with high water content (Figure 6.4). At this salt solution, the microbeads were very stable and maintained their size and shape during the storage. The

amount of tryptophan released in the salt solution was very small, with maximum of 0.01% tryptophan contained in the microbeads. This result reinforced the assumption that the most of retained tryptophan was encapsulated in the oil phase and oil-protein interface, while that placed in the carrageenan layer was released to the salt solution. Once again the value of pH did not influence the tryptophan release from microbeads, showing very similar behaviors for both pH (Figure 6.2) since the main difference between the microbeads with different pH was in the position of polysaccharide (Figure 6.2). After the storage, almost 100% of the encapsulated tryptophan remained in the microbeads, which is equivalent to 100 mg tryptophan per 100 g of microbeads.

6.3.2.3. Rheological properties

The rheological properties of microbead suspensions were evaluated in order to determine the influence of the incorporation of microbeads on the texture of food products (Figure 6.4). The flow curves showed different behaviors depending on the volume fraction of suspensions. No suspension showed yield stress (σ_o) or time dependence (thixotropy or rheopexy), as verified for κ-carrageenan – sodium caseinate microgels at the highest volume fraction (60%) (Chapter 3). These differences could be attributed to the lower aspect ratio (higher sphericity) of microbeads containing oil and the lubrication of particle motion due to the presence of oil in the microbead surface. With the increase of volume fraction, the suspensions tended to show shear thinning behavior and a greater viscosity (Figure 6.4). The flow curves were well fitted to power law model and the flow behavior index (n), as well as the apparent viscosity at 50 s^{-1} are shown in Figure 6.5.
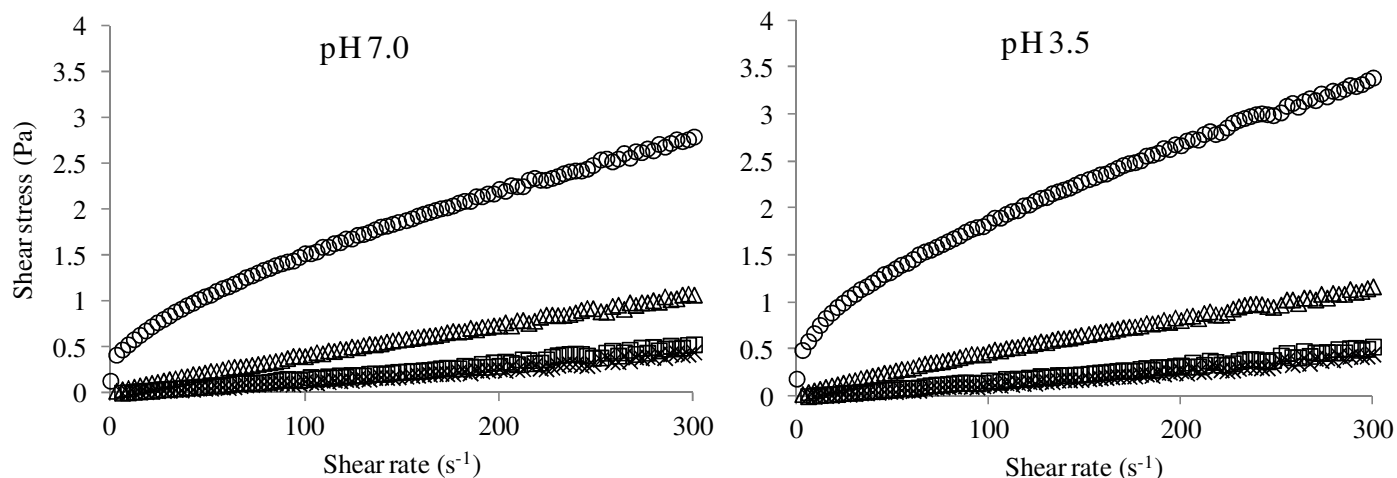
Figure 6.4. Flow curves of suspensions of microbeads composed by 10% (v/v) soybean oil, 0.25% (w/v) sodium caseinate and 1.5% (w/v) κ-carrageenan at pH 7.0 and 3.5 in KCl solution. Volume fraction: ($\times$) 10%, ($\square$) 20%, ($\triangle$) 40% and ($\bigcirc$) 60%.

The flow behavior index (n) decreased from ~1.2 (shear thickening behavior) to ~0.4 (shear thinning behavior) as the volume fraction of suspension was increased from 10 to 60% (Figure 6.5A). The shear thickening behavior occurred for lower volume fractions because the increase in shear rate in these samples led to a greater interaction between the particles, causing the increase in dispersion viscosity. This behavior is expected to occur in all suspensions (BROWN et al., 2010). However, the increase of volume fraction can result in a confinement or flocculation of particles in the suspensions, resulting in a shear thinning behavior that hides the shear thickening (BROWN et al., 2010). The values of apparent viscosity at 50 s^{-1} ($\eta_{50\,s}^{-1}$) were evaluated (Figure 6.5B) in order to compare the behavior of the suspensions at a shear rate typical of chewing (STEFFE, 1996). The evaluation of apparent viscosity confirmed the tendency of suspension to become more viscous with the increase of volume fraction. Nevertheless, the apparent viscosity of microbead suspensions

was very low, indicating that the addition of microbeads exerted small influence on the rheological behavior of food products. It occurred due to the reduced size and high sphericity of microbeads (Figure 6.1). The maximum apparent viscosity at 50 s^{-1} (volume fraction = 60%) was around 0.030 and 0.025 Pa.s, which is still relatively low when compared to some food products. This range of apparent viscosity can be compared to some fruit juices, such as mango ($\eta_{50\ s}^{-1}$ = 0.03 Pa.s) (DAK et al., 2007) and pineapple juice ($\eta_{50\ s}^{-1}$ = 0.024 Pa.s) (SHAMSUDIN et al., 2009). However, Krasaekoopt and Kitsawad (2010) observed that the addition of 10% (w/w) alginate beads containing encapsulated probiotic into orange and grape juices affected their turbidity and the swallow ability of potential consumers. These beads showed mean diameter around 100-200 µm, which was similar than the microbeads containing 1.5% (w/v) κ-carrageenan in the present work. Thus, it can be concluded that although the addition of 60% microbeads exert small influence on the viscosity of solution, the sensorial properties are affected with only 10% beads. It is also interesting to note that the influence of beads on sensory attributed is lower for products with higher viscosity or thicker texture, such as yoghurt (KRASAEKOOPT & KITSAWAD, 2010).
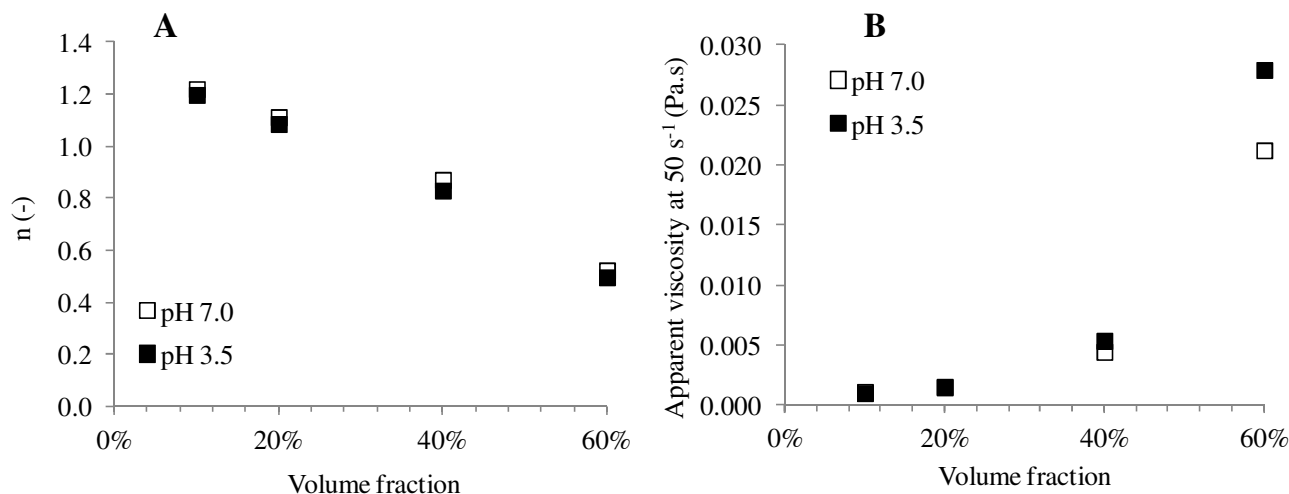
Figure 6.5. Flow behavior index and relative viscosity at 50 s^{-1} as a function of volume fraction of microbead suspensions.

6.4. CONCLUSIONS

The viability to encapsulate tryptophan in Na-CN - κ-carrageenan microbeads for application in high moisture products was assessed. The encapsulation efficiency of tryptophan was quite low (~30%). This was attributed to the high porosity of the gels, which resulted in tryptophan leakage during the beads production. Nevertheless, the biopolymer layer at the interface contributed for retaining the tryptophan in the oil phase, since the leakage of this compound in aqueous solution (0.75% KCl) was negligible (0.01%) over 1 day. Therefore, gelled microbeads are not the suitable technology for encapsulating tryptophan. In fact, we can conclude that the best technology to encapsulate tryptophan should be designed considering the Retrodesign approach as described by Braga and Ubbink (2012). Following this approach we would probably have predicted the low encapsulation efficiency. One should also think ahead about the characteristics of the final product, since we have seen during this work that the beads made of carrageenan are only

stable in solutions with minimum 0.75% KCl. Considering future applications, we can imagine the Na-CN - κ-carrageenan microbeads system being used to encapsulate nutraceuticals with higher molecular weight and showing higher oil solubility and affinity. Nevertheless, if the nutraceutical needs to be stabilized, e.g. oxidation, one should still investigate if the biopolymer interfacial layer is adequate for the requirements.

Our rheological data have shown a slight increase of overall viscosity up to 40% particles in KCl solution. Nevertheless, not only the rheological data should be considered for evaluating the feasibility of particles addition in food products. The particles produced had a mean size between 100-200 micrometers, which in principle could be perceived in mouth. Previous study done by Krasaekoopt and Kitsawad (2010) has shown that the addition of 10% of 200 µm probiotics beads to fruit juices affects its turbidity and the swallow ability of potential consumers. Therefore, we can suggest applying up to 10% of the Na-CN - κ-carrageenan microbeads with other hydrophobic nutraceutical in salty, turbid and viscous products.

6.5. ACKNOWLEDGEMENTS

6.6. REFERENCES

ALVIM, I. D.; GROSSO, C. R. F. Microparticles obtained by complex coacervation: influence of the type of reticulation and the drying process on the release of the core material. **Ciência e Tecnologia de Alimentos**, v. 30, n. 4, p. 1069-1076, 2010.

AZARNIA, S.; LEE, B. H.; ROBERT, N.; CHAMPAGNE, C. P. Microencapsulation of a recombinant aminopeptidase (PepN) from *Lactobacillus rhamnosus* S93 in chitosan-coated alginate beads. **Journal of Microencapsulation**, v. 25, n. 1, p. 46-58, 2008.

BRAGA, A. L. M.; UBBINK, J. An industrial approach to design / screen encapsulates for best performance in products: fish oil case. **Proceedings of the 1st South-American Symposium on Microencapsulation**. To be published in April 2012.

BROWN, E.; FORMAN, N. A.; ORELLANA, C. S.; ZHANG, H.; MAYNOR, B. W.; BETTS, D. E.; DESIMONE, J. M.; JAEGER, H. M. Generality of shear thickening in dense suspensions. **Nature Materials**, v. 9, p. 220-224, 2010.

CHAN, E. –S. Preparation of Ca-alginate beads containing high oil content: Influence of process variables on encapsulation efficiency and bead properties. **Carbohydrate Polymers**, v. 84, n. 4, p. 1267-1275, 2011.

CHAN, E. –S.; LEE, B. –B.; RAVINDRA, P.; PONCELET, D. Prediction models for shape and size of ca-alginate macrobeads produced through extrusion-dripping method. **Journal of Colloid and Interface Science**, v. 338, n. 1, p. 63-72, 2009.

CHEN, L.; REMONDETTO, G. E.; SUBIRADE, M. Food protein-based materials as nutraceutical delivery systems. **Trends in Food Science & Technology**, v. 17, n. 5, p. 272-283, 2006.

DAK, M.; VERMA, R. C.; JAAFFREY, S. N. A. Effect of temperature and concentration on Rheological properties of "Kesar" mango juice. **Journal of Food Engineering**, v. 80, n. 4, p. 1011-1015, 2007.

ELLIS, A.; JACQUIER, J. C. Manufacture of food grade κ-carrageenan microspheres. **Journal of Food Engineering**, v. 94, n. 3-4, p. 316-320, 2009.

GEORGE, M.; ABRAHAM, T. E. pH sensitive alginate-guar gum hydrogel for the controlled delivery of protein drugs. **International Journal of Pharmaceutics**, v. 335, n.1-2, p. 123-129, 2007.

GUZEY, D.; MCCLEMENTS, D. J. Formation, stability and properties of multilayer emulsions for application in the food industry. **Advances in Colloid and Interface Science**, v. 128-130, p. 227-248, 2006.

HEILIG, A.; GÖGGERLE, A.; HINRICHS, J. Multiphase visualization of fat containing β-lactoglobulin - κ-carrageenan gels by confocal scanning laser microscopy, using a novel dye, V03-01136, for fat staining. **LWT – Food Science and Technology**, v. 42, n. 2, p. 646-653, 2009.

KRASAEKOOPT, W.; KITSAWAD, K. Sensory characteristics and consumer acceptance of fruit juice containing probiotics beads in Thailand. **Assumption University Journal of Technology**, v. 14, n. 1, p. 33-38, 2010.

MARKUS, C. R.; FIRK, C.; GERHARDT, C.; KLOEK, J.; SMOLDERS, G. F. Effect of different tryptophan sources on amino acids availability to the brain and mood in healthy volunteers. **Psychopharmacology**, v. 201, n. 1, p. 107-114, 2008.

MUHAMAD, I. I.; FEN, L. S.; HUI, N. H.; MUSTAPHA, N. A. Genipin-cross-linked kappa-carrageenan/carboxymethyl cellulose beads and effects on beta-carotene release. **Carbohydrate Polymers**, v. 83, n. 3, p. 1207-1212, 2011.

NAYAK, A. K.; PAL, D. Development of pH-sensitive tamarind seed polysaccharide – alginate composite beads for controlled diclofenac sodium delivery using response surface methodology. **International Journal of Biological Macromolecules**, v. 49, n. 4, p. 784-793, 2011.

NILSANG, S.; LERTSIRI, S.; SUPHANTHARIKA, M.; ASSAVANIG, A. Optimization of enzymatic hydrolysis of fish soluble concentrate by commercial proteases. **Journal of Food Engineering**, v. 70, n. 4, p. 571-578, 2005.

SHAMSUDIN, R.; DAUD, W. R. W.; TAKRIF, M. S.; HASSAN, O.; ILICALI, C. Rheological properties of Josapine pineapple juice at different stages of maturity. **International Journal of Food Science and Technology**, v. 44, n. 4, p. 757-762, 2009.

SPIES, J. R. Determination of tryptophan in proteins. **Analytical Chemistry**, v. 39, p. 1412-1445, 1967.

STEFFE, J. F. **Rheological methods in food process engineering**. Michigan: Freeman Press, 1996.

CAPÍTULO 7.   CONCLUSÕES GERAIS

O presente trabalho mostrou que microgéis puderam ser produzidos com sucesso a partir de soluções ou emulsões multicamadas contendo caseinato de sódio e κ-carragena através da extrusão em solução salina. As principais conclusões obtidas neste trabalho estão enumeradas a seguir:

1) Emulsões multicamadas

A partir do estudo das emulsões multicamadas foi possível avaliar a interação proteína – polissacarídeo na interface óleo-água. Em pH 7, a κ-carragena foi fracamente adsorvida na superfície das gotas, já que tanto a proteína quanto o polissacarídeo estavam carregados negativamente. Assim, o aumento na concentração de κ-carragena levou ao aumento na concentração de polissacarídeo livre na fase aquosa, o que promoveu a floculação por depleção. Por outro lado, a κ-carragena carregada negativamente foi fortemente adsorvida na superfície das gotas cobertas pela proteína carregada positivamente em pH 3,5. Neste caso, as emulsões apresentaram floculação por ponte (*bridging flocculation*) nas menores concentrações de polissacarídeo e completa cobertura das gotas em elevadas concentrações de κ-carragena. Na maior concentração de κ-carragena (1% m/v), as emulsões foram estáveis em ambos os valores de pH devido ao aumento da viscosidade da fase contínua. A partir desses resultados, concluiu-se que os complexos eletrostáticos proteína-polissacarídeo produzidos nessa concentração de κ-carragena foram eficientes na estabilização das emulsões, inclusive em valores de pH próximos ao ponto isoelétrico da proteína. Estas emulsões estáveis puderam ser utilizadas para a produção de sistemas de encapsulação.

2) Produção dos microgéis / microesferas

Com relação ao processo de extrusão, a morfologia e o tamanho das partículas

164

formadas foram influenciados por: 1) vazão de alimentação, 2) vazão de ar comprimido, 3) diâmetro de saída de fluido do bico atomizador, 4) distância entre o bico atomizador e a solução salina e 5) viscosidade, tensão superficial, composição e pH das soluções biopoliméricas. Os resultados mostraram que o aumento na vazão de ar comprimido e a redução na vazão de alimentação, diâmetro de saída de fluido e viscosidade da solução polimérica promoveram a formação de microgéis menores. Entretanto, o *aspect ratio* das partículas foi principalmente influenciado pela tensão superficial das soluções e pela distância entre o bico atomizador e a solução salina, sendo que maiores tensões superficiais e maiores distâncias levaram à formação de partículas mais esféricas. A composição de biopolímeros também afetou a morfologia dos microgéis devido à interação entre proteína e polissacarídeo. No caso das soluções aquosas, microgéis mistos (κ-carragena / Na-CN) foram maiores do que os puros (κ-carragena) provavelmente devido à incompatibilidade entre proteína e polissacarídeo. Já para as emulsões, microesferas foram maiores quando produzidas em pH 3,5, o que pode ser atribuído ao aumento da espessura da membrana interfacial durante a gelificação das partículas, o que não ocorreu para as microesferas produzidas em pH 7.

Com relação à estabilidade, os microgéis / microesferas foram altamente instáveis quando dispersos em água, porém mantiveram seu formato quando diluídos em soluções salinas (> 0,75% KCl para as microesferas e > 10% KCl para os microgéis). Além disso, as microesferas preparadas em pH 3,5 foram mais estáveis do que aquelas preparadas em pH 7 quando diluídas em água e soluções de sacarose, o que pode ser atribuído à maior interação eletrostática entre os biopolímeros nessa condição. A avaliação da reologia das suspensões de microgéis em solução salina mostrou que diferentes comportamentos reológicos podem

ser obtidos dependendo da fração volumétrica e do tamanho e formato das partículas. Suspensões contendo microgéis grandes e com formato irregular apresentaram comportamento de fluidos complexos com a presença de tensão residual quando utilizadas as maiores frações volumétricas (40 e 60%). Já as suspensões contendo partículas menores e mais esféricas apresentaram comportamento variando desde dilatante até pseudoplástico com o aumento na fração volumétrica. As suspensões de microesferas, em especial, apresentaram relativamente baixas viscosidades mesmo nas maiores frações volumétricas.

3) Aplicação das microesferas para encapsulação do triptofano

Após o estudo do processo de fabricação dos microgéis / microesferas, estes foram testados com relação à encapsulação de triptofano. A eficiência de encapsulação do triptofano nas microesferas foi baixa (~30%), o que pode ser atribuído ao elevado tamanho dos poros da rede de gel que não impediu a difusão deste aminoácido. O triptofano que permaneceu encapsulado provavelmente estava localizado no óleo e na interface óleo-água, o que explica o mesmo valor de eficiência de encapsulação obtido para as microesferas produzidas nos diferentes valores de pH. Apesar da baixa eficiência de encapsulação, a quantidade de triptofano liberada durante a estocagem em solução aquosa (0,75% KCl) foi muito baixa (~0,01%), o que indica a elevada estabilidade das microesferas nessas condições.

Neste exemplo de aplicação, observou-se que o processo de encapsulação utilizado não foi o mais adequado para encapsulação do triptofano. O processo apropriado para a encapsulação do triptofano poderia ser definido através da metodologia do "Retro-Design". Nesta metodologia primeiramente define-se o produto que se deseja adicionar as microcápsulas e o local de liberação do composto encapsulado, para depois decidir os materiais e o processo de encapsulação a serem empregados, sendo um método pensado de

forma oposta àquela utilizada neste trabalho. No entanto, as microesferas produzidas a partir da gelificação iônica de emulsões multicamadas podem ser uma alternativa promissora para a encapsulação de outros compostos bioativos hidrofóbicos.